GEORG-AUGUST-UNIVERSITÄT
GÖTTINGEN

Analysis of the role of Mdm38 in respiratory chain biogenesis

Dissertation
for the award of the degree
"Doctor rerum naturalium"
of the Georg-August-Universität Göttingen

submitted by
Christine Vollmer
from Göttingen

Göttingen 2011

Member of the Thesis Committee (First Reviewer):
Prof. Dr. Peter Rehling
Department of Biochemistry II
Center for Biochemistry and Molecular Cell Biology
Georg-August University, Goettingen

Member of the Thesis Committee (Second Reviewer):
Prof. Dr. Stefanie Pöggeler
Department of Genetics of Eukaryotic Microorganisms
Institute of Microbiology and Genetics
Georg-August University, Goettingen

Member of the Thesis Committee
Prof. Dr. Michael Thumm
Department of Biochemistry II
Center for Biochemistry and Molecular Cell Biology
Georg-August University, Goettingen

Member of the Thesis Committee:
Prof. Dr. Marina Rodnina
Department of. Physical Biochemistry
Max Planck Institute for Biophysical Chemistry, Goettingen

DATE OF ORAL EXAMINATION: 31.05.2011

Affidavit:

I herewith declare that this thesis has been written independently and with no other sources and aids than explicitly quoted.

Christine Vollmer

TABLE OF CONTENTS

LIST OF FIGURES

LIST OF TABLES

1. INTRODUCTION

1.1 Mitochondria: semi-autonomous cell organelles

1.1.1 Origin and evolution of mitochondria

Ever since the evolution of complex life on earth, multicellular organisms have immensely flourished, which is regarded by many to be directly linked to the development of the compartmentalized eukaryotic cell. One of the pioneering works on this evolutionary event proposed the endosymbiotic theory of plastid and mitochondrial origins, introduced by Andreas Schimper in 1883 and Konstantin Mereschkowsky in 1905. The theory postulates that a proto-eukaryotic cell without mitochondria evolved first and subsequently captured a proto-bacterium via endocytosis.

A more contemporary view of eukaryotic evolution was proposed in the 20th century, which suggests that a fusion event occurred over a billion years ago between an anaerobic archeo-bacterium (host) and a respiration-competent proto-bacterium (symbiont). After establishing a symbiotic relationship, the vast majority of the bacterial symbiotic genome was transferred to the host nucleus and integrated into the nuclear chromosomes. It is hardly traceable which factors might have driven the ancient bacterial symbiont to surrender its genome (Embley et al. 2006). The contemporary mitochondrial genomes range from 3 (in the human malaria parasite *Plasmodium falciparum*) to 67 (in the freshwater protozoan *Reclinomas americana*) protein-coding genes (Gray et al. 1999; Dyall et al. 2004). This reveals that many genes have been lost throughout evolution, such as e.g. complex I (*nad*) genes of the respiratory chain in the yeast *Saccharomyces cerevisiae* (*S. cerevisiae*) (Gray et al. 2001). At this point in evolution, mammals' mitochondrial genome encodes 13 proteins (Scheffler 2001), whereas the model organism *S. cerevisiae*, which was mainly used in the present work, possesses eight mitochondria encoded proteins.

1.1.2 Function and morphology of mitochondria

The key role of mitochondria is to provide energy in the form of adenosine triphosphate (ATP). Furthermore the last years of research have shown the organelle to be vital in many other cellular functions, including ß-oxidation and the citric acid cycle, heme and iron-sulphur biosynthesis, Ca^{2+} homeostasis, amino acid metabolism and even apoptosis (Graier et al. 2007; Tong et al. 2007; Rimessi et al. 2008; Youle et al. 2011).

The number and shape of mitochondria exhibit an extremely large variability, depending on tissue, physiological state or developmental stage of the cell. Moreover the shape of the cristae membranes also vary; tubular, lamellar and even triangle shaped cristae have been observed (Zick et al. 2009). Mitochondria consist of four distinct sub-compartments: the outer membrane, the intermembrane space, the inner membrane and the matrix. The outer membrane (OM) forms an envelope, which represents a barrier only for macromolecules. The intermembrane space (IMS) is contiguous to both membranes, while the inner membrane (IM) surrounds the matrix. In contrast to the OM, the IM acts as a real barrier: not even small solutes like ions and metabolic substances can diffuse through it.

Electron tomography and computer-assisted three-dimensional imaging have revealed that the inner membrane is organized into two morphologically distinct domains: the inner boundary membrane (IBM) and the cristae membrane (CM), which is connected by narrow, tubular cristae junctions (Vogel et al. 2006) (Figure 1.1).

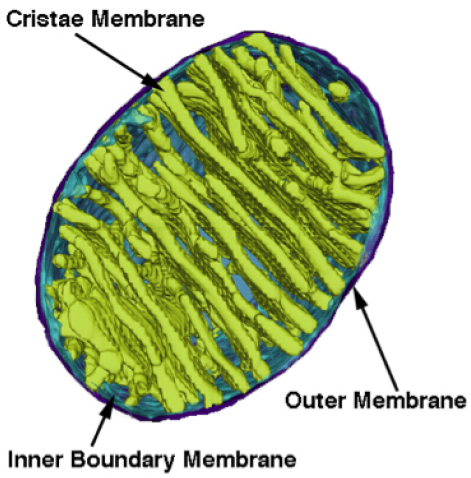

Figure 1.1: 3D computer model of the mitochondrial membranes generated from electron tomogram of a mitochondrion.
The image shows the outer membrane in dark blue, inner boundary membrane in turquoise and all the cristae in yellow. Picture is taken from (Perkins et al. 1997)

Compared to other biological membranes, the inner mitochondrial membrane is extremely rich in proteins and has a protein : lipid mass ratio of 75 : 25 (Simbeni et al. 1991), suggesting that the proteins are densely packed within the membrane. Moreover protein distribution varies between the inner boundary membrane and the cristae membrane. Fluorescence microscopy studies done by Wurm and Jakobs (2006) and quantitative immunoelectron microscopy performed by Vogel et al. (2006) (both in *S. cerevisiae*) have shown that TIM23 complex components and the presequence translocase-associated motor (PAM) are strongly enriched at the IBM, while the F_1F_0-ATP-Synthase as well as the respiratory chain complexes III and IV are located in the cristae-containing interior of mitochondria. Moreover studies done in the past few years provided support to the presumption that the F_1F_0-ATP-Synthase (complex V) is important for cristae formation (Giraud et al. 2002; Rabl et al. 2009; Velours et al. 2009; Zick et al. 2009).

The respiratory chain complexes are located within the IBM. They are involved in oxidative phosphorylation (OXPHOS) and guarantee the energy supply of the cell through the production of ATP. These multi-subunit protein complexes generate an electrochemical gradient across the inner membrane using energy harvested from electron flux between the complexes. The pumping of protons from the matrix to the intermembrane space establishes this gradient. The electrochemical gradient is referred to as the mitochondrial membrane potential ($\Delta\Psi$) and measures approximately −180 mV in respiring mitochondria (Mitchell et al. 1965). Eventually, the energy is utilized by the F_1F_0-ATP Synthase (Complex V) to produce ATP from ADP and inorganic phosphate (P_i) (Mitchell et al. 1968; Yoshida et al. 2001), and additionally to fuel a number of pre-protein transport processes (see 1.1.3). The reduction equivalents NADH and $FADH_2$ are produced in the citric acid cycle and subsequently oxidized within the respiratory chain. Respiratory chain of *S. cerevisiae*, unlike that of mammals, lacks complex I. Here, electrons are transferred to ubiquinone by NADH dehydrogenases (Boumans et al. 1998). Three additional electron-transport complexes follow the NADH dehydrogenases: succinate dehydrogenase (complex II), ubiquinol cytochrome *c* reductase or *bc1* complex (complex III) and cytochrome *c* oxidase (complex IV). The latter transfers electrons to O_2, which is subsequently reduced to water. Electron transport is mediated by different redox-centers within the complexes and supported by mobile electron carrier shuttles, termed Ubiquinone (coenzyme Q) and cytochrome *c*. It

has been shown that these electron carriers do not exhibit pool behavior in *S. cerevisiae*, implying that the respiratory chain in yeast is one functional unit (Boumans et al. 1998).

It has been shown that this electron-transporting complexes are not randomly distributed within the inner mitochondrial membrane, but assembled into high-molecular structures termed respirasomes (Schagger et al. 2000). In yeast, the *bc1* complex exists in three different forms: complex III dimer (III_2) or as supercomplex with one (III_2IV) or two (III_2IV_2) complex IV monomers. In mammals, complex III associates also with complex I in order to form different supercomplexes: I/III_2 or $I/III_2/IV_n$. The observed oligomerization probably allows for fast electron transport by substrate channeling and reduction of diffusion distances for electron shuttles (Acin-Perez et al. 2008; Lenaz et al. 2009).

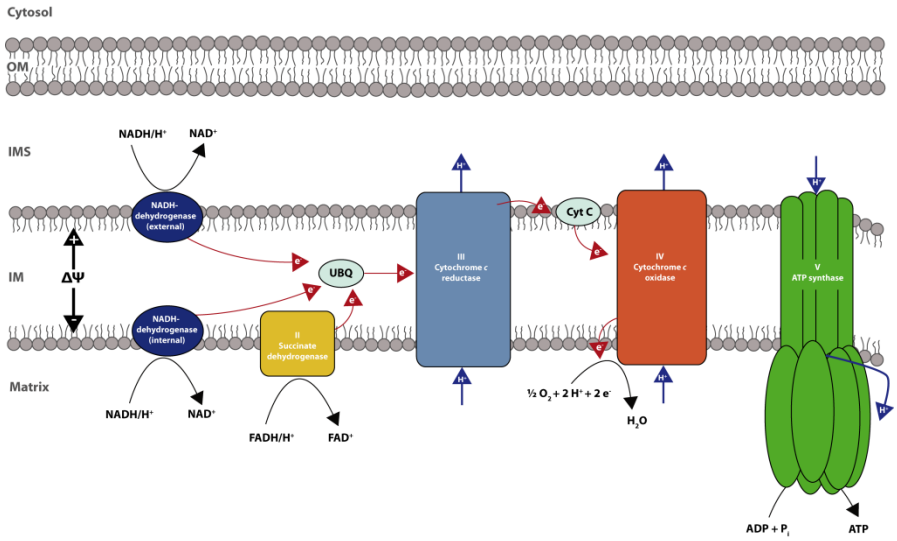

Figure 1.2: Schematic representation of the oxidative phosphorylation system in the yeast *S. cerevisiae*
Schematic representation of the NADH-dehydrogenases, the respiratory complexes (II-IV), the F_1F_0-ATPase (V), the mobile electron carrier ubiquinone (UBQ) and cytochrome *c* (cyt C) in the inner mitochondrial membrane (IM). Electron flux (e^-) is shown in red, proton flux (H^+) is shown in blue. Electrons are transferred from UBQ to complex III and further shuttled via CytC to complex IV ultimately to be reduced to water. During electron transport, complexes III and IV pump protons from the matrix trough the inner membrane (IM) into the intermembrane space (IMS), thereby generating an electrochemical proton-gradient. OM: outer mitochondrial membrane.

1.1.3 Mitochondrial protein translocases

As mitochondria are involved in numerous cellular processes (see 1.1.2), a huge number of proteins are required to fulfill all their tasks. Recent studies revealed that the

proteome of the *S. cerevisiae* mitochondria contains approximately 1.000 proteins (Sickmann et al. 2003; Prokisch et al. 2004; Reinders et al. 2006), while the mammalian counterpart contains around 1.500 proteins (Foster et al. 2006). The vast majority of mitochondrial proteins (> 99%) are encoded within the nuclear DNA. They are synthesized in the cytosol and post-translationally transported into the organelle. Transport is mediated by sophisticated protein translocases regulating precursor protein import and sorting into the different mitochondrial sub compartments (Figure 1.3). It can be assumed that all the different import pathways as well as the export pathway, which mediates the transport of the mitochondria encoded proteins from the matrix side into the IM, (see 1.2.3) are highly adapted to the requirements of the organelle. However, current knowledge on mitochondrial transport pathways mostly derived from analyses of the import machineries, which are therefore much more precisely described than the export machinery.

The import is driven either by membrane potential, ATP, or redox reactions (Chacinska et al. 2009). To reach their final destinations, mitochondrial precursor proteins carry targeting signals, which are recognized by different receptor proteins. These mitochondrial targeting signals are diverse and can be located in various positions within the sequence (Rehling et al. 2004; Mokranjac et al. 2009). The best-described targeting signal is an N-terminal amphipathic α-helix of approximately 10 to 80 amino acids, also known as a presequence. This presequence predominantly destines the particular pre-protein to the mitochondrial matrix, but also directs a small number of proteins to the inner membrane or intermembrane space.

Many mitochondrial proteins contain non-cleavable, internal targeting signals, which can be distributed over the entire precursor protein. This is typical for outer membrane proteins, but can also be found in many intermembrane or inner membrane proteins (Rapaport 2003; Bolender et al. 2008). These signals are still poorly characterized; however, Kutik et al. (2008) have identified a C-terminal sorting signal specific to mitochondrial ß-barrel proteins, which mediates a two-stage insertion mechanism into the outer mitochondrial membrane.

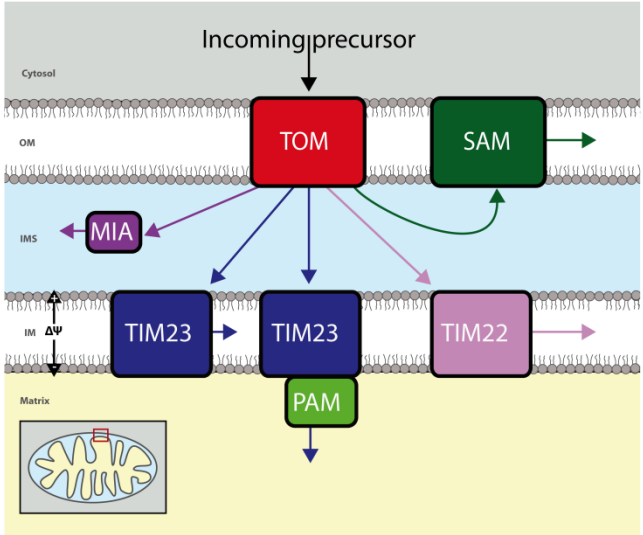

Figure 1.3: Mitochondrial protein pathways
Proteins destined for the mitochondrion, termed precursors until they reach their correct location, utilize the Translocase of the Outer Membrane (TOM) to cross the organelle. Afterwards they can use the SAM complex (sorting and assembly machinery) to enter into the outer membrane or the Translocases of the Inner Membrane (TIM), TIM23 and TIM22, to assemble into or to cross the inner membrane (IM), respectively. Import of cysteine-motif containing proteins into the inter membrane space (IMS) is organized by MIA (mitochondria intermembrane space import and assembly).

1.1.3.1 Protein import complexes of the outer mitochondrial membrane

TOM complex

Acting as a central entry gateway, TOM complex deciphers the targeting signals and determines the following import pathway of the majority of all nuclear encoded mitochondrial proteins destined for the inner membrane, intermembrane space or matrix. The translocase of the outer membrane is composed of seven distinct proteins which form a high molecular weight complex (Meisinger et al. 2001). Tom20, Tom22 and Tom70 are the receptor proteins, which recognize incoming mitochondrial proteins and guide them as unfolded polypeptide chains through the pore component, Tom40 (Model et al. 2008). Three small Tom proteins, Tom5, Tom6 and Tom7, regulate the assembly and stability of the complex (Model et al. 2001). After passing through the TOM complex, the precursor protein can follow one of the five major pathways to reach its final location (Figure 1.4).

SAM complex

The outer mitochondrial membrane contains numerous ß-barrel proteins, which are translocated and assembled into the outer membrane by the SAM (Sorting and assembly machinery of the outer membrane) complex.

After passing the TOM complex, the ß-barrel precursor proteins are transferred into the intermembrane space to the chaperone complexes Tim9-Tim10 and Tim8-Tim13. Subsequently they are guided to the SAM complex, in order to be inserted into the outer membrane (Wiedemann et al. 2003; Zeth 2010).

The core channel subunit of the complex is a ß-barrel protein termed Sam50 (Kozjak et al. 2003). During protein import it interacts with two receptors, Sam35 and Sam37, which have domains expose into the cytosol. In order to insert incoming precursor proteins into the outer membrane, Sam50 interacts with Sam35, while its interaction with Sam37 accomplishes the precursor to be released into the outer membrane (Milenkovic et al. 2004; Chan et al. 2008) (Figure 1.4).

1.1.3.2 Protein import into the mitochondrial intermembrane space

The MIA machinery consists of a disulfide relay system driving the import of a specific class of cysteine containing proteins into the mitochondrial intermembrane space, which utilizes an oxidative folding mechanism. All substrates contain conserved cysteine residues arranged in a typical twin Cx(3)C or Cx(9)C motif forming disulfide bonds and/or binding metal ions (Chacinska et al. 2008; Hell 2008). The key components of the disulfide relay system are the redox-regulated import receptor Mia40 and the sulfhydryl oxidase Erv1, which interact via disulfide bonds (Hofmann et al. 2005; Chacinska et al. 2008; Terziyska et al. 2009).

Like most of the mitochondrial proteins, small IMS proteins are synthesized on the cytosolic ribosomes and subsequently enter mitochondria through the TOM complex. They pass the outer membrane in reduced form and upon entering the IMS they can interact with Mia40. Mia40 exists in two different states, oxidized and reduced, while only the oxidized form can interact with substrates. Mia40 donates disulfide bonds to the substrate through a transient disulfide intermediate, which allows substrate- folding and -retention in the IMS. After having released the substrate, Mia40 is in a reduced, inactive form, hence incapable to react with new substrate. In order to

enable a new round of substrate oxidation, Erv1 facilitates oxidation and therefore activation of Mia40 (Chacinska et al. 2008; Hell 2008). In turn, Erv1 is oxidized through donation of electrons to the cytochrome *c* of the respiratory chain (Allen et al. 2005) (Figure 1.4)

1.1.3.3 Protein import complexes of the inner mitochondrial membrane

Import across or into the inner membrane is achieved by two different translocases, TIM22 and TIM23. While the latter mediates translocation of preproteins across and their insertion into the mitochondrial inner membrane, the TIM22 complex is specialized in the insertion of polytypic proteins into the inner membrane.

The TIM23 complex can be found in two different forms: $TIM23_{SORT}$ for inner membrane insertion and $TIM23_{MOTOR}$ for protein translocation into the matrix (Chacinska et al. 2010). The core of both TIM23 complex forms consists of three membrane embedded proteins: Tim17, Tim23 and Tim50.

Tim23 exposes its N-terminus to the intermembrane space to interact with incoming polypeptides (Bauer et al. 1996), whereas Tim17 plays an important role in lateral protein sorting into the inner membrane and interacts also with Pam18, a component of the PAM complex (Chacinska et al. 2005).

The intermembrane space domain of Tim50 induces TIM23 channel closure in a precursor dependent manner. This mechanism prevents ion leakage across the inner membrane and stabilizes the tightly regulated electrochemical gradient across the inner membrane (Meinecke et al. 2006; van der Laan et al. 2006) (Figure 1.4).

$TIM23_{Motor}$ complex

During protein translocation into the mitochondrial matrix, the PAM complex (presequence translocase associated motor) interacts with the membrane embedded part of the TIM23 complex and forms the $TIM23_{MOTOR}$ form of the translocase (Chacinska et al., 2005). PAM is a multi-subunit protein complex containing six components: mtHsp70 (Ssc1 in yeast), Tim44, Mge1, Pam16, Pam17 and Pam18 (Figure 1.2).

During protein translocation, Tim44 recruits mtHsp70 to the import channel. Mt-Hsp70 is an essential subunit of the PAM complex. It associates with the polypeptide in transit and exerts an import-driving activity on incoming polypeptides via a cycle of

ATP binding and hydrolysis (Voisine et al. 1999; Geissler et al. 2000; Gebert et al. 2010). Its activity is regulated by two other members of the PAM complex: Mge1 and Pam18. The nucleotide exchange factor Mge1 regulates ADP releasing and ATP binding cycles from Hsp70 (Miao et al. 1997), whereas Pam18's J-domain stimulates its ATPase activity (Truscott et al. 2003). Pam16 antagonizes Pam18's function (Li et al. 2004), and together they form a heterodimer known as the J-complex. The integrity of the J-complex is maintained by Pam17, which stabilizes also the interaction between TIM23 and PAM complexes by interacting with Tim23 (van der Laan et al. 2005; Hutu et al. 2008).

Once the precursor-protein reaches the matrix, its presequence is cleaved by the matrix-processing peptidases (MPP) generating the mature protein (Taylor et al. 2001).

$TIM23_{SORT}$ complex

For the insertion of preproteins into the mitochondrial inner membrane the TIM23 complex releases the PAM complex and recruits an additional protein, Tim21. This form of the complex is known as $TIM23_{SORT}$ (Wiedemann et al. 2007) and mediates the import of precursor proteins containing an additional hydrophobic sorting signal. Tim21 promotes reorganization of the complex and interacts with the mitochondrial respiratory chain supercomplex consisting of complexes III and IV. It is proposed that this interaction stimulates preprotein insertion into the inner membrane (van der Laan et al. 2006; Wiedemann et al. 2007) (Figure 1.4).

TIM22 complex

Polytopic inner membrane proteins such as mitochondrial carrier proteins are transported and inserted into the inner membrane by the TIM22 complex. It consists of three inner membrane proteins, namely Tim18, Tim22, and Tim54, as well as three peripherally associated proteins, Tim9, Tim10, and Tim12 (Rehling et al. 2003). The import of hydrophobic metabolite carriers into the mitochondrial inner membrane has been divided into five stages. In stage I the precursors of hydrophobic metabolite carriers are guided by cytosolic chaperones to finally reach the receptor protein Tom70 (stage II). The precursors cross the TOM complex in a loop formation. In the IMS, Tim9 and Tim10 guide the precursor to the TIM22 complex to prevent its aggregation (stage III). Subsequently, Tim9 and Tim10 interact with Tim12 and associate with Tim54,

enabling the precursor to dock into the TIM22 complex (stage IV) (Figure 1.4). Actual membrane insertion of the precursor occurs in two steps, promoted by energy from the membrane potential (Rehling et al. 2003). The insertion is completed when the inserted protein assembles into a dimer (stage V); however, this release process is still ill-defined (Wagner et al. 2008).

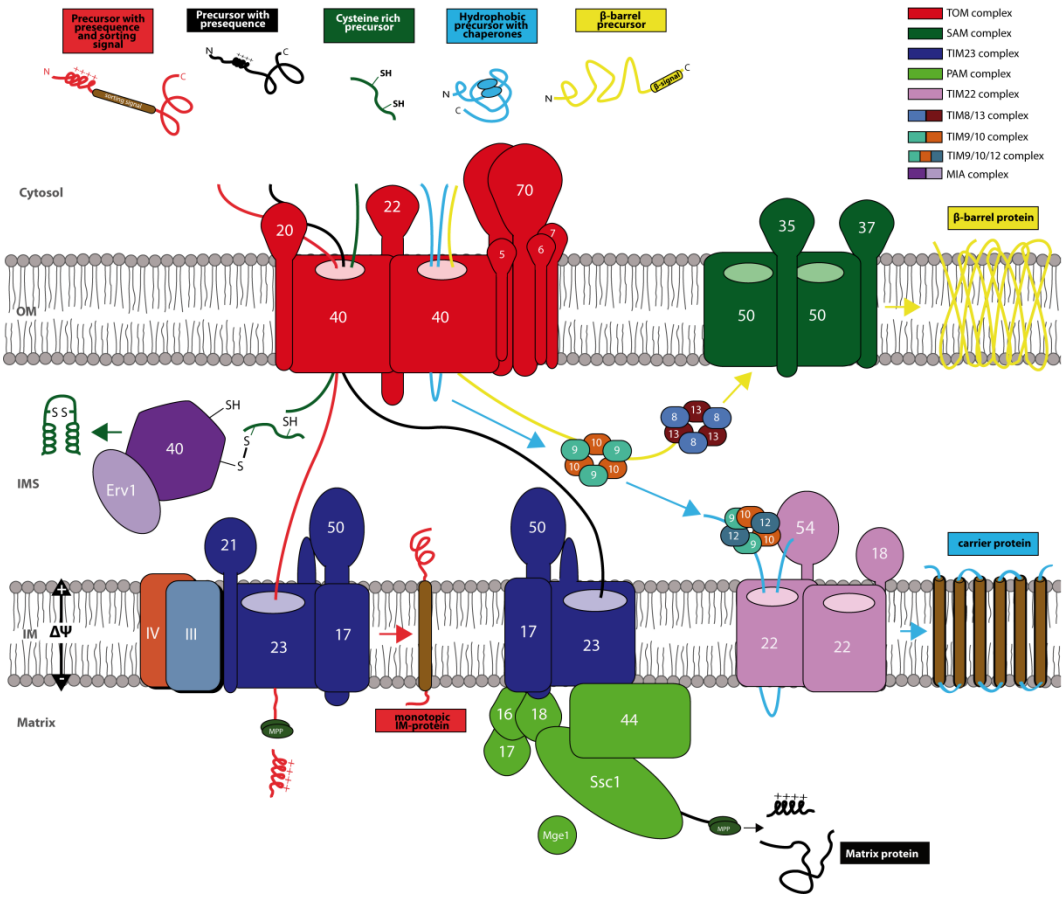

Figure 1.4: The main mitochondrial protein import pathways in mitochondria
Protein transport across the outer membrane (OM) is achieved via the TOM complex (red). The SAM complex mediates the insertion of outer membrane proteins. Import of cysteine-motif containing proteins into the inter membrane space is organized by MIA. The TIM23 complex mediates membrane insertion of monotopic membrane proteins into the inner membrane and cooperates with the PAM complex for the translocation of presequence containing proteins into the matrix. Inner membrane carrier proteins are transported and integrated into the inner membrane by the TIM22 complex.

1.2 Mitochondrial protein-biosynthesis machinery

The mitochondrial protein-biosynthesis machinery is a sophisticated system adapted to the specific requirements of mitochondria in different organisms. This chapter will mainly focus on the characteristics of the protein-biosynthesis machinery (particularly the mt-translation machinery) in the model organism used in the present work, the baker's yeast *S. cerevisiae.*

1.2.1 Mitochondrial genome

Ever since the 1960s, when mitochondrial DNA was discovered, it has been clear that due to its wide range of variations, mtDNA is not comparable to bacterial or eukaryotic nuclear DNA. When human and bovine mtDNA were compared, one major difference was discovered to be, that mitochondria's genetic code is not universal but, to the contrary, differs between species (Hudspeth et al. 1982). Moreover, both the termination and initiation codons were shown to be distinct from those used by prokaryotic or eukaryotic cytoplasmic translation machineries. Interestingly there are species-specific differences within the mtDNAs as well, or even different mt-genomes within one single cell, caused by mutations. Therefore it is difficult to summarize all differences. Compared to its ancestor, the mitochondrial genome is considerably reduced in size and oftentimes encodes no more than mitochondrial tRNAs, rRNAs, as well as a few additional proteins (Burger et al. 2003). In fact, the size of the mitochondrial genome significantly varies between organisms, e.g. the human mitochondrial genome encodes for 13 proteins, whereas the mitochondrial genome of *S. cerevisiae* encodes for only eight. Foury et al. (1998) published the first complete sequence of a mitochondrial genome, namely of the *S. cerevisiae* strain FY1679. Before then, only partial sequences had been derived from a dozen different *S. cerevisiae* backgrounds. The full sequence was assembled into a circular map of 85.779 base pairs (bp) and 19 ORFs were identified, encoding for 11 common and 8 hypothetical proteins. Seven of the common ORFs encode for core subunits of the respiratory chain complexes, i.e. cytochrome *b* of the cytochrome *c* reductase as well as Cox1, Cox2, Cox3 of cytochrome *c* oxidase (COX) and Atp6, Atp8 and Atp9 of the F_1F_o-ATPase. All these proteins are known to be very hydrophobic and it is widely believed that therefore their mitochondrial genes remained in the matrix rather than being transferred to the

nucleus. It is believed that in order to avoid aggregation, newly synthesized peptides are directly inserted into the inner membrane following or even during translation (for further details see section 1.2.3). Besides the seven hydrophobic membrane proteins, Var1 is the only mitochondria encoded matrix protein. It is assembled into the small ribosomal subunit and postulated to be involved in the assembly of the mitochondrial ribosome (Terpstra et al. 1979; Terpstra et al. 1979; Fiori et al. 2003) (Figure 1.5).

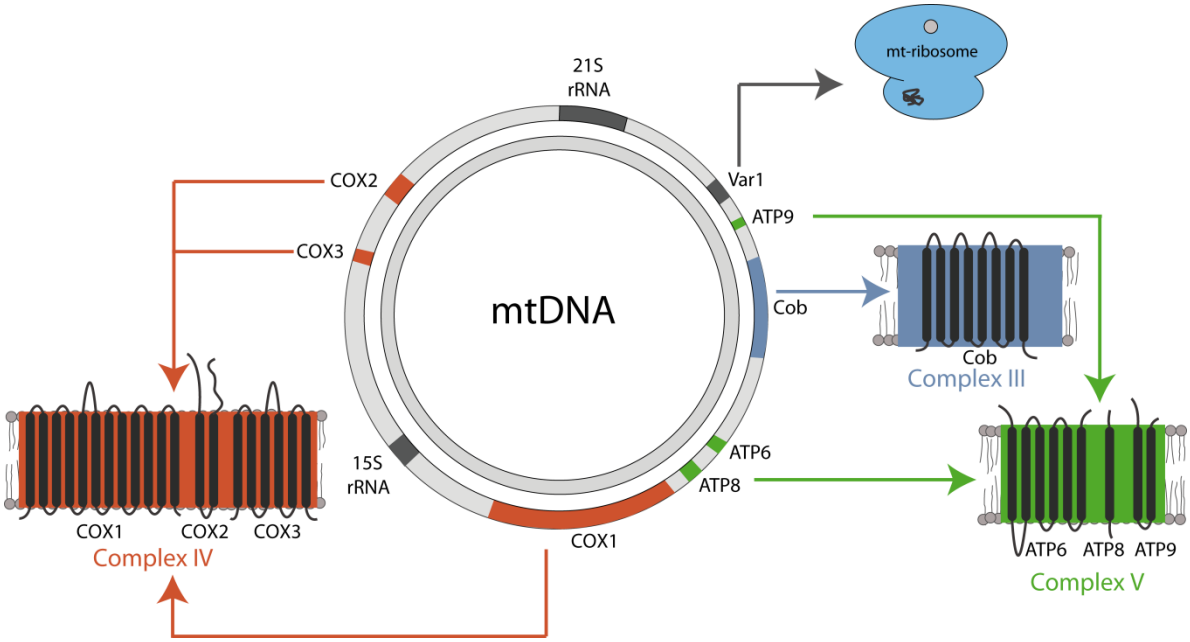

Figure 1.5: Overview of the mitochondrial genome in the yeast *S. cerevisiae*
S. cerevisiae mtDNA encodes eight polypeptides as well as 15S and 21S rRNA. Seven of the polypeptides are subunits of the respiratory chain complexes (topology is illustrated in dark grey). The eighth one, termed Var1, is a component of the small ribosomal subunit.

Although mitochondrial DNA is preferentially depicted as a circular map, circular molecules represent only a small fraction of isolated mtDNA, and *in vivo*, the population may in fact consist of long linear concatemers, as shown by pulsed field gel electrophoresis (PFGE). The linear monomer of a mt-yeast genome (approx. 75 kb) measures 25µm in length and is compacted into a globular nucleoid structure with an average diameter of approximately 0.3 µm in aerobic cells (Chen et al. 2005). It was suggested that the replication of *S. cerevisiae* mtDNA occurs via rolling circle mechanism as evidenced for the yeast *Torulopsis glubrutu* by electron microscopy (Maleszka et al. 1991). Unfortunately, since there is no *in vitro* system available to study replication, the hypothesis of *S. cerevisiae* duplicating by rolling circle mechanism cannot yet be verified (Grivell 1995).

1.2.2 Mitochondrial ribosomes

Mitochondrial ribosomes (also referred to as mt-ribosomes) are perfectly adapted to the requirements of the mitochondrial translation machinery. Therefore, in *S. cerevisiae* they are tightly associated to the inner mitochondrial membrane in order to ensure translation of polypeptides close to their insertion site on the inner membrane (Marzuki et al. 1986). They consist of two different RNA-molecules and mitochondrial ribosomal proteins (MRPs). Although the mt-ribosome shows similar sensitivity to antibiotics as its eubacterial ancestor (sensitivity to chloramphenicol, and insensitivity to cycloheximide), only a minority of all MRPs show similarity to any cytoplasmic or *E. coli* counterpart (Scheffler 1999). Moreover, most of these proteins contain additional domains, making them considerably larger than their counterparts (Sharma et al. 2003; Smits et al. 2007). Various approaches including sequence analysis, genetic complementation, one or two dimensional (2D-) PAGE, purification and amino-acid sequencing revealed up to 77 MRPs; at least 50 of which belong to the large ribosomal subunit (Kitakawa et al. 1997; Lee et al. 2002). Graak and Wittmann-Liebold (1998) estimated an even higher number of mitochondrial ribosomal proteins. They speculated that differences in staining and migration of the individual proteins as well as choice of PAGE method could affect the analyses and thereby assumed that the actual mitochondrial ribosome contains approximately 100 proteins.

In general, yeast mitochondrial ribosomes exhibit a higher protein to nucleic acid ratio compared to their eubacterial counterparts. It was also revealed that *E. coli* ribosomes contain proteins and RNAs in a mass ratio of 1 : 2, whereas in yeast mitoribosomes this ratio is increased to 1 : 1 (Graack et al. 1998) and even up to 2 : 1 in bovine mitoribosomes (O'Brien 2003). The increase in protein ratio was followed by a decrease of rRNA. *S. cerevisiae* ribosomes contain two RNA species: 15S (S= sedimentation-coefficients) rRNA and 21S rRNA. These resemble *E. coli´s* 16S rRNA and 23S rRNA. However, *E. coli* additionally has 5S rRNA, which is absent in yeast. Also, due to the loss of secondary structural elements, the mitoribosomal rRNAs are significantly shorter.

It remains elusive why the mitochondrial ribosome, despite only synthesizing eight proteins itself, contains a perplexing quantity of proteins. Gene disruption and other mutations were able to support the concept that most of the unique mitochondria

encoded proteins are essential to the stability of mitochondrial DNA. Interestingly, those MRPs that have bacterial counterparts and do not seem to be essential for bacterial ribosomal functions are the ones indispensable in yeast mitochondria (Graack et al. 1998). It seems that, dependent on the species, mitochondrial ribosomes exhibit wide variation in their features as well as the number and properties of their constituents (Graack et al. 1998). They vary in sedimentation-coefficients (*s*) between 55S and 80S (Kitakawa et al. 1991) and molecular masses between 2.5 and 3.6 MDa (Smits et al. 2007). The mitochondrial ribosome of yeast has a sedimentation-coefficient of 74S, which is composed of the 54S and 37S subunits.

Despite the quantity of examples demonstrating the differences in composition of bacterial and mitochondrial ribosomes, it could be shown that at least one part has been conserved from bacteria to mitochondria. It is arguably the most important part within the ribosome, namely the catalytic center. The mitochondrial proteins and rRNA domains which contribute to decoding and peptide bond formation share high degrees of homology with their bacterial counterparts (Ott et al. 2010).

First structural data on mitochondrial ribosomes could be obtained via cryo-electron microscopy (cryo-EM) of the 55S bovine mitochondrial ribosome. Unlike other ribosomes, it revealed a highly porous structure (Sharma et al. 2003). Unfortunately, at a resolution of 13.5 Å, further sub-mitochondrial localization of proteins was not feasible; therefore this approach could not provide further insight as to the exact composition of proteins within the mt-ribosome. Interestingly, however, the structural analysis revealed that mitochondrial bovine ribosomes have an additional opening next to the ribosomal polypeptide exit tunnel (RET), termed polypeptide accessible site. Whether this region really does form a tunnel or simply represents a region of low electron density is unclear, but it was speculated that such a tunnel might be used by a subset of proteins for their interaction with specific biogenesis factors (Ott et al. 2010). Chemical cross-linking, combined with mass-spectrometry revealed that the mitochondrial ribosomal proteins Mrpl3, Mrpl13 and Mrpl27 as well as the ribosome receptor Mba1 are located in close proximity to the RET. The RET is unique in architecture and composition (Gruschke et al. 2010), presumably due to those MRPs found exclusively around the RET of mitochondrial ribosomes. These MRPs and their homology to bacterial ribosomal proteins (*S. cerevisiae* Mrpl22, Mrp20, Mrp40, Mrpl4 are homologous to *E. coli* L22, L23, L24 and L29, respectively) suggest, that similar to the

whole ribosome, the RET has been modified considerably throughout evolution as well.

The exact function of the MRPs is unknown, but they are presumed to either provide assembly and stabilization for the ribosome or to compensate for the loss of rRNA. It is very probable that some are involved in the unique mitochondrial translation system ensuring that the ribosome is assembled to the inner membrane. However, only future research will help understanding the functional implications of their existence.

1.2.3 Mitochondrial protein export machinery

Co-translational insertion of mitochondria encoded proteins from the matrix site into the inner membrane is mediated by the OXA1 complex. This complex is still ill-defined compared to other mitochondrial complexes. The central component of the export machinery is the Oxa1 protein. It was initially detected in genetic screens searching for components involved in the assembly of cytochrome *c* oxidase (Oxidase assembly mutant 1) (Bonnefoy et al. 1994, Bauer et al. 1994). The OXA1 translocase is an interesting example of conservation of translocase machinery during evolution (Kutik et al. 2009). Bacteria and chloroplasts were shown to contain proteins, namely YidC and Alb3, which are homologous to Oxa1. Therefore, they are all considered members of the "YidC/Alb3/Oxa1 family". All three are involved in membrane insertion of newly synthesized proteins (Funes et al. 2011). Each contains five hydrophobic transmembrane spans able to substitute for one another (Funes et al. 2004; Preuss et al. 2005; van Bloois et al. 2005; Funes et al. 2009). X-ray scattering of YidC crystals and cryo-EM of recombinant Oxa1 support the hypothesis of the dimeric nature of both proteins. This dimeric structure could lead to the formation of a protein translocase channel and would also enable lateral protein release into the membrane (Nargang et al. 2002; Kohler et al. 2009).

Besides the aforementioned five transmembrane spans, Oxa1 consists of a unique C-terminal extension of roughly 100 positively charged amino acids, which faces the mitochondrial matrix. Additionally, the protein possesses a smaller loop between transmembrane segments one and two, which also extends into the matrix. It was shown that Oxa1 binds to the mitochondrial ribosome via its C-terminal extension and facilitates translocation and lateral exit of mt-encoded protein to the lipid bilayer (Jia et al. 2003). This interaction is likely indicated by the opposing charges of the positively

charged α-helical domain of Oxa1 and negatively charged RNA, and is further supported by the smaller loop of Oxa1 interacting with the mt-ribosome (Figure 1.6).

Various approaches confirmed the association of Oxa1 with the mitochondrial ribosome. Using low-salt sucrose gradients, Bonnefoy et al. (2009) demonstrated that the C-terminal domain of Oxa1 is important for its co-fractionation with mitochondrial ribosomes. Physical interaction of Oxa1 and mt-ribosome was additionally supported by RNAse treatment, which led to the disintegration of the ribosomes and prevented the co-migration of Oxa1 and mt-ribosomes on sucrose gradients (Ott et al. 2006). Chemical cross-linking revealed a binding site of Oxa1 to the large ribosomal subunit. The protein bound in direct proximity to Mrpl40 and Mrp20, two components of the large ribosomal subunit, located next to the RET (Jia et al. 2009).

The physical association of Oxa1 and the ribosome is important for the insertion of the newly synthesized proteins but the protein is not involved in the regulation of translation. Treatment with puromycin (an inhibitor of translation via premature nascent chain release) did not affect the cross-linking efficiency of Oxa1 to the ribosome (Jia et al. 2003; Ott et al. 2006).

Interestingly the OXA1 translocase is not only specialized in the transport of mt-encoded proteins, but also facilitates export from the matrix side and insertion of nuclear encoded proteins into the inner membrane (Bohnert et al. 2010). Presumably, membrane protein domains that do not sort laterally through the TIM23 complex are dependent on this mechanism. This route seems to have evolved from the insertion process of the bacterial ancestors and was therefore named the “conservative sorting” pathway (Hartl et al. 1986). Import of Oxa1 itself has been shown to be dependent on this pathway (Herrmann et al. 1997). Oxa1 is a nuclear encoded protein, which is synthesized with a presequence in the cytosol and transported into the matrix. After cleavage of the presequence, the N-terminus and the first TM are exported across the inner membrane into the intermembrane space. The additional four TMs are inserted pairwise to achieve a N_{out}-C_{in} topology within the inner membrane.

The role of Oxa1 in the export of mitochondrial-encoded proteins into the inner membrane, with regards to Cox2, has been shown to be strictly dependent on the translocase (He et al. 1997, Hell et al. 1997). The other mitochondria encoded translation products integrate into the inner membrane only with reduced efficiencies in the absence of Oxa1. Considering this, Oxa1 likely cooperates with other proteins or

components in order to ensure an optimal insertion process. The two most important proteins, which have already been shown to support Oxa1 in its function, are Cox18 and Mba1. Cox18 is a mitochondrial Oxa1 homologue and a member of the YidC/Alb3/Oxa1 family, but derived from a different subfamily (Bonnefoy et al. 2009). Like Oxa1, Cox18 (termed Oxa2 in *Neurospora crassa*) is an integral inner membrane protein with five transmembrane segments and exhibits a N_{out}-C_{in}–topology. However, it lacks a C-terminal ribosome-binding site. It is uncertain why mitochondria contain two distinct members of the export family. Although in different stages during insertion, both Cox18 and Oxa1 are specifically required for insertion of Cox2 (Saracco et al. 2002). Cox2 contains two transmembrane spans with a large hydrophilic C-terminal domain (144 aa) and a short N-terminal domain (26 aa), both located on the intermembrane (*trans*) side of the inner membrane (see Figure 3). In yeast, its N-terminus contains a 15 amino acids leader peptide, which initiates membrane insertion by Oxa1 (He et al. 1997), whereas the C-terminal domain is translocated by Cox18 in a membrane potential dependent manner (Fiumera et al. 2007).

Besides Cox18, Mba1 was shown to support Oxa1 in its function. It is a nuclear encoded 26 kDa protein, peripherally attached to the inner mitochondrial membrane (Preuss et al. 2001). Mba1 (Multicopy bypass of AFG3 mutant 1) was described as a multicopy suppressor of a mutant lacking Yta10 (Afg3; m-AAA-protease), together in one screen with Oxa1 (Saint-Georges et al. 2001). Yta10 is involved in protein homeostasis control and mediates degradation of misfolded or unassembled proteins.

Mba1 was suggested to act as a receptor for mitochondrial ribosomes (Ott et al. 2006). The protein binds to the large ribosomal subunit in proximity to the RET and ensures the RET's direct alignment with the insertion machinery of the inner membrane. Deletion of Mba1 alone leads to a weak growth phenotype on non-fermentable carbon source, but simultaneous deletion of Mba1 and Oxa1 C-terminal domain cause a dramatic respiration-deficient phenotype. Moreover, co-translational membrane insertion of newly synthesized mitochondria encoded proteins is severely impaired in *mba1Δ/oxa1ΔC* mitochondria and translation products are found in association with matrix chaperone Hsp70 (Ott et al. 2006). In conclusion, Oxa1 and Mba1 cooperate to position the ribosome polypeptide exit tunnel to the proper site of the inner membrane (Figure 1.6).

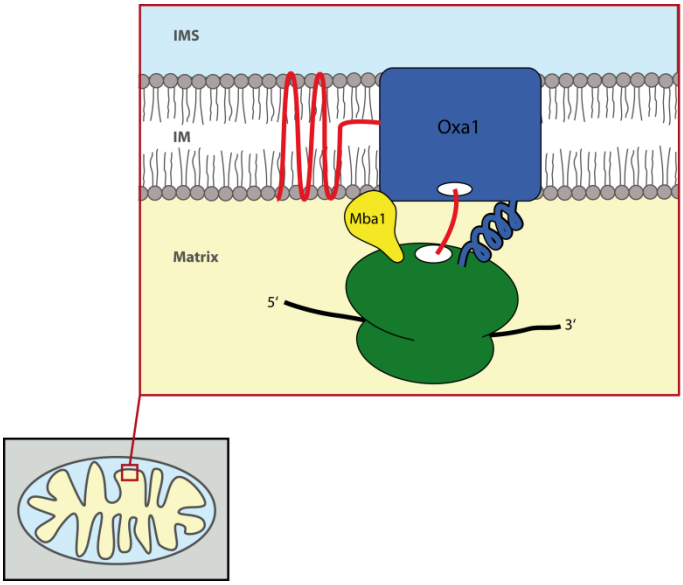

Figure 1.6: Functional model of co-translational protein insertion into the inner membrane of mitochondria
Oxa1 binds with its C-terminal domain close to the mt-ribosomal polypeptide exit tunnel to ensure translocation of newly synthesized mt-encoded polypetides into the inner mitochondrial membrane (IM) directly after they emerge from the polypeptide exit tunnel. Mba1 acts as a ribosome anchor. It tethers the ribosome in close proximity to the IM and supports Oxa1 in its function. IMS: mitochondrial inter membrane space.

1.2.4 Mitochondrial translation

A small number of genes encoded by mtDNA are transcribed and translated within the organelle. In yeast, seven of the eight mitochondrial translation products interact with the nuclear encoded polypeptides to form the complexes of the respiratory chain (Steele et al. 1996). The translation of mitochondria encoded proteins in yeast occurs on the matrix side of the inner mitochondrial membrane. This ensures an optimal co-translational insertion of nascent, hydrophobic pre-proteins into the inner membrane immediately after their emergence from the ribosomal polypeptide exit tunnel. The translation apparatus itself has been documented for years; however, a functional *in vitro* mitochondrial translation system is yet to be devised, making it impossible to achieve advanced characterization of the system. Knowledge pertaining to the functionality of mitochondrial translation was obtained exclusively by the characterization of individual components in addition to *in vivo* and *in organello* analyses of the translation system. Several fundamental components of mitochondrial translation (mostly studied in yeast), have been identified up to now: the translation

initiation factor IF-2 (Vambutas et al. 1991) and its supporting proteins Rsm28 (Williams et al. 2007) and AEP3 (Lee et al. 2009). Three elongation factors mEF-Tu, mEF-G1/G2 (Nagata et al. 1983; Vambutas et al. 1991), the termination factor mRF-1 (Pel et al. 1992; Towpik et al. 2004), as well as the mitochondrial ribosome recycling factor Rrf1 (Teyssier et al. 2003).

S. cerevisiae benefits from a unique and highly specific translation regulatory system. Translation of mitochondrial mRNAs encoding subunits of respiratory chain complexes requires dedicated translation activator proteins with the ability to recognize the 5′ untranslated leader sequences (UTLs) of their cognate mRNAs (Mick et al. 2011). These activator proteins regulate the translation initiation process by binding to the 5'-UTLs of mitochondrial mRNAs and positioning the ribosomes to the specific initiation codon (Fox 1996). Seven of the eight mitochondria encoded proteins in yeast have been shown to be dependent on specific translation activators, albeit only five have been extensively analyzed (Table 1.1).

mRNA of	Translation activator	Reference
COB	Cbs1p; Cbs2p Cbp6p Cbp1p	(Rodel 1986) (Dieckmann et al. 1985) (Dieckmann et al. 1982)
COX1	Pet309p Mss51p	(Manthey et al. 1995) (Siep et al. 2000)
COX2	Pet111p	(Poutre et al. 1987)
COX3	Pet54p; Pet122p; Pet 494p	(Costanzo et al. 1988)
ATP9	Aep1p Aep2p	(Payne et al. 1993) (Finnegan et al. 1995)

Table 1.1: Overview of the best-studied mRNA translation activator proteins in the yeast *S. cerevisiae*.

Besides their role in translational activation, the translation activators, as indicated above, serve other purposes, such as regulating both the location and level of translation, as well as stabilizing the mt-mRNAs (Manthey et al. 1995). Their position within the inner mitochondrial membrane allows for direct mediation of translation, insertion, and the assembly of mitochondrial gene products to their defined insertion sites within the inner membrane (Naithani et al. 2003). Furthermore, they indirectly

modulate the level of translation of the individual mt-mRNAs, as the quantity of the nuclear encoded translation activators itself is regulated in response to functional states of the mitochondrion (see 1.2.3.1).

Mitochondrial translation seems to be highly organized and precisely regulated, as many of the translation activators establish a regulatory network by mutual interaction. This behavior has been observed for all three *COX3*-specific activators (Pet54, Pet122, Pet494) forming a complex to mediate the interaction of the COX3 mRNA with mitochondrial ribosomes on the surface of the inner membrane (Brown et al. 1994). Moreover, Pet309 (*COX1*) interacts with all three *COX3* activator proteins, while Pet111 (*COX2*) interacts with Pet54 (*COX3*) and Pet494 (*COX3*), suggesting that synthesis of Cox1, Cox2, and Cox3 must be co-localized in a way that facilitates the assembly of the core of complex IV (Naithani et al. 2003). The interaction of translational activators, however, is not limited to distinct complexes (e.g. of cytochrome *c* oxidase), as the analysis of a high molecular weight complex (approx. 900 kDa) revealed *COB* mRNA activators Cbp1, Cbs1, Cbs2 as well as *COX1* mRNA activator Pet309 to be components of the complex (Krause et al. 2004).

Nevertheless, the specialized translational activation system is not the only adaption to the requirements of the genetic system in yeast mitochondria. Yeast mitochondrial mRNAs also display unique characteristics. They are uncapped (Christianson et al. 1983), and lack conventional poly(A) tails (i.e. posttranscriptionally added) (Moorman et al. 1978) as well as a typical Shine-Dalgarno sequence (Grivell 1989). However, most unusual and unique are their long untranslated 5'-leader sequences (UTLs), which are recognized by the translation activator proteins. Their size varies from 54 nucleotides (*COX2*) to 954 nucleotides (*COB*), and they are rich in adenosine and uracil (Fox 1996). Little is known about the target sequences within the 5'-UTLs and about their ability to guide the ribosome to the translation initiation site. Presumably, yeast mitochondrial ribosomes recognize a common feature in mRNA 5'-UTLs. A putative candidate for such a consensus sequence is the octanucleotide UAUAAAUA, which was identified by functional analysis of COX2 mRNA 5'-UTL with other 5'-UTLs (Dunstan et al. 1997). This octanucleotide is complementary to several sites in the small mitochondrial subunit rRNA and could be involved in mRNA-rRNA base pairing (Green-Willms et al. 1998). Indeed, different studies also show that some small ribosomal subunit proteins are involved in the translation activation pathway

(McMullin et al. 1990; Green-Willms et al. 1998), where they work in conjunction with mRNA-specific activators to recognize targets in mRNA 5'-UTLs (Fox 1996). Most of these proteins are not conserved in other systems and belong to the unique group of mt-ribosomal proteins specifically adapted to the mitochondrial genetic system (see also 1.2.2).

As a further adaption, the mitochondrial genome of *S. cerevisiae* was shown to contain „optional introns". These type I and II introns are found in the genes encoding 21S rRNA, cytochrome *b* (*COB*) and Cox1 (*COX1*). Their number differs within different yeast strains. For instance, the *COB*-gene exists both in a short form containing 2 introns (bl4; bl5), and in a long form, containing 5 introns (Lazowska et al. 1980; Labouesse et al. 1984). Some introns encode for activities for their own removal, which are required for splicing and their mobility (Grivell et al. 1989; Keating et al. 2010). These optional introns account for a substantial part of the size variations in mtDNAs (Scheffler 1999).

1.2.4.1 Regulation of mitochondrial translation

In *S. cerevisiae*, mitochondrial respiratory complex assembly is highly regulated on the translational level. However, the functionality of translation activators could only be thoroughly described for the biogenesis of yeast mitochondrial *COX1* gene (encoding subunit I of the cytochrome *c* oxidase). *COX1* translation has been shown to be directly coupled to complex IV assembly. Translation of *COX1* mRNA is initiated by the translation activators Pet309 and Mss51 (Perez-Martinez et al. 2003; Barrientos et al. 2004). However, although these two proteins play a similar role in *COX1* translational activation, they remain distinct in almost all other functional aspects. Pet309 contains seven pentatricopeptide repeats (PPRs) located within the central part of the protein. This motif has been suggested to face a central cavity, which was postulated to be involved in mRNA-binding (Tavares-Carreon et al. 2008). Indeed, it was shown that all the seven PPRs present in Pet309 are necessary for *COX1* mRNA translation, but are expendable in terms of the mRNA stability function of Pet309.

The second *COX1*-specific translation activator, Mss51, does not contain any common motifs or structure elements. Furthermore, its functionality differs from other translation activators; it has namely been shown to be involved in more than merely translation activation. Mss51 interacts with the 5'-UTL of *COX1* mRNA (Zambrano et al.

2007), as well as with a distinct target in the protein coding sequence of *COX1* mRNA, perhaps to promote elongation (Perez-Martinez et al. 2003). Furthermore it is speculated that Mss51 interacts also with the nascent Cox1 polypeptide (Perez-Martinez et al. 2003). This mechanism is unique and indicates that translation activators play a key role in coupling mt-encoded protein synthesis to respiratory chain complexes assembly (Perez-Martinez et al. 2009). The role of Mss51 in Cox1 translation and assembly is shown in detail in Figure 1.7.

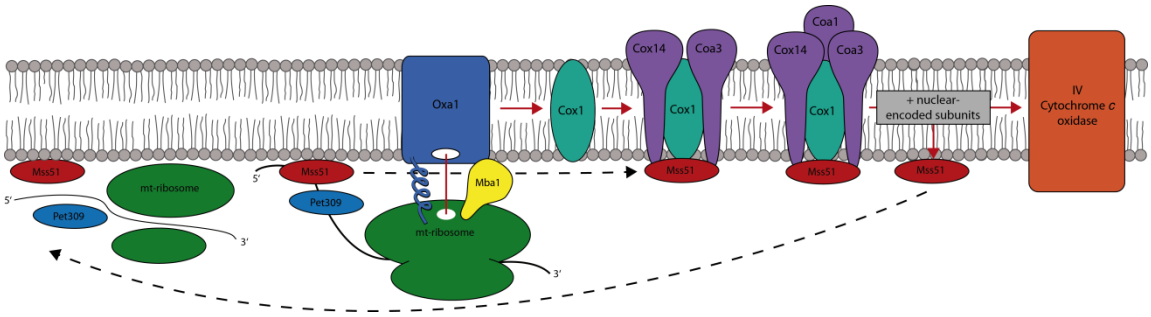

Figure 1.7: Mss51 function in translation and assembly of Cox1
Mss51 interacts with *COX1* mRNA 5' UTL and additionally with newly synthesized Cox1 protein in order to couple the Cox1 synthesis with the assembly of cytochrome *c* oxidase. Interaction of Mss51 or Pet309 with *COX1* mRNA 5' UTL activates the translation; coupling of Mss51 to newly synthesized Cox1 prevents new rounds of COX1 mRNA translation as long as the translation activator is bound in the Cox1-Cox14-Coa3/+Coa1 assembly intermediate complexes. Addition of further nuclear encoded subunits leads to final assembly of cytochrome *c* oxidase and sequesters Mss51. Released Mss51 can initiate new rounds of COX1 mRNA translation.

First, Mss51 and Pet309 bind to the 5'-UTL of Cox1 mRNA, initiating its translation. Cox1 is then synthesized by the mitochondrial ribosome and subsequently inserted into the inner membrane via the Oxa1 translocase. Afterwards, Mss51 associates with the newly synthesized Cox1 protein and the assembly factors Cox14 and Coa3 (cytochrome *c* oxidase assembly 3) forming an intermediate complex within the inner membrane (Barrientos et al. 2004; Mick et al. 2010; Fontanesi et al. 2011). Cox14 and Coa3 are necessary to stabilize Cox1 within the complex and furthermore to repress the translation activation activity of Mss51 through physical interaction with the protein. How this intermediate complex represses Mss51's pro-translational function remains an open question (Mick et al. 2011). The role of this intermediate complex seems to be confined to controlling Cox1 assembly, as the absence of Cox1 synthesis causes the loss of Mss51 and Cox14 or Coa3 interaction (Mick et al. 2010). Subsequent binding of Coa1 (cytochrome *c* oxidase assembly 1) to the complex converts Mss51 to an inactive state;

the translation activator is arrested within the complex and prevented from promoting additional cycles of Cox1 mRNA translation (Mick et al. 2007; Pierrel et al. 2007).

Cox1 probably needs to be fully assembled into the cytochrome *c* oxidase complex to trigger the dissociation of Mss51 from the intermediate complex, enabling Mss51 to start a new translation cycle. However, the exact assembly state of Cox1 in the moment of Mss51's release is not known. The dissociation of Mss51 from the assembly intermediate complex is mediated by the interaction of nuclear encoded cytochrome *c* oxidase subunits, such as Cox6, with an ill-defined intermediate containing Cox1. This feedback mechanism prevents excess Cox1 from being synthesized, and therefore protects the mitochondrion from harmful reactive oxygen species arising from unassembled Cox1 (Khalimonchuk et al. 2007).

Interestingly, Mss51 was shown to interact with mt-Hsp70 within the mitochondrial matrix, and also was found in larger complexes containing mt-Hsp70, Cox1, Coa3 and Cox14 (Fontanesi et al. 2010; Fontanesi et al. 2011). Mt-Hsp70 (Ssc1 in yeast) is known to act also as a chaperone for mt-encoded proteins, especially for Var1, Atp6 and Atp9, and to play a role in the assembly of supramolecular complexes (Herrmann et al. 1994). The interaction of Mss51 and mt-Hsp70 has been proposed as COX assembly-controlled translational auto-regulation of Cox1, however, the precise role of mt-Hsp70 in the Mss51 intermediate complex remains to be characterized (Fontanesi et al. 2010).

In addition to the previously described translation regulatory mechanism, translation of mt-mRNAs is controlled by the quantity of translocation activators within the mitochondrion (Costanzo et al. 1990; Dieckmann et al. 1994). In regards to Pet111, Pet122 and Pet494, it was shown that the translation and expression of their corresponding genes is subject to regulation by the local oxygen and/or carbon source (Fox 1996). For instance, Steele et al. (1996) showed that PET494 is normally expressed at very low levels and its expression is further down-regulated in response to glucose repression. Taken together, these features open the possibility for subtle regulatory effects on individual translation products, adding an additional layer of regulation over and above the general regulation of the mitochondrial transcription and translation systems controlled largely by the environment (Grivell 1995).

1.2.5 Mdm38

The existence of a mitochondrial export machinery has been documented for years; however, its exact composition is still elusive. Three components have been identified, namely Oxa1 (Bonnefoy et al. 1994), Cox18 (Souza et al. 2000) and Mba1 (Ott et al. 2006) (see 1.2.3). Furthermore, biosynthesis of mitochondria encoded proteins depends on a unique regulatory mechanism, whose functionality has yet to be fully clarified. With this in mind it would seem obvious that additional yet to be discovered proteins exist. These proteins are likely involved in the biosynthesis of mt-encoded proteins or in the organization of a functional export complex mediating conservative sorting.

Interestingly, Mdm38, a 65 kDa protein of the inner mitochondrial membrane was also proposed to play a role in the export of mitochondria encoded proteins into the inner membrane (Frazier et al. 2006). Mdm38 was identified in a systematic genome-wide screen in *S. cerevisiae* for genes important for mitochondrial distribution and morphology (MDM) (Dimmer et al. 2002). Dimmer and co-workers proposed that Mdm38 is essential for the establishment of normal mitochondrial morphology, as mitochondria of cells lacking Mdm38p appeared enlarged with very few branches often forming rings or lariat-like structures (Figure 1.8).

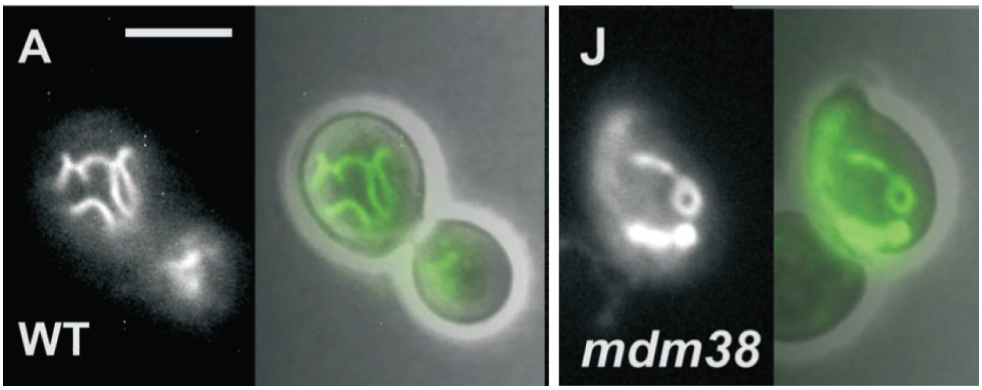

Figure 1.8: Mitochondrial morphology of WT and Δ*mdm38* yeast cells
Strains expressing mitochondria-targeted GFP were grown in YPD medium at 30°C until the logarithmic growth phase and subjected to fluorescence microscopy. A: wild-type (WT) mitochondrial cell; J: *mdm38Δ* cell. Left panel of each picture: mitochondrial morphology of representative cells; right panel: overlay with the corresponding phase contrast image. Bar indicates 5 µm. Picture is taken from Dimmer et al. (2002).

Besides the morphological defects, growth of *Δmdm38* cells on non-fermentable carbon sources is reduced, indicating that the protein is required for respiration (Frazier et al. 2006). Furthermore, Blue native PAGE analysis of the respiratory chain complexes of

Δmdm38 mitochondria revealed that the levels of complexes III and IV were significantly decreased (Frazier et al. 2006). Concomitantly to the severe defects in respiratory chain biogenesis, the insertion of newly synthesized cytochrome *b* and Atp6 into the inner membrane was also affected in *Δmdm38* mitoplasts (mitochondria containing a disrupted outer membrane). Furthermore, mt-encoded cytochrome *b,* Cox1, Cox2, Cox3, Atp6 and Atp9 were co-purified with Mdm38, leading one to believe that Mdm38 plays a role in protein export of mt-encoded proteins (Frazier et al. 2006), as was previously shown for Oxa1 (Jia et al. 2003). Speculations about a putative export-function of Mdm38 were fueled by successful co-isolation of Mdm38 with mitochondrial ribosomal proteins (Frazier et al. 2006).

S. cerevisiae mitochondria possess a protein with high sequence homology to Mdm38, termed Ylh47 (Yeast LETM1 homologue of 47 kDa). Sub-mitochondrial localization of these proteins revealed that Ylh47 and Mdm38 are found in the inner membrane. Furthermore, each protein has a putative transmembrane domain. Both proteins are postulated to expose their C-terminal domains into the mitochondrial matrix (Nowikovsky et al. 2004; Frazier et al. 2006). Interestingly, Ylh47 was also shown to interact with mitochondrial ribosomes. However, these proteins lack further functional similarities, highlighted by Ylh47's expendability in respiratory chain function (Frazier et al. 2006).

A more promising candidate for an Mdm38 homologue, also taking function into account, is the human protein LETM1. The 83.6 kDa protein was shown to be localized to mitochondria (Schlickum et al. 2004). It possesses a single transmembrane domain, two possible EF-hand motifs (one likely functional), a leucine zipper, and several alpha-helical structures with high probabilities of forming coiled coils (Endele et al. 1999). Since Mdm38 was also suggested to contain two coiled coil domains within its C-terminus, it is tempting to speculate that LETM1 localizes to the same vicinity as Mdm38 in yeast mitochondria. A recent study showed that adenovirus-mediated overexpression of LETM1 induced AMP-activated protein kinase (AMPK) leading to a subsequent inhibition of cell cycle progression in lung tumor cells (Hwang et al. 2010). LETM1 was therefore suggested to function as a tumor suppressor gene for lung cancer.

Regarding its homology to Mdm38, LETM1 was shown to suppress the growth defect of *Δmdm38* mutants on non-fermentable carbon sources, indicating that yeast Mdm38 is a functional counterpart of human LETM1 (Nowikovsky et al. 2004). Different

experiments elucidated that Mdm38 and LETM1 are not only similar in topological aspects, but also in their functions. Deletion of *MDM38* in yeast led to a loss of complexes III and IV of the respiratory chain (Frazier et al. 2006), an effect, which could also be seen for LETM1, since the formation of the respiratory chain complexes I, II and IV was impaired by *LETM1* knockdown (Tamai et al. 2008). Like Mdm38, LETM1 was also shown to interact with the mitochondrial ribosome and was therefore proposed to be involved in mitochondrial biogenesis (Piao et al. 2009). Additionally, both proteins were shown to be involved in ion homeostasis. Since LETM1 was identified to act as a Ca^{2+}/H^{+} antiporter in the inner mitochondrial membrane (Jiang et al. 2009), Nowikovski and co-workers provided indication for K^{+}/H^{+} exchange activity of Mdm38 in yeast mitochondria (Nowikovsky et al. 2004; Froschauer et al. 2005; Zotova et al. 2010). They observed that an artificial H^{+}/K^{+} exchanger (Nigericin), supplemented to the growing medium of *mdm38Δ* cells, is able to rescue the growth defect. An additional study revealed the Drosophila gene CG4589 to be an ortholog of LETM1 (McQuibban et al. 2010). They postulated the *D. melanogaster* ortholog of LETM1 to be a mitochondrial osmoregulator with mitochondrial K^{+}/H^{+} exchange (KHE) activity.

It is currently unclear, why both proteins are involved in two processes, which *prima facie* show no connection. This represents a unique future challenge in unraveling the ultimate specific function of Mdm38 and LETM1. A promising hint lies in the fact, that *LETM1* was originally identified as one of the genes, which are chromosomally deleted in patients suffering from Wolf-Hirschhorn syndrome (WHS). This congenital malformation syndrome arises from the deletion of sections of the distal short arm of chromosome 4. The disease is characterized by growth and mental retardation, congenital hypotonia, distinct facial appearance, congenital heart defects, midline defects, and seizures (Endele et al. 1999; Rauch et al. 2001; Zollino et al. 2003). Although WHS has been the object of various researches throughout the last years (Dietze et al. 2004; Rosello et al. 2009), the exact role *LETM1* deletion plays in regards to the clinical manifestations of the disease still remains unclear. It is however speculated that the WHS-typical symptom of seizures is provoked by *LETM1* deletion.

It is encouraging that due to the unique similarities in homology shared by Mdm38 and LETM1, a comprehensive understanding of Mdm38 will allow for powerful conclusions to be drawn on the role LETM1 plays in WHS, hopefully establishing new possibilities to treat this disease.

1.3 Aims of the work

The present work focuses on Mdm38, a mitochondrial protein in *S. cerevisiae*, whose deletion was initially identified to cause changes in mitochondrial distribution and morphology (Dimmer et al. 2002). It was also postulated to be involved in ion homeostasis, acting as a K^+/H^+ antiporter in the inner mitochondrial membrane (Nowikovsky et al. 2004). However, in a subsequent study, Frazier et al. (2006) showed Mdm38 to be specifically required for the biogenesis of respiratory chain complexes. Mdm38 possesses an N-terminal transmembrane span and a C-terminal domain, which is exposed into the mitochondrial matrix, interacts with mitochondrial ribosomes, and was suggested to participate in the export of mitochondrial-encoded proteins across the inner mitochondrial membrane (Frazier et al. 2006). The protein is orthologous to the human protein LETM1, which has been implicated in the pathology of the mitochondrial disorder Wolf-Hirschhorn syndrome (Endele et al. 1999; Zollino et al. 2000).

Although Mdm38 was proposed to be required for respiratory chain biogenesis and for interaction with the mitochondrial ribosome (Frazier et al. 2006), the exact molecular function of the protein is still unknown. Therefore one aspect of the present work was to analyze the molecular function of the Mdm38-ribosome interaction. Special interest was focused on identifying the ribosome binding-region within Mdm38. It was presumed that the identification of this region could contribute to the differentiation of both postulated functions, namely ion homeostasis and ribosome binding. Another objective was to uncover in which steps in the biogenesis of respiratory chain complexes III, IV and V Mdm38 could be involved. In order to gather more information on the interaction of Mdm38 with the mitochondrial ribosome and its role in the export of mitochondria encoded proteins, the objective was to identify new interacting partners of Mdm38, which could be components of a putative Mdm38 complex. Moreover, the structural homology of Mdm38 to LETM1 was to be analyzed, especially in regards to the question whether LETM1 fulfills a similar function in respiratory chain biogenesis and ribosome-binding in human cells as Mdm38 does in yeast.

2. MATERIAL & METHODS

2.1 Material

2.1.1 Chemicals, reagents and enzymes

Standard chemicals and buffer substances were obtained from AppliChem (Darmstadt), Carl Roth (Karlsruhe), Serva (Heidelberg), Sigma-Aldrich (Taufkirchen) and Merck (Darmstadt). Specific chemicals, reagents and enzymes are listed below:

Chemicals, reagents, enzymes	Supplier
Acetic acid 100% Rotipuran	Roth
Acrylamide 30% (w/v)-Bisacrylamide (37.5 : 1) Solution	AppliChem or Roth
Adenosine-5'-triphosphate (ATP)	Roche
Agar-Agar	BD
Agar-Agar Kobe I	Roth
Agarose NEEO	Roth
Alkaline Phosphatase	Roche
Ampicillin	AppliChem
Acrylamide for Blue native PAGE	Serva
Ammoniumperoxodisulfat	Merck
Acetone	Merck
Bis Tris Buffer Grade	AppliChem
Bovine Serum Albumin	Sigma
Bio-Rad D_c Protein Assay	Bio Rad
Complete EDTA-free	Roche
Coomassie Brilliant Blue G250	Serva
Coomassie Brilliant Blue R250	Serva
Cycloheximide	Sigma

Chemicals, reagents, enzymes	Supplier
Chloramphenicol	Serva
1.4 Dithiothreitol (DTT)	Roth
D (+) Galactose	Roth
D (+) Glucose	Roth
D (+) Saccharose	Roth
D (+) Sorbitol	Roth
Developer G 153 f12	AGFA
Digitonin (high purity)	Calbiochem
DNA ladder mix “Gene ruler”	Fermentas
DNase I	Roche
dNTPs	NEB
Dodecylsulfat Na-salt Pellets	Serva
Ethylenediaminetetraacetic acid (EDTA)	Roth
Ethanol Rotipuran	Roth
ECL Western Blotting Detection Reagents	GE Healthcare
Ethidiumbromid 0.07% Dropper-bottle	AppliChem
Fidelitaq DNA Polymerase	USB
Fixer G354 f18	AGFA
Glutathione Sepharose 4B	GE Healthcare
Glycerol	Sigma-Aldrich
Glycine p.a.	Roth
Hering Sperm DNA	Promega
Hydrochloric acid 37 %	Roth
IgG, goat α mouse	Dianova
IgG, goat α rabbit	Dianova
IgG; Bovine	BioRad

Chemicals, reagents, enzymes	Supplier
Imidazole	Merck
Isopropyl-β-D-1-thiogalactopyranoside (IPTG)	AppliChem
KOD HOT Start DNA Polymerase	Novagen
Leupeptin	Roche
3-(N-morpholino)propanesulfonic acid (MOPS)	Sigma
ß-Mercapthoethanol	Roth
[^{35}S]- L-Methionine	Hartmann Analytic
Nicotinamide-adenine-dinucleotide hydrate (NADH)	Roche
Nigericin sodium salt	Sigma
Ni^{2+}-NTA Agarose	Qiagen
Novex Sharp Protein Standard	Invitrogen
Oligonucleotides	Metabion
Pefa bloc	Sigma
Peptone	BD
Phenylmethylsulfonylfluorid (PMSF)	Roth
Precision Plus Protein Standard “All Blue”	Bio Rad
Puromycin	PAA
Protein G Sepharose™ 4 Fast Flow	GE Healthcare
Restriction enzymes HF	NEB
Rotiphorese Gel A (Acrylamide 30%)	Roth
Roti-Quant	Roth
SDS-PAGE Molecular Weight Standards, Broad Range	Bio Rad
Seleno-DL-Methionine	Sigma
Sequencing mix and buffer	Applied Biosystems
Taq DNA Polymerase	USB
Tetramethylethylenediamine (TEMED)	Roth

Chemicals, reagents, enzymes	Supplier
TEV Protease	Invitrogen
Triton X-100	Sigma
Tryptone	BD
Tween 20	Roth
Yeast Extract	BD
YNB w/o aa	BD
Zymolyase 20 T	Seikagaku Biobusiness

2.1.2 Disposables

Disposables were obtained from various common suppliers; some selected ones are listed below:

Disposables	Supplier
Amicon Ultra centrifugal filter 50 k	Millipore
Filter (0.20 – 0.45 µm) for use with syringe	Satourius AG
Hyperfilm ™ ECL (5 x 7; 8 x 10 inches)	GE Healthcare
Mobicols, Bottom Plug for Mobicol, Filter for Mobicol (35µM)	Mo Bi Tec
PVDF Membrane	Millipore
Sterile Syringe 5ml	BD
Vivaspin 30.000 MWCO	Satorius AG
Whatman	Heinemann Labortechnik GmbH

2.1.3 Kits

Kits	Supplier
Pure yield ™ Plasmid Miniprep system 50 preps	Promega
Rapid DNA Ligation Kit	Fermentas
Thrombin Cleavage Capture Kit	Novagen
Wizard Plus SV Miniprep DNA	Promega
Wizard SV Gel and PCR clean-up system	Promega
ABI PRISM® BigDye® Terminator v1.1 Cycle Sequencing Kits	Applied Biosystems

2.1.4 Laboratory equipment

Name of product	Supplier
Superdex 75 PC 3.2/ 30	Pharmacia
Superdex 200 PC 3.2/ 30	Pharmacia
Autoradiography Storage Phosphor Screen	GE Healthcare
Autoclave 3870 EL	Tuttnauer Systec
Autoclave Systec DX-200	Systec
BioPhotometer	Eppendorf
Western-blotting chamber	PeqLab
Centrifuge 5804R	Eppendorf
Christ alpha 1-4/ speed vac	W.Kranich
Developing machine CURIX 60	AGFA
DNA-gel electrophoresis apparatures, Mini Sub cell GT	Biorad
BN-PAGE HOEFER SE600 Ruby	Hoefer
Electrophoresis system Mini PROTEAN 3	Biorad
Electrophorsis Power Supply EPS 601	GE Healthcare

Name of product	Supplier
Elisa Reader Tecan spectra	SLT
Emulsi Flex C5	Avestin
Excella E10 Platform Shaker	New Brunswick Scientific
French press cell SLM AMINCO FA003	Thermo Electron Corporation
French press cell SLM AMINCO FA032	Thermo Electron Corporation
French pressure cell press	SLM-AMINCO
Hood Lamin Air HB 2472	W.H.MAHL
Incubator Shaker Innova 44	New Brunswick
Incubator Shaker Model G25	New Brunswick
Innova 2300 Platform Shaker	New Brunswick Scientific
LAS 3000 Intelligent Dark Box	Fuji/ Raytest, Benelux
Magnetic stirrer MR 3001	Heidolph
Milli-Q-Water Purification System	Millipore
Mini-SUB Cell GT	Biorad
Model 250 EX Incubator	Life Technologies
NanoVue	GE Healthcare
Optima ™Max-xp Ultracentrifuge	Beckman Coulter
PCR cycler T personal 48	Biometra
pH-Meter	InoLab
Photostation for agarose gels	Canon-Kamera
Pipet (2µl; 10µl; 20µl; 100µl; 200µl; 1000µl; 5000µl)	Gilson
Potter S	Satorius
Scale BP 3100P	Satorius
Shaker DRS 12 Skyline	ELMI
Sorvall RC12 BP Centrifuge	Thermo Scientific
Sorvall RC6Plus Centrifuge	Thermo Scientific

Name of product	Supplier
Speed Vac Concentrator	Savant
Starion FLA-9000	Fuji
Table-Centrifuge 5415R	Eppendorf
Table-Centrifuge 5417R	Eppendorf
Thermomixer comfort	Eppendorf
Transilluminator UV solo	Biometra
Smart System	Pharmacia
Video copy processor	Mitsubishi
Vortex-genie 2	Scientific Industries
Water bath SWB25	Thermo Electron
ÄKTA Purifier 10	GE Healthcare

2.1.5 Vectors

Name	Tag	Expression/Use	Source
pGEX- 4T2	N-terminal GST	bacteria	GE Healthcare
pGEX- 4T3	N-terminal GST	bacteria	GE Healthcare
pYM10	C-terminal Prot.A-His7	yeast	Rehling group

2.1.6 Antibodies

All antibodies directed against proteins of *S. cerevisiae* were obtained by immunisation of rabbits. Monoclonal His6-or HA-antibody, PAP-antibody and GST-antibody were obtained commercially (Dianova). In table 2.1 are the most often used primary antibodies of this work listed with description. The polyclonal sera were used for Western blot analysis, immunoprecipitation and co-immunoprecipitation. Secondary antibodies were HRP conjungated and raised in goat.

Antibody directed against	Dilution	Description
Mdm38 (a. purified)	1:300	Against Mdm38 C-terminus Sequence IPADQAAKTFVIKKD
Ylh47	1:300	Against Ylh47 C-terminus Sequence HDTKPIGEAAAIKEK
Mba1	1:100	Against Mba1 C-terminus Sequence YEDDAKVAIHRMK
Mrp51	1:1000	From Prof. Fox
Mrpl39	1:200	Against Mrpl39 C-terminus Sequence AKKRKVAERKPLDFLRTAK
Tom70	1:250	Against the cytosolic domain of Tom70
Tim44	1:500	From Prof. Pfanner (Freiburg)
Tim23	1:500	Against Tim23 N-terminus Sequence MSWLFGDKTPTDDANC
Aco1	1:5000	From Prof. Pfanner (Freiburg)
Tim10	1:500	Against full length protein
Mge1	1:500	From Prof. Pfanner (Freiburg)
Rip1	1:1000	Against Rip1 C-terminus Sequence LEIPAYEFDGKVIVG
Cox1	1:500	Against Cox1 C-terminus Sequence LTSPPAVHSFNTPAVQS
Tim22	1:500	Against the C-terminus of Tim22

Table 2.1: Most often used primary antibodies

2.1.7 Microorganisms

2.1.7.1 *E. coli* strains

Strains	Genotypes	Ref.
XL1-Blue	*supE*44, *hsdR*17, *recA*1, *endA*1, *gyrA*96, *thi*-1, *relA*1, *lac*-, F'[*proAB*+, *lacI*^{q} *lacZ*ΔM15,Tn*10*(tet^r)]	1
Bl21(DE3)	F$^-$ *omp*T *gal dcm lon hsdS*B(rB$^-$ mB$^-$) λ(DE3 [*lacI lac*UV5-T7 gene 1 ind1 sam7 nin5])	2
C43	F$^-$*ompT gal hsdS$_B$* (rB$^-$mB$^-$) *dcm lon* λDE3 and two uncharacterized mutations described in the reference.	3

Legend: 1 = Stratagene; 2= Novagen; 3= (Miroux et al. 1996)

2.1.7.2 *S. cerevisiae* strains

Strains	Genotypes	Ref.
W303-1A (WT)	*MATa ade2-1 his3-11,15 leu2-3,112 ura3-1 trp1-1*	1
HHY299 (Δ*mba1*)	*MATa ade2-1 his3-11,15 leu2-3,112 ura3-1 trp1-1 mba1::HIS5MX6*	2
DaMY17 (Δ*mdm38*)	*MATa ade2-1 his3-11,15 leu2-3,112 ura3-1 trp1-1 mdm38::TRP1*	2
DaMY18 (Δ*mdm38/* Δ*mba1*)	*MATa ade2-1 his3-11,15 leu2-3,112 ura3-1 trp1-1 mba1::HIS5MX6 mdm38::TRP1*	2
AFY25 (*mdm38$_{ProtA}$*)	*MATa ade2-101 his3-Δ200 leu2-Δ1 ura3-52 trp1-Δ63 lys2-801 mdm38::MDM38ProtA-HIS3MX6*	3
YPH499 (WT)	*MATa ade2-101 his3-Δ200 leu2-Δ1 ura3-52 trp1-Δ63 lys2-801*	4

Legend: 1 =(Thomas et al. 1989); 2=(Bauerschmitt et al. 2010); 3=(Frazier et al. 2006); 4= (Sikorski et al. 1989)

2.2 Media & growth conditions

Buffers, stock solutions and media

Buffers and stock solutions were prepared using double-distilled water (ddH_2O) and autoclaved 20 min at 121°C and 2 bar. Buffers and solutions containing heat-sensitive substances were sterilized by filtration through 0.2 µm or 0.45 µm filters. Stock solutions were stored at -20°C. The pH of the buffers was adjusted with KOH, NaOH or HCl.

2.2.1 Media and growth conditions for *E. coli*

2.2.1.1 Media for *E. coli*

LB-medium	1.0 % (w/v) Bacto Tryptone 0.5 % (w/v) Yeast extract 1.0 % (w/v) NaCl pH 7.0
LB-Amp medium	LB-medium supplemented with 100 µg/ml of ampicillin

Above-mentioned compositions of the media were used for preparing liquid cultures. For preparation of LB or LB-Amp plates 1.5 % (w/v) Bacto Agar was added to the liquid media solutions and autoclaved for 20 minutes at 121°C. The ampicillin was added after the media had been cooled down below 50°C.

Auto-induction medium (ZYP-5052)

Autoinduction medium was used to express proteins without addition of IPTG.

This medium contains glucose, which represses T7-polymerase, expression of which is controlled by the LacUV5 promoter. At higher cell densities the glucose is used up and the lactose induces the expression of the T7-polymerase. Subsequently the genes (MDM38) under the control of the T7 promoter will be expressed.

Stock solutions for auto-induction medium:

Buffer	Component	Concentration
ZY	Tryptone Yeast extract $(NH_4)_2SO_4$	1 % 0.5 % 0.5 M
20x NPS; pH 6,75	KH_2PO_4 Na_2HPO_4 Glycerol	1 M 1 M 0.5 %
50x5052*	Glucose Alpha-lactose	0.05 % 0.2 %

All media solutions have been autoclaved for 20 minutes at 120°C. To obtain the final ZYP-5052 rich medium for auto-induction, stock solutions were mixed (sterile) as following (Table 2.2):

Component	**1 liter**	**Concentration**
ZY	~ 928 ml	-
1M $MgSO_4$	1 ml	1 mM
50 x 5052	20 ml	1x
20 x NPS	50 ml	1x
Ampicillin (50 mg/ml)	1 ml	50 µg/ ml

Table 2.2: Auto-induction medium

M9 medium with incorporation of selenomethionine

The M9 medium was used for production of proteins with incorporation of selenomethionine to allow phase determination by multiwavelength anomalous diffraction (MAD). The media was obtained by mixing M9 medium with freshly prepared SolX solution.

M9 medium

Component	Concentration
Na_2HPO_4x $2H_2O$	50 mM
KH_2PO_4	24 mM
NaCl	9 mM
$(NH)_4Cl$	12 mM

SolX solution

Component	Concentration (@200 ml)
$MgCl_2$	50 mM
$CaCl_2$	2.5 mM
Glucose	10 % (w/v)
Seleno-Methionine	1.25 mg/ml (Sigma-Aldrich: Seleno-DL-Methionine; S3875-1G)
Lysine	2.5 mg/ml
Threonine	2.5 mg/ml
Phenylalanine	2.5 mg/ml
Leucine	1.25 mg/ml
Isoleucine	1.25 mg/ml
Valine	1.25 mg/ml

2.2.1.2 Cultivation of *E. coli*

Growth in LB medium

5-50 ml of liquid LB-Amp medium was inoculated with a single colony from a plate and grown overnight at 37°C while shaking at 140 rpm.

Protein overexpression in LB medium

The MDM38 ORF was cloned into the pGEX-4T2 or pGEX-4T3 plasmid. The plasmid was transformed in BL21 (DE3) cells and an expression culture was prepared: 1.5 l LB-Amp was inoculated to OD 0.1 and grown at 37°C 140 rpm until OD 0.6. Protein expression was induced with 0.5 mM IPTG (3h 37°C 140 rpm). Cells were harvested by centrifugation (5000 rpm; 4°C, 15 min), aliquoted to portions of 0.5 g and frozen (- 20°C).

Protein overexpression in auto-induction medium

The open reading frame of MDM38 was cloned into the pGEX-4T2 or pGEX-4T3 plasmid. The plasmid was transformed in BL21 (DE3) cells and an expression culture was prepared: 5 ml LB-Amp liquid medium was inoculated with a single colony from the plate and grown for 12-16 hours at 30°C while shaking at 300 rpm until the culture is turbid but not saturated. After appropriate time 200 µl of the inoculum culture have been transferred in a 2-liter Erlenmeyer flask containing 400 ml ZYP-5052+ampicillin medium (to obtain optimal gas exchange of the culture) and shaken at 300 rpm at 30°C until the cells reached OD_{600} 0.5. Subsequently the temperature was reduced to 18°C and the culture incubated for further 24 h, 140 rpm. At OD_{600} of 10-12 the cells were harvested by centrifugation (5000 rpm; 4°C, 15 min).

Protein overexpression in M9 medium with incorporation of selenomethionine

The ORF of MDM38 was cloned under the control of the t7 promoter into pGEX-4T3. This plasmid was transformed in BL21 (DE3) cells and an expression culture was prepared: 100 ml LB-Amp liquid medium was inoculated with a single colony from the plate and grown for 12-16 hours at 37°, shaking at 180-220 rpm. The cells have been harvested by centrifugation, washed and the pellet was resuspended in 5ml LB-Amp medium. For the main culture 1 liter M9 medium (see 2.2.1.1) + 40 ml SolX solution (see

2.2.1.1) + antibiotic have been mixed. Each was inoculated with 1 ml of pre-washed LB-Amp culture. The main cultures were grown at 37°C/220 rpm to an OD_{600} of 0.4-0.6 and induced with 1 mM IPTG. After incubation at 37°C/220 rpm for 12-16 hours the cells were harvested by centrifugation (5000 rpm; 4°C, 15 min).

2.2.1.3 Growth phase analysis of cultures

The optical density of bacterial cultures was determined with BioPhotometer (Eppendorf) OD_{600} of 1 was assumed to $3x10^7$ cells/ml culture.

2.2.1.4 Preparation of permanent (glycerol) cryo-stocks

For storage of bacterial strains over a longer time period, glycerol stocks have been generated. For this, *E.coli* cells have been taken out of liquid culture and incubated with glycerol freezer medium in a 1:1 ratio. The stocks were frozen at -80°C.

LB+40% Glycerol freezer media	1.0 % (w/v) Tryptone 0.5 % (w/v) Yeast Extract 1.0 % (w/v) NaCl 40 % (v/v) Glycerol

2.2.2 Media and growth conditions for *S. cerevisiae*

2.2.2.1 Media for *S. cerevisiae*

Selective media (SM)	0.67 % (w/v) yeast nitrogen base w/o amino acids 0.07 % (w/v) Drop-out mix 2 % (w/v) Glucose
YPG (glycerol)	1 % (w/v) yeast extract 2 % (w/v) bacto-peptone 3 % (w/v) glycerol
YPD (glucose)	1 % (w/v) yeast extract 2 % (w/v) bacto-peptone 2 % (w/v) glucose
YPS (saccharose)	1 % (w/v) yeast extract 2 % (w/v) bacto-peptone 2 % (w/v) sucrose

YPGal (galactose)	1 % (w/v) yeast extract 2 % (w/v) bacto-peptone 2 % (w/v) galactose
YPG (glycerol) + Nigericin*	1 % (w/v) yeast extract 2 % (w/v) bacto-peptone 3 % (w/v) glycerol 0.5 µM Nigericin*
YPD (glucose) +Nigericin*	1 % (w/v) yeast extract 2 % (w/v) bacto-peptone 2 % (w/v) glucose 0.5 µM Nigericin*

* Nigericin was added to the autoclaved medium when the medium was cooled down below 50°C. Nigericin plates were always prepared fresh.

Above-mentioned compositions of the media were used for preparing liquid cultures. For preparation of solid agar plates 2.5 % (w/v) bacto-agar was added to the liquid media solutions and autoclaved for 20 minutes at 121°C.

2.2.2.2 Cultivation of *S. cerevisiae*

Yeast cells were streaked out of a glycerol stock on YPD-plate or selective plates and incubated at 30°C. After 2-3 days a culture of 5 ml was inoculated. Yeast strains were cultivated in YP medium supplemented with 2 % carbon source (glucose, galactose, saccharose or glycerol (3 %)) or in corresponding selective media. Cells were grown at 30°C and shaken at 120 rpm.

2.2.2.3 Growth test of *S. cerevisiae* on agar plates

For analyses of the growth phenotype 5 ml cultures were inoculated from YPD plates (see 2.2.2.2) and grown at 30°C while shaking at 120 rpm to a high cell density. OD_{600} was adjusted to 1.0 and serial 1:10 dilutions were spotted on agar plates with different carbon sources. Plates were incubated at 30°C. (Temperature- sensitive cells have been grown at indicated temperature).

2.2.2.4 Preparation of cryo-stocks

For storage of yeast strains over a longer time period, glycerol stocks have been generated. For this, *S. cerevisiae* cells have been taken out of liquid culture (mid log, OD approx. 0.6) and incubated with YPAD freezer media in a 1 : 1 ratio. The stocks were frozen at -80°C.

YPAD freezer media for yeast	1 % (w/v) yeast extract 2 % (w/v) peptone 2 % (w/v) glucose 30 µg/ml Adenine sulfate 15 % (v/v) glycerol Stir to dissolve. Dispense 3 ml in each vial. Autoclave 20 min

2.2.2.5 Isolation of mitochondria from *S. cerevisiae*

Mitochondria were isolated from *S. cerevisiae* following the method previously described by (Daum et al. 1982; Meisinger et al. 2006). Mitochondria were isolated from exponentially growing cultures (OD 1.5-2.0). Yeast cells with OD_{600} 1.5-2.0 were harvested by centrifugation (15 min/4500 rpm/RT). Subsequently the cells were washed with ddH_2O and the weight of the pellet was determined. The pellet was resuspended in DTT buffer (2ml/g wet weight) and incubated for 20 minutes at 30°C with shaking at 80 rpm. In order to remove residual DTT buffer, the cell suspension was centrifuged (10 min/4000 rpm) and the pellet was washed with 1.2 M Sorbitol. For digestion of the cell wall, the pellet was resuspended in zymolyase buffer (7ml/g wet weight)* with 3mg zymolyase/g wet weight and the suspension was incubated at 30°C for 60 minutes under moderate shaking conditions. The spheroplasts were isolated by 5 min centrifugation at 4000 rpm and the pellet was washed in zymolyase buffer without zymolyase (7ml/g wet weight). All subsequent steps were performed at 4°C to avoid proteolysis. The pellet was resuspended in cold homogenizing buffer (7.0 ml/g wet weight) and the spheroplasts were homogenized with 15 strokes using a glass-Teflon homogenizer ("potter S"/Sartorius). Cell Debris and unopened cells were pelleted by

* To check the level of cell wall digestion, 50µl cell suspension (in zymolyase buffer without zymolyase) was diluted with 2 ml dH_2O. Lysis efficiency was compared with a sample following zymolyase treatment. Spheroplasting was complete when the OD of the H_2O dilution following zymolyase treatment was 10-20 % of the OD of the sample prior to zymolyase treatment. The solution of spheroplasts in pure H_2O becomes clear because spheroplasts burst under these conditions (osmosis).

two centrifugation steps at 5 min 3000 rpm and 10 min 4000 rpm. Subsequently mitochondria were pelleted at 12.000 rpm for 15 min and washed with ice-cold SEM buffer and the total protein concentration has been determined. Mitochondria were adjusted to a final protein concentration of 10mg/ml (with cold SEM buffer), aliquoted, shock-frozen in liquid nitrogen and stored at -80°C.

DTT-buffer	0.1 M Tris H_2SO_4 pH 9.4 10 mM DTT
Zymolyase-buffer	20 mM KPi-Buffer pH 7.4 1.2 M Sorbitol
Homogenizing- buffer	10 mM Tris/HCl pH 7.4 0.6 M Sorbitol 0.5 mM EDTA 0.2 % (w/v) BSA 1 mM PMSF
SEM buffer / pH 7.2 (KOH)	250 mM Saccharose 10 mM MOPS 1 mM EDTA

2.3 Methods in molecular biology

2.3.1 Isolation of DNA

2.3.1.1 Isolation of yeast genomic DNA

For a small-scale preparation of yeast genomic DNA, 5ml culture of YPH499 was grown (see 2.2.2.2) to OD_{600} of 0.5 to 0.7. The cells were harvest by centrifugation (5min/ 5000 rpm), resuspended in 150 µl solution A and incubated for 1 hour at 37°C. Upon addition of 20 µl of 10 % SDS and 100 µl 8M ammonium acetate the sample was incubated at -20°C for 10-15 minutes and DNA was separated from cell wall and membranes by centrifugation at 14.000 rpm for 15min at 4°C. The supernatant was transferred to a new tube and DNA was precipitated by addition of the same volume of isopropanol. After centrifugation (14.000 rpm/15min/4°C), the pellet was washed with 70 % ethanol, centrifuged, dried at RT, resuspended in 25µl TE buffer and stored at -20°C.

Solution A	50 mM Tris/HCl pH 7.5 10 mM EDTA 0.3 % ß-mercaptoethanol 0.5 mg/ml Zymolyase (add fresh)
10X TE buffer	100 mM Tris-HCl (pH 7.5) 10 mM EDTA

2.3.1.2 Isolation of plasmid DNA from *E. coli*

Plasmid DNA from *E. coli* was isolated using "Wizard® Plus SV Minipreps DNA purification system" according to the manufacturers instructions.

Cell Resuspension Solution (CRA)	50 mM Tris-HCl (pH 7.5) 10 mM EDTA 100 µg/ml RNase A
Cell Lysis Solution (CLA)	0.2 M NaOH 1 % SDS
Neutralization Solution (NSB)	4.09 M guanidine hydrochloride 0.759 M potassium acetate 2.12 M glacial acetic acid Final pH is approximately 4.2
Column Wash Solution (CWA)	60 % ethanol 60 mM potassium acetate 8.3 mM Tris-HCl 0.04 mM EDTA

2.3.1.3 Measurement of DNA concentration

To determine DNA concentration the absorption of DNA solutions was measured at 260 nm by using NanoVue (GE Healthcare). One OD 260 was assumed to correspond to 50 µg/ml of dsDNA (Sambrook et al. 1989).

2.3.2 Cloning of DNA fragments

2.3.2.1 DNA amplification by Polymerase Chain Reaction (PCR)

DNA fragments were amplified by polymerase chain reaction (PCR) as initially described

by Mullis (1990). Two different proofreading polymerases have been used: "FideliTaq™DNA Polymerase"(Usb) and "KOD HOT Start DNA Polymerase"(Novagen). Reaction setups have been performed according to the recommended instructions of the producer (Table 2.3). The annealing temperature of the primers was calculated according to online calculators* or estimated using the following equation: T_m (°C)= 2(A+T)+4(G+C). The cycler (see 2.1.4) was programmed according to table 2.4.

Component	50µl reaction (FideliTaq)	50µl reaction (KOD)
PCR Buffer	1x	1x
$MgSO_4$	-	1.5 mM
dNTPs	0.2 mM (each)	0.2 mM (each)
Forward primer	0.2 µM	0.3 µM
Reverse primer	0.2 µM	0.3 µM
Template DNA	10-100ng	10-100ng
DNA polymerase	0.05 U/µl	0.02 U/µl

Table 2.3: Reaction setups for FideliTaq and KOD polymerases

Cycle step	FideliTaq Temperature [°C]	Time [s]	KOD Temperature [°C]	Time [s]
1) Denaturation	95	120	95	120
2) Denaturation	95	30	95	20
3) Annealing	55	30	55	10
4) Extension	68	60 → 2) 5x	70	90 → 2) 5x
5) Denaturation	95	30	95	20
6) Annealing	52	30	52	10
7) Extension	68	60 → 5) 25x	70	90 → 5) 25x
8) Extension	68	320	-	-
9) Cooling	4	∞	4	∞

Table 2.4: PCR-program for FideliTaq and KOD polymerases

* http://www.bioinformatics.org/sms2/pcr_primer_stats.html

2.3.2.2 Agarose gel electrophoresis of DNA

DNA fragments were separated by horizontal Agarose gel electrophoresis. 0.8-1% Agarose Gels were prepared in TAE buffer, containing Ethidium bromide. 5x Loading Dye was added to DNA samples and electrophoresis was performed at 120 V. Separation of the DNA fragments was documented using the UV-solo-transilluminator. "Gene Ruler" (Fermentas) was used as a standard to estimate the size of the separated fragments.

25X TAE buffer stock solution	1 M Tris base 2.85 % (v/v) Acetic acid 25 mM EDTA pH 8.0
5X loading dye	30 % (v/v) glycerol 0.25 % (w/v) bromphenol-blue 0.25 % (w/v) xylencyanol

2.3.2.3 Isolation of DNA from agarose gels

DNA bands were excised from the gel with a sterile scalpel under UV light. The "Wizard SV Gel and PCR Clean-Up System" (Promega) was used to extract the DNA out of the gel according to the manufacturers instructions.

Membrane Binding Solution	4.5 M guanidine isothiocyanate 0.5 M potassium acetate (pH 5.0)
Membrane Wash Solution	(after ethanol addition) 10 mM potassium acetate (pH 5.0) 80 % ethanol 16.7µM EDTA (pH 8.0)

2.3.2.4 Digestion of DNA with restriction endonucleases

Buffer and digestion conditions were used according to the manufacturer's recommendations (New England bioLabs). DNA was usually digested for 1 h at 37°C in the buffer specific for the restriction enzyme. Digested DNA fragments were analyzed by agarose gel electrophoresis and used for ligation reactions.

2.3.2.5 Ligation of DNA fragments

Digested DNA fragments were ligated using "rapid DNA ligation kit" (Fermentas) according to the manufacturer's recommendations. Linearized vector (100 ng) and 3-fold molar excess of the insert DNA were incubated in a 20 µl reaction with 4 µl of 5 x rapid ligation buffer and 1 µl (5 U) T4 DNA ligase (Fermentas) for 1 h at 22°C.

2.3.3 Transformation of *E. coli* cells

2.3.3.1 Preparation of transformation competent *E. coli* cells

A 500 ml LB culture in mid log phase (OD 0.5) was chilled on ice for 10 min *E. coli* cells were centrifuged for 10 min/2000 rpm/4°C and the pellet gently resuspended in 250 ml of cold, sterile $CaCl_2$ (50mM). The cells were left on ice for 15 min. A second centrifugation was performed (10 min/2000 rpm/4°C), and the *E. coli* cells were finally resuspended in 25 ml of cold, sterile $CaCl_2$ (50 mM). Glycerol was supplemented (final concentration of 15 %) to cells, which were not immediately used. Cells are stored frozen at -80°C.

2.3.3.2 Transformation of $CaCl_2$ competent *E. coli* cells by heat shock

100µl of $CaCl_2$ competent *E. coli* cells were thawed on ice and incubated with 50 ng plasmid or 10 µl of the ligation mixture for 30 minutes on ice. A heat shock was performed at 42°C for 45 sec. Subsequently the culture was cooled down for two minutes on ice. 900 µl of SOC or LB medium was added and bacteria were incubated for one hour at 37°C/700 rpm. Finally, the transformed cells were centrifuged down (5 min/10.000 rpm) and resuspended in 30 µl LB. The bacterial suspension was plated on LB agar plates with the respective antibiotic for the transformed plasmid.

2.3.3.3 Sequencing of DNA

DNA sequencing of new constructed plasmids was performed by the dideoxy chain-termination method (Sanger et al. 1977). For the sequencing reaction 200-400 ng plasmid, 8 pmol primer, 1.5 µl sequencing mix and 1.5 µl sequencing buffer (ABI PRISM® BigDye® Terminator v1.1 Cycle Sequencing Kits) were mixed and filled up with water to

a final volume of 10 µl. "PCR" was performed according to the program in table 2.5. The reaction was purified by addition of 1 µl 125 mM EDTA and 1 µl 3M NaAc and precipitated by addition of 50 µl of 100 % ice-cold EtOH. The solution was carefully mixed and incubated for five minutes at RT. Subsequently it was centrifuged (15 min/14.000 rpm) and the pellet was washed with 70 µl of 70 % EtOH (5 min/14.000 rpm) and vacuum-dried. For sequencing the pellet was resuspended in 15 µl formamide (HiDye) and sent to the Göttinger Center for Molecular Biosciences (GZMB*) where it was analyzed in a Genetic Analyzer 3100 (Applied Biosystems). The sequences were analyzed using software "ApE (Universal)" or "Geneious".

Cycle step	Temperature [°C]	Time [s]
1) Initial denaturation	96	120
2) Denaturation	96	10
3) Annealing	55	15
4) Extension	60	240 → 2) 25x
5) Cooling	4	∞

Table 2.5: PCR-program for sequencing of DNA

2.3.4 Cloning strategies for plasmid used for recombinant protein expression

The open reading frame was cloned into pGEX-4T2 or pGEX-4T3 and fused in frame to GST (Gluthation S transferase) under the control of the lac promoter. The plasmids were verified by sequencing.

2.3.4.1 Cloning of different domains of Mdm38 and LETM1 in bacterial GST-expression vector pGEX-4T2/ pGEX-4T3

An overview on the different constructs used in the present work, their generation and the corresponding primer sequences, are given in tables 2.6 and 2.7.

* GZMB, Georg-August University, Goettingen (www.gzmb.uni-goettingen.de)

Name	Mdm38^{CTD}	Mdm38^{RBD}	LETM1^{RBD}
Aa sequence	159-573	182-408	250-612
N-terminal tag	GST	GST	GST
C-terminal tag	His_6	His_6	His_6
Backbone	pGEX 4T3	pGEX 4T2	pGEX 4T2
Restriction sites	*SalI* and *NotI*	*Bam*HI and *Not*I	*Bam*HI and *Not*I
Primers	(Frazier, Taylor et al. 2006	CV 18 (for) and CV 19 (rev) (Table 2.7)	CV 13 (for) and CV 15 (rev) (Table 2.7)
Reference	(Frazier, Taylor et al. 2006	This work	This work

Table 2.6: Cloning of Mdm38 and LETM1 constructs

CV 13 (for)	5`- GGTGGTGGATCCAAGAAGGAGCTTCGGGTCAAG -3`
CV 15 (rev)	5`- GGTGGTGCGGCCGCTCAGTGATGGTGATGGTGATGCACCCTTTTTGTCAATCTCTTG -3`
CV 18 (for)	5`- GGTGGTGGATCCAAGCTCATCGAGATCAGAAAAAAG-3`
CV 19 (rev)	5`- GGTGGTGCGGCCGCCTAATGGTGATGGTGATGGTGGTTGTAAACGGGATCTGGAATGGA-3`

Table 2.7: Primer sequences used for generation of truncation constructs

2.3.5 Chromosomal integration of yeast cells

2.3.5.1 Amplification of yeast integration cassettes

For generation of yeast cells expressing TEV-protein-A fusion proteins, PCR amplified tagging cassettes have been chromosomally integrated into the yeast genome. For this, DNA cassettes have been generated by PCR according to (Knop et al. 1999) with pYM10.

2.3.5.2 Transformation of yeast cells by lithium acetate method

Transformation of yeast cells has been performed according to Gietz et al. (2007). 10 ml YPD medium was inoculated with a single colony from the used strain and grown over night at 30°C while shaking at 130 rpm. Next morning the main culture (5 ml/transformation) was inoculated to OD_{600} 0.1 and shaken at 30°C/130 rpm until the cells reached OD_{600} 0.6. The cells have been harvested by centrifugation (3.500 x g/5

min), washed first with 1 ml dH_2O and then with one ml of 100 mM LiAc. Subsequently the pellet was resuspended in two ml LiAc-TE solution. An aliquot of 100 µl competent cells was mixed with 10 µl ssDNA (salmon sperm DNA 10 mg/ml) and 50µl of the DNA (PCR), which had to be transformed. After addition of 600 µl LiAc-TE-PEG solution, the mix was incubated for 30 min at 30°C, 70µl DMSO were added and the solution was heat shocked for 10 minutes at 42°C. The cells were harvested by centrifugation (2 min/4.000 rpm/RT); the pellet was resuspended in 100 ml ddH_2O and plated out on a minimal selection plate.

LiAc solution	10 mM Tris/HCL pH7.5 1 mM EDTA 100 mM Lithiumacetat
LiAc-PEG solution	40 % (w/v) PEG 3350 (in LiAc solution)

2.4 Biochemical methods

2.4.1 Purification of recombinant proteins from *E. coli*

2.4.1.1 Cell wall disruption of *E. coli* cells by French press or EmulsiFlex

For protein purification in a preparative scale, the cell pellet was resuspended in 1 x PBS-buffer containing 10 % Triton-X 100, DNase1, 1 mM PMSF, 20 µM Leupeptin, 0.4 mM Pefabloc and 1 EDTA-free-protease- inhibitor cocktail tablet (Roche)/ 50 ml buffer. The bacterial cell walls were disrupted by pressure (15000 Psi) generated by French press or EmulsiFlex (see 2.1.4) and soluble proteins were separated from insoluble ones by by centrifugation (30 min/45.000 x g / 4°C) and transferred to Glutathione Sepharose (see 2.4.1.2).

10 x PBS buffer	1.4 M NaCl 27 mM KCl 101 mM Na_2HPO_4 18 mM KH_2PO_4 pH 7.4

2.4.1.2 Affinity purification via Glutathione Sepharose 4B

For protein purification in a preparative scale, the cell lysate was bound to the Glutathione Sepharose 4B in a batch. The amount of used Sepharose varied with the amount of recombinant protein; approximately 8 mg recombinant protein/ ml medium has been used. For equilibration the Sepharose was sedimented by centrifugation at 500 x g/5 min and washed twice with 5 times excess of PBS buffer. Afterwards the cell lysate was incubated in a batch (50 ml Falcon tubes) at 4°C overnight with end-over-end rotation. After 16 h of incubation the resin was sedimented by centrifugation (500 x g/5 min/4°C) and washed ten times by adding 5ml PBS binding buffer to each ml of slurry. Elution of the protein was performed by addition of 0.5 ml Thrombin cleavage buffer per 1 ml slurry of Glutathione Sepharose, spiked with thrombin (one unit equates to 0.9 µl and cleaves 100 µg recombinant protein). For this, the slurry was incubated in a batch (50 ml Falcon tubes) at 4°C for 16 hours with end-over-end rotation. Prior to elution the Sepharose was transferred to a gravity flow column. Drop wise elution was performed by gravity flow and the eluate was collected in a Falcon tube on ice. Afterwards it was transferred to a second affinity purification column, to Ni^{2+} NTA (see 2.4.1.3).

The regeneration procedure of the column was performed as described in the producers' handbook.

10 x Thrombin cleavage buffer	200 mM Tris-HCl pH 8.4 1.5 M NaCl 20 mM EDTA 50 % Glycerol

2.4.1.3 Affinity purification via Ni^{2+} NTA

The recombinant Mdm38 truncation construct was purified via double affinity purification. For this, the eluate from the GSH-Sepharose was directly transferred to Ni^{2+}NTA Agarose. Prior to it, the resin was equilibrated with wash buffer. For big scale preparation also the Ni^{2+} NTA material was incubated with the recombinant protein in a batch (50 ml Falcon tube) at 4°C over night with end-over-end rotation. The amount of used Ni^{2+} NTA Agarose varied with the amount of recombinant protein; approximately 50 mg His-tagged protein/ ml resin has been used. Next morning the Ni^{2+} NTA Agarose was sedimented by centrifugation (200x g/ 5 min/4°C), the unbound fraction was

removed and the beads resuspended in wash buffer and subsequently transferred in a gravity flow column. After 10 times wash by adding 5ml wash buffer to each ml of slurry, the recombinant protein was eluted with elution buffer.

Binding/wash buffer	10 mM Tris pH 7.4 20 mM Imidazole
Elution buffer	1 M Tris pH 7.4 400 mM Imidazole

2.4.1.4 Size-exclusion chromatography using Superdex 200

For final purification of the recombinant protein, size-exclusion chromatography was performed. For this purpose, Mdm38 protein solution was concentrated by centrifugation in Vivaspin centrifugal filters (Sartorius) to a final volume of 1 ml, filtered through a 0.20 µm filter and injected a Superdex™ S200 column connected to a ÄKTA purifier (GE Healthcare). The purity of the elution fractions has been analyzed by SDS-PAGE and Western blotting. Marker proteins determined the molecular weight of the eluted proteins:

Marker protein	Size (kDa)
Thyroglobulin	669.000
Ferritin	440.000
Aldolase	158.000
Conalbumin	75.000
Ovalbumin	43.000
Carbonic-Anhydrase	29.000
Ribonuclease A	13.700
Aprotinin	6.500

2.4.2 Protein analyses

2.4.2.1 SDS-Polyacrylamide gel electrophoresis (SDS-PAGE)

The proteins were separated electrophoretically according to their molecular weights under denaturing conditions using one-dimensional vertical SDS-polyacrylamide gel electrophoresis (SDS-PAGE) (Laemmli 1970). Two electrophoresis systems have been used**:** a self-made gel equipment* (gel size: 16.5 cm x 14 cm x 1mm) and a Mini-PROTEAN II Bio-Rad system (gel size: 10 cm x 5.5 cm x 0.75). The polyacrylamide concentrations of the separating gel were chosen according to the molecular sizes of proteins of interest. Before loading, the samples were resuspended in SDS-sample buffer and heated to 95°C for 5 min. The electrophoresis was performed at 20-35 mA (2.5-3 hours) for large gels, and at 25 mA (approx. 1 hour) for Bio-Rad gels. Subsequently, separated proteins were either stained with Coomassie Brilliant Blue staining buffer or transferred onto a PVDF-membrane (see 2.1.2).
The following protein markers have been used:

I.	SDS-PAGE Molecular Weight Standards, Broad Range SDS-PAGE Molecular Weight Standards, BioRad.
II.	Precision Plus All Blue Protein Standards, BioRad.
III.	Novex® Sharp Protein Standard, Invitrogen.

4x SDS (Laemmli) sample buffer	8 % (w/v) SDS 40 % (w/v) glycerol 240 mM Tris/HCl pH 6.8 0.2 % (v/v) ß-Mercaptoethanol 0.04 % (w/v) Bromophenol blue
Acrylamide/bis-acrylamide	30 % acrylamide 0.8 % bis-acrylamide

* Self-made gel-equipment was produced by the in-house work shop.

1x SDS- running buffer	25 mM Tris 191 mM glycine 0.1 % (w/v) SDS
Stacking gel buffer	0.5 M Tris/HCl, pH 6.8 0.1 % (w/v) SDS
Separating gel buffer	1.5 M Tris/ HCl, pH 8.8 0.4 % (w/v) SDS
Ammonium-peroxidiulfate (APS)	10 % (w/v) APS
SDS solution	10 % (w/v) SDS
TEMED	Undiluted

2.4.2.2 Blue native-polyacrylamide gel electrophoresis (BN-PAGE)

Blue native-polyacrylamide gel electrophoresis was performed according to Schagger et al. (1991), with small variations. Mitochondria (100-300 µg) were thawed on ice, pelleted (5 min/ 14.000 rpm/ 4°C) and resuspended in 100-300 µl ice-cold solubilization buffer (containing 1% digitonin). The samples were incubated for 15 minutes on ice and the non-solubilized material was removed by centrifugation (5 min/ 14.000 rpm/ 4°C). 5 µl 10 x loading dye was added to 45µl sample (supernatant) and the samples were directly applied to Blue native PAGE. Electrophoresis was performed in a cooled (4°C) gel-chamber. Conditions for running through the stacking gel were 100-400 volt; those were switched to 600 volt for running the gradient gel. Overnight runs have been performed at 70-80 volt (gradient gel). After the blue dye front had moved half way through the gel, the cathode buffer was exchanged against fresh cathode buffer without Coomassie dye. The electrophoresis was stopped when the blue dye front was running out of the gel into the anode buffer. Subsequently the gels had been transferred to PVDF membrane (see 2.1.2) or dried on a gel drier.

Acrylamide for BN-PAGE	Acrylamide 48.0 % (w/v) Bis-Acrylamide 1.5 % (w/v)
Cathode Buffer with Coomassie 10X	500 mM Tricine 150 mM Bis-Tris pH 7.0 0.2 % (w/v) Coomassie G250

Cathode Buffer w/o Coomassie 10X	500 mM Tricine 150 mM Bis-Tris pH 7.0
Anode Buffer 40X	2M Bis-Tris /HCl pH 7.0
3 X Gel Buffer	150 mM Bis-Tris/ HCl pH 7.0 200 mM e-Amino-n-caproic acid
10 X Loading Dye	100 mM Bis-Tris/ HCl pH 7.0 500 mM e-Amino-n-caproric acid 5 % w/v Coomassie G250 pH 7.0
Digitonin Buffer	1 % Digitonin 20 mM Tris/ HCl pH 7.4 0.1 mM EDTA pH 8.0 50 mM NaCl 10 % Glycerol 1 mM PMSF

2.4.2.3 Coomassie staining of polyacrylamide gels and PVDF membranes

The gel was incubated with Coomassie Brilliant Blue staining solution for at least 3 hours. Subsequently the background staining was removed by repeated washes with destaining solution. To verify protein transfer efficiency (see 2.4.2.4) and to visualize marker protein's bands, also the PVDF membranes were shortly immersed in Coomassie Brilliant Blue staining solution and rinsed afterwards with destaining solution.

Coomassie Blue Stainer	40 % (v/v) Methanol 7 % (v/v) Acetic acid 0.2 % (w/v) Coomassie R250
Destainer	26 % (v/v) Methanol 7 % (v/v) Acetic acid

2.4.2.3 Transfer of proteins onto PVDF membrane

For immunochemical detection, the proteins were separated by SDS-PAGE and subsequently transferred to polyvinylidene fluoride (PVDF)-membrane (pore diameter 0.45 µm, Millipore) using semi-dry method (2-2.5 h, 250 mA). The membrane was

activated by a short incubation in methanol for 2 minutes and rinsed afterwards with transfer buffer in order to remove residual methanol. The transfer was performed by placing the gel onto the PVDF membrane, sandwiched by three Whatman papers on each side. To verify transfer efficiency and to visualize marker protein's bands, the membrane was reversibly stained in Coomassie staining buffer (see 2.4.2.3).

Transfer buffer	20 mM Tris 150 mM Glycine 0.02 % SDS (w/v) 20 % (v/v) Methanol
Western buffer (TBS-T)	1 x TBS 0.1 % Tween 20 (w/v)
20 X TBS	400 mM Tris 2.5 M NaCl pH 7.5 (HCl)

2.4.2.4 Immunodecoration

The membrane was blocked by incubation in TBST with 5% low fat milk powder either for 1 hour at RT or over night at 4°C. Subsequently the membrane was incubated with the appropriate antibody (2h/RT or 4°C/over night). Next the membrane was washed in TBS-T for 3 x 15 min and incubated in HRP-linked secondary antibody. After a second washing step (3 x 15 min in TBS-T), the detection was performed using "ECL-Western blotting-detection and analysis system" (GE Healthcare) according to the manufacturer's recommendations.

2.4.2.5 Affinity purification of antibody against Mdm38

In order to reduce the cross-reactivity of the Mdm38 antiserum, the antibody was purified by affinity chromatography. For this purpose an affinity column was prepared. The antigen was solved in coupling buffer and incubated with CNBr activated beads either at RT for 2 hours or over night at 4 °C. Subsequently, the excess antigen was washed away with 5 volume columns of coupling buffer and the remaining actives groups were blocked by incubation with 5 ml 0.1 M Tris/HCL pH 8.0 at RT for two hours.

The excess Tris/HCL solution was removed by an alternative washing with two different washing buffers.

Coupling buffer	0.1 M $NaHCO_3$ pH 8.3 0.5 M NaCl
Wash buffer 1	0.1 M Na-acetate pH 4.0 0.5 M NaCl
Wash buffer 2	0.1 M Na-acetate pH 8.0 5 M NaCl

For affinity purification Mdm38 serum was diluted 1:1 with TBS and incubated with the affinity column. The unbound material was removed by intensive washing with TBS. The Mdm38 antibodies were released from the column with 100 mM glycine pH 2.5 and collected in tubes containing Tris/HCl pH 8.0 in order to neutralize the low pH of Glycine. After purification the column was washed with TBS and stored in TBS + 0.02 % Na-azide at 4°C.

2.4.2.6 Determination of protein concentration by Bradford method

Determination of protein concentration was performed by Bradford method using "Bio-Rad- D_c Protein Assay" Kit according to the producer's recommendations. Protein concentration was determined using a BSA-standard curve.

2.4.3 Protein interaction analyses

2.4.3.1 Co-immunoprecipitation experiments

For coupling of antibodies to protein G Sepharose (PGS), 50 µl of the 50 % PGS slurry were filled into a Mobitec column (see 2.1.2) and washed twice by centrifugation with 500 µl 0.1 M KPi pH 7.4 at 100 g for 30 seconds. Subsequently affinity purified HA-antibody has been diluted in a 1 : 3 ratio with 0.1 M KPi pH 7.4 to a total volume of 400 µl and incubated with the Sepharose beads for one hour at RT while mixing end-over-end. Afterwards the column material was sedimented by centrifugation (100g/30 sec.) and the column washed twice with 0.1 M sodium borate. The protein G-antibody interaction was strengthened by cross linker DMP. For this, 350 µl of DMP solution

(5mg/ml DMP in 0.1 M sodium borate) was incubated for 30 minutes at RT while mixing end-over-end. Subsequently the DMP solution was spun out (100 g/1min) and the slurry was washed with 20mM Tris pH 7.4. For final quenching of the cross linker 500 µl 20 mM Tris pH 7.4 were incubated with the column beads overnight at 4°C. Next morning Tris was spun out and the column washed three times with 1x TBS by centrifugation (100 g/1 min). The column was stored in 1 x TBS with 2 mM sodium azide at 4°C.

For performing the Co-IP, 50 µl mitochondria (10µl/µl) from a HA-tagged strain were thawed on ice and subsequently pelleted (14.000 rpm/4°C/ 10min). The pellet was resuspended in 500 µl solubilization buffer and incubated for 30 min at 4°C, mixing end-over-end. Subsequently the solubilizate was cleared by centrifugation (15 min/4°C/14.000 rpm) and transferred to the Mobitec column (was washed and equilibrated prior to use) for incubation with the beads. After one hour incubation at 4°C (end-over-end), the beads were centrifugated and the column washed two times by centrifugation (200 g/ 1min/4°C). Elution was performed with 0.1 M glycine pH 2.8.

Solubilization buffer	50 % Glycerol 1 % Digitonin 20 mM Tris pH 7.4 50 mM NaCl 1 mM EDTA 2 mM PMSF
Wash buffer	50 % Glycerol 20 mM Tris pH 7.4 50 mM NaCl 1 mM EDTA 0.3 % Digitonin 1 mM PMSF

2.4.3.2 Isolation of protein complexes via IgG chromatography

1 mg of isolated mitochondria from yeast strains expressing Protein A tagged proteins was centrifuged for 10 minutes at 14.000 rpm/4°C. The mitochondrial pellet was solubilized in solubilization buffer for 30 min at 4°C (end-over end shaker). The lysate was cleared (15 min/ 14.000 rpm/ 4°C) and incubated with IgG Sepharose (previously

washed with 2 x 500 µl acetate buffer and 4x with 250 µl solubilization buffer) for 2 hours at 4°C (end-over-end shaker). The unbound material was removed by an intensive washing step. Subsequently Protein A tagged proteins coupled to IgG Sepharose beads were incubated with TEV protease over night at 4°C. The isolated tagged proteins were cleaved from Protein A by TEV-protease. TEV-protease was bound to 30 µl of Ni^{2+}-NTA-Agarose and elution was performed by centrifugation. SDS-Leammli buffer was added to the beads for a second elution.

Solubilization buffer	50 % Glycerol 1 % Digitonin 20 mM Tris pH 7.4 50 mM NaCl 1 mM Pefabloc 1 mM EDTA 2 mM PMSF 1 µg/ml Leupeptin
Wash buffer	50 % Glycerol 20 mM Tris pH 7.4 50 mM NaCl 1 mM EDTA 0.3 % Digitonin 1 mM PMSF
Acetate buffer	0.5 M HAc 0.5 M NH_4Ac pH 3.5
TEV cleavage buffer	10 % Glycerol 0.3 % Digitonin 20 mM Tris pH 7.4 50 mM NaCl 2 mM PMSF

2.4.3.3 *In vitro* binding experiments

To analyze Mdm38 interactions *in vitro*, purified GST-Mdm38 (see 2.4.1.2) was used. Protein concentrations of the bait proteins were determined using Bradford assay and SDS-PAGE and identical amounts of different recombinant proteins (GST and GST-Mdm38 fusions) were incubated with 1 mg of mitochondria solubilized in buffer containing 1 % digitonin or 0.3 % Triton X-100. After 2 hours incubation (4°C, end-over-

end shaking) the GST-fusion protein and the specific interacting mitochondrial proteins, were bound to GSH-Sepharose (in a Mobitec column). After 30 minutes incubation (4°C/ end-over-end shaking) the column was washed with 10 times 500µl wash buffer and subsequently eluted by addition of SDS-Laemmli buffer. Co-isolated mitochondrial proteins were separated by SDS-PAGE and analyzed by immunodetection.

1X PBS-buffer / cell opening buffer	140 mM NaCl 2.7 mM KCl 10 mM Na_2HPO_4 1.8 mM KH_2PO_4 1.5 mM PMSF 0.75 % Triton X-100 DNase1 (10 mg/ml) Complete EDTA-free protease inhibitors (1 Tab/50ml) 1 µg/ml Leupeptin 1 mM Pefabloc 0.675 mM EDTA
Solubilization buffer	0.3 % Triton 50 % Glycerol 20 mM Tris pH 7.4 50 mM NaCl 5 mM EDTA 1 mM Pefabloc 2 mM PMSF 1 µg/ml Leupeptin
Wash buffer	0.15 % Triton 20 mM Tris pH 7.4 50 mM NaCl 50 % Glycerol 5 mM EDTA 1 mM Pefabloc 2 mM PMSF 1 µg/ml Leupeptin
Glutathione cleavage buffer	140 mM NaCl 2.7 mM KCl 10 mM Na2HPO4 1.8 mM KH2PO4 10 mM Glutathione

2.4.4 Labeling of mitochondrial translation products

2.4.4.1 *In organello* labeling of mitochondrial translation products

In organello labeling of mitochondrial translation products was performed as initially described by Celis (1994). Per labeling reaction 4 µl of mitochondria (10 mg/ml) have been carefully mixed with 40 µl translation buffer (freshly prepared), 3 µl pyruvate kinase (0.5 mg/ml) (freshly prepared) and 11 µl H_2O. After equilibration at 30°C for two minutes the labeling was started by addition of 2 µl ^{35}S-methionine (10 mCi/ml). Translation was stopped after 20-30 minutes at 30°C/300 rpm by addition of 10 µl 0.2 M non-labeled methionine and mitochondria were further incubated for 5 min at 30°C before the reaction was cooled down on ice. Mitochondria were collected by centrifugation (10 min/14.000 rpm/ 4°C) and washed with 150 µl SEM buffer + 5 mM methionine. The pellet was resuspended in 30 µl SDS-Laemmli buffer while shaking at RT for 30 minutes and finally subjected to SDS-PAGE. After electrophoresis the radiolabeled translation products were analyzed by digital autoradiography.

Component	Concentration	Storage [°C]
Sorbitol	0.9 M	RT
KCl	225 mM	RT
Kpi pH 7.2	22.5 mM	RT
Tris pH 7.2	30 mM	RT
$MgCl_2$	19 mM	RT
BSA f.a. free	4.5 mg/ml	-20
ATP pH 7.2	6 mM	-20
GTP pH 7.2	0.75 mM	-20
α-Ketoglutarate	9 mM	-20
phosphoenolpyruvate	10 mM	-20

Amino acids-mix-methionine	0.15 mM	-20
Cyclohexamide (CHX)	7.5 µg/ml	Fresh

Table 2.8: Components for 1.5x translation buffer

2.4.4.2 *In vivo* labeling of mitochondrial translation products

To analyze the pattern of mitochondrial protein synthesis in living cells (Douglas et al. 1976), yeast cells from a fresh plate were inoculated in 5-10 ml YPGal (see 2.2.2.1) medium and grown to an optical density of OD_{600} 0.5-1.0. The cells were harvested by centrifugation (1Min/5000 rpm/RT) and the pellet was washed in 500 µl labeling buffer (centrifuging at RT/1 min/ 5000 rpm). Cells were resuspended in 500 µl labeling buffer and incubated for 10 minutes at 30°C while shaking at 1000 rpm. Cytosolic translation was stopped by addition of 10 µl fresh cyclohexamide (CHX: 7.5 mg/ml). After a 5 minutes incubation period 2µl ^{35}S-methionine was added to the sample and mitochondrial translation products were labeled for 5-30 min (Pulse). Subsequently, 10 µl 0.2 M non-labeled methionine were added and a chase of 5 minutes was performed (for pulse-chase experiments the incubation time with non-labeled methionine was increased to 80 minutes). The reaction was put on ice and whole cell extracts were prepared: Cells were centrifuged down and resuspended in 500µl ddH_2O. After addition of lysis solution (75 µl 2M NaOH, 6 µl ß-ME), the sample was mixed and incubated on ice for 10 minutes. For precipitation of proteins, 80 µl 50% (w/v) trichloroacetic acid (TCA) were added. The sample was incubated on ice for 20 minutes and subsequently centrifuged at max. speed for 20 minutes/ 4°C. The pellet was resuspended in 50µl SDS-sample buffer while shaking at RT for 30 minutes. Samples were subjected to SDS-PAGE and digital autoradiography.

Labeling buffer	40 mM KPi pH 6.0 2 % Galactose

2.5 Structural biology methods

All analyzes concerning the crystallization procedure and the resolution of the structure have been performed in collaboration with Domenico Lupo; University of Heidelberg.

3. RESULTS

3.1 Mdm38 interacts with the mitochondrial translation machinery

3.1.1 Establishment of an Mdm38 interaction assay

3.1.1.1 Cloning and expression of the Mdm38 truncation construct in *E. coli*

Mdm38 is a mitochondrial inner membrane protein of 65 kDa and was suggested to be involved in the export of newly synthesized, mitochondria encoded proteins into the inner membrane (Frazier et al. 2006). However, the molecular function of Mdm38 remains enigmatic, therefore, it was of importance to identify new interaction partners of the protein in order to obtain knowledge on the role of Mdm38 in the mitochondrial export machinery. For this purpose, a recombinant Mdm38 truncation construct suitable for an *in vitro* binding assay, was generated.

Interestingly, Mdm38 was predicted to contain coiled coil motifs in its C-terminal domain (aa 411-438, aa 507-538) (Figure 3.2). Coiled coil motifs are known to mediate protein-protein interactions and suggested to have a similar function in Mdm38. Moreover, Mdm38 is predicted to possess one transmembrane span at the N-terminus between aa 137-157 (Figure 3.1; 3.2). An overview of the predicted domains of Mdm38 is given in figure 3.1.

In order to analyze the interaction partners of Mdm38 *in vitro*, the truncation construct was expressed and purified from *E. coli*. To optimize the solubility of the construct, an area behind the predicted transmembrane span of Mdm38 was chosen (aa 159-573), termed Mdm38^{CTD} (Figure 3.3).

Figure 3.1: Scheme of Mdm38 domains (aa 1-573)
Schematic overview of Mdm38 including all predicted protein domains. Abbreviations: PS (presequence); TM (transmembrane span); CC (coiled coil); numbers indicate amino acids.

A

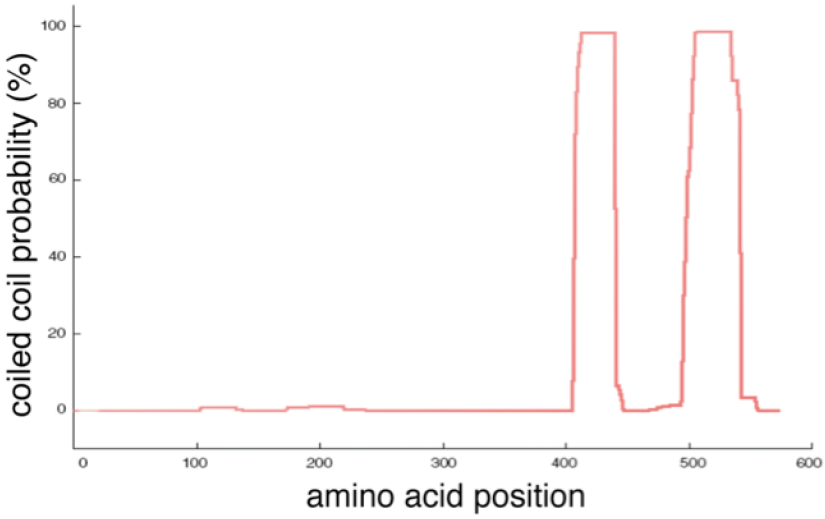

B

```
1         10        20        30        40        50        60        70        80
MLNFASRASC VTRRQASLYF VKNQGPRLIA STIPSCHWPL RAQGVQPNLS LRFYSTDKSK SVTKPVAPTS TDAPAKPKET

          90       100       110       120       130       140       150       160
LMVKVKHALK HYANGTKLLG YEIKVSTKLL IKFAQGYELS RRERNQLRRT MGDVFRLIPF SAFLIIPFAE LFLPFALKLF
                                                                 transmembrane span
         170       180       190       200       210       220       230       240
PNLLPSTYES GKDKQAKRNK LIEIRKKTSE FLHETLEESN LITYNTIENA EKKQKFLNFF RKLYSAKEGK IMTFQHDEIS

         250       260       270       280       290       300       310       320
AIAQMFKNDS VLDNLSRPQL AAMSKFMSLR PFGNDNMLRY QIRSKLKDIM NDDKTIDYEG VESLSQEELY QACVSRGMKA

         330       340       350       360       370       380       390       400
YGVSKEDLVD NLKVWLELRL RQKIPSVLMV LSSTFTFGGL PKENYSKAFS PLAEKKETKS KYDDLLDLYY DGILQVLSSI

         410       420       430       440       450       460       470       480
PDPVYNVAKL DVSESKSSAA ETEAEKQVAE KKIKTEEKPE ETAIPKEEAT AKESVIATTA SAVTPKLVVV NEKAETAKTE
           coiled coil
         490       500       510       520       530       540       550       560
EISQEKENAE PTDSAEATEA EEKKTSDDNE FKLNVLKEQE ELIKKEEEEA KQRASREHVP DDINLDEEEE AKSVPPIPAD
                                 coiled coil
         570  572
QAAKTFVIKK D*
```

Figure 3.2: Overview of predicted domains in Mdm38
A: Coiled coil probability of Mdm38's amino acid sequence: Coiled coil prediction was performed using http://www.ch.embnet.org; B: Amino acid sequence of Mdm38: Overview of the amino acid sequence of Mdm38 was generated with Geneious Pro 4.8.3. Predicted transmembrane span and coiled coil domains are marked by blue arrows.

Figure 3.3: Overview of full-length Mdm38 (aa 1-573) and generated C-terminal truncation construct (aa 159-573)
Specific protein domains are indicated in dark grey, numbers indicate amino acids.

The $Mdm38^{CTD}$ construct was generated with an N-terminal GST-tag as well as a C-terminal His_6 tag to enable double affinity purification. Therefore, the open reading frame of *MDM38*, encoding for residues 159-573 (C-terminus without transmembrane span), was amplified by PCR from yeast genomic DNA (see 2.3.1.1) and primers were designed to add flanking restriction sites for *Sal*I and *Not*I (see 2.3.2.4) to the PCR-product. To increase solubility and to enable detection as well as purification of the recombinant protein, the PCR product was cloned in the pGEX-4T3 vector, adding a GST-tag (see 2.3.2.5). Ligated plasmids were transformed into *E. coli* XL1 Blue cells (see 2.3.3.2), plasmid DNA was isolated (see 2.3.1.2) and clones were sequence-verified (see 2.3.3.3). For recombinant protein expression, plasmids were transformed into the BL21 (DE3) *E. coli* strain (see 2.1.7.1).

To optimize GST-$Mdm38^{CTD}$-His_6 expression in BL21 cells (see 2.2.1.2), different induction times were used: Cells were harvested after 1.5 h or 3 h of 0.5 mM IPTG addition and collected by centrifugation. The cell pellet was resuspended in SDS-Loading buffer (Laemmli), subjected to SDS-PAGE (see 2.4.2.1), and subsequently analyzed by either Coomassie staining (see 2.4.2.3) or immunodetection (2.4.4.5) (Figure 3.4).

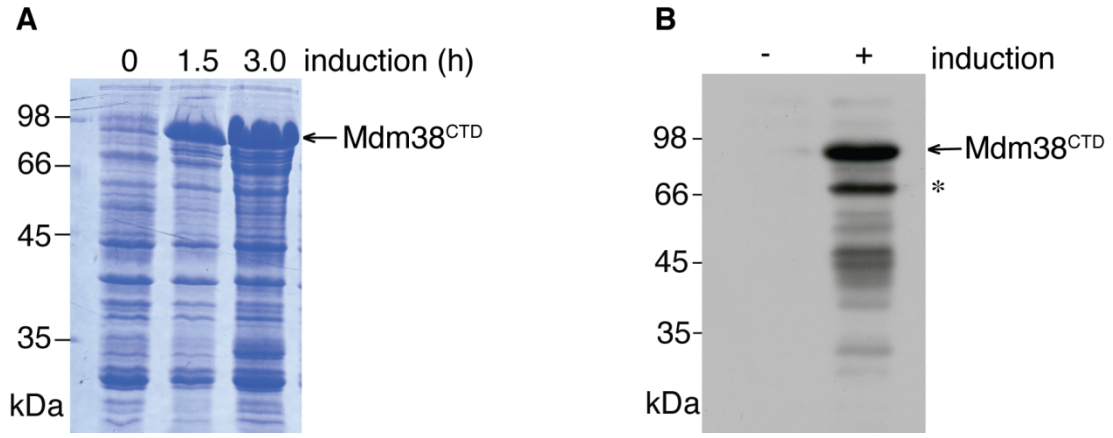

Figure 3.4: Expression of GST-Mdm38^{CTD}–His$_6$
A: Coomassie stained SDS-PAGE analysis of harvested *E. coli* cells after 1.5 h and 3.0 h of expression of the GST-Mdm38^{CTD}-His$_6$ construct, induced by 0.5 mM IPTG (control lane without IPTG induction). B: Western blot and immunodetection using an antibody directed against the Mdm38 C-terminus. Arrows point to the signals of interest (GST-Mdm38^{CTD}-His$_6$ construct). * Unspecific signal.

To analyze the protein solubility, 0.5 g of *E. coli* cells expressing GST-Mdm38^{CTD}-His$_6$ construct (see 2.2.1.2) were resuspended in 1x PBS (see 2.4.3.2) and disrupted via French press (see 2.4.1.1). Insoluble particles were pelleted via centrifugation and soluble proteins were further analyzed. Samples were taken after cell disruption (=T [total]) and after centrifugation: S (soluble fraction), P (pellet). As a control, the same procedure was performed with *E. coli* cells expressing an insoluble protein construct (Shy1 [aa 50-389]-10His). All samples were separated by SDS-PAGE (see 2.4.2.1) followed by Coomassie staining (2.4.2.3) (Figure 3.5).

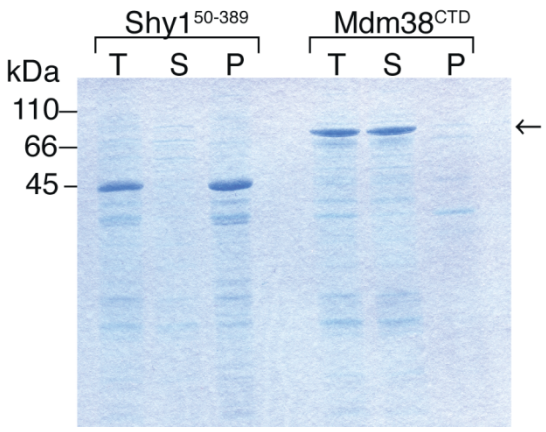

Figure 3.5: Test for solubility of GST-Mdm38^{CTD}-His$_6$ construct
To investigate the solubility of the GST-Mdm38^{CTD}-His$_6$ construct, *E. coli* cells were induced with 0.5 mM IPTG. After 3 h of induction, *E. coli* cells were harvested and disrupted by French press. Over-expression was confirmed using an aliquot of total lysate after French press disruption (= total [T]). Soluble (S) and insoluble (P) material was further separated by centrifugation and aliquots were analyzed by SDS-PAGE followed by Coomassie staining. Left hand side shows an insoluble construct of the protein Shy1 [aa 50-389]-10His, used as a control; right hand side shows the soluble

GST-Mdm38^{CTD}-His$_6$ construct. The signal of interest (GST-Mdm38^{CTD}-His$_6$ construct) is denoted by an arrow.

It could be shown that soluble GST-Mdm38^{CTD}-His$_6$ can be expressed in high amounts in *E. coli* BL21 (DE3) cells when cultured at 37°C and induced with 0.5 mM IPTG for 1.5–3 h. This led to the possibility of recombinant expression and purification of the Mdm38^{CTD} construct and, therefore further use in *in vitro* binding assays to determine its interaction partners.

3.1.1.2 Establishment of the Mdm38^{CTD} binding-assay

The recombinantly expressed GST-Mdm38^{CTD}-His$_6$ was used to examine mitochondrial interaction partners of Mdm38. For this purpose, a Glutathione-S-Transferase (GST)-binding-assay was established: Prior to performing the binding assay, the bait protein, GST-Mdm38^{CTD}-His$_6$, was purified (Step 1). In order to assess the binding specificity between the bait protein and the substrate, and further to exclude that the interaction was mediated by the GST-tag, GST (Step1) was also purified and used as a control. Purification was performed by binding the GST moiety to the glutathione coupled Sepharose matrix (I.), removing of contaminations by extensive washing (II.), and subsequent elution with reduced glutathione (III.). To control the efficiency of immobilization and purification of Mdm38^{CTD} and GST (control) prior to incubation with solubilized mitochondria, a small fraction of the eluate was analyzed by SDS-PAGE followed by Coomassie staining (IV.) (Figure 3.6). An estimation of the Mdm38^{CTD} and GST concentrations in the eluate was performed by Bradford protein determination.

Subsequently, an *in vitro* binding-assay, using purified GST-Mdm38^{CTD}-His$_6$ was established: Isolated mitochondria (see 2.2.2.5) were solubilized in buffer containing 0.3% Triton X-100 (V.) and incubated with purified Mdm38^{CTD} or GST (VI). Interacting proteins (bait + mitochondrial proteins) were rebound to GSH-Sepharose (VII). Unspecific binding of mitochondrial proteins to the bait protein was removed by extensive washing (VIII.). Finally, elution of GST-Mdm38^{CTD}-His$_6$ or GST and bound proteins was performed with reduced glutathione (IX.). The elution fractions containing specific protein complexes were analyzed by SDS-PAGE (X.) (see 2.4.2.1) and immunoblotting (see 2.4.2.4; 2.4.2.5). A schematic overview of the experimental procedure is given in figure 3.7.

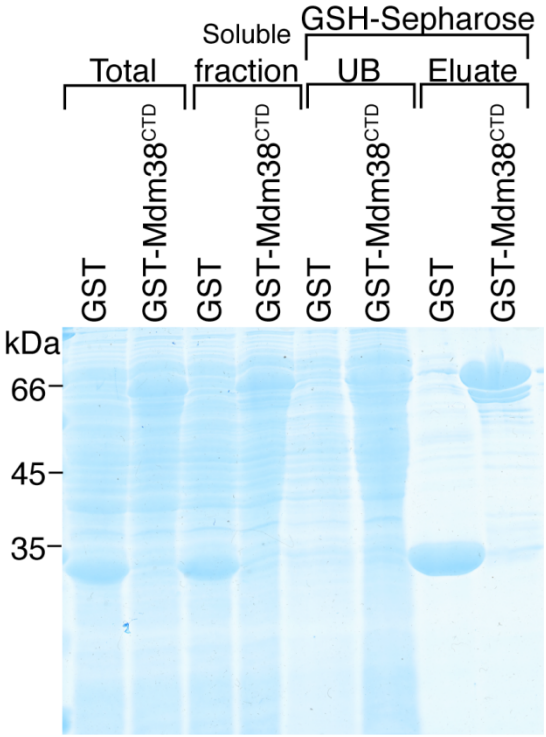

Figure 3.6: Purification of bait protein
E. coli cells expressing GST or GST-Mdm38^{CTD}(bait) were disrupted by French press (Total). Soluble fractions were harvested by centrifugation (Soluble fraction) and incubated with GSH-Sepharose in a Mobicol column. The unbound (UB) fraction was removed by centrifugation. Elution was performed with 10 mM Glutathione (Eluate).

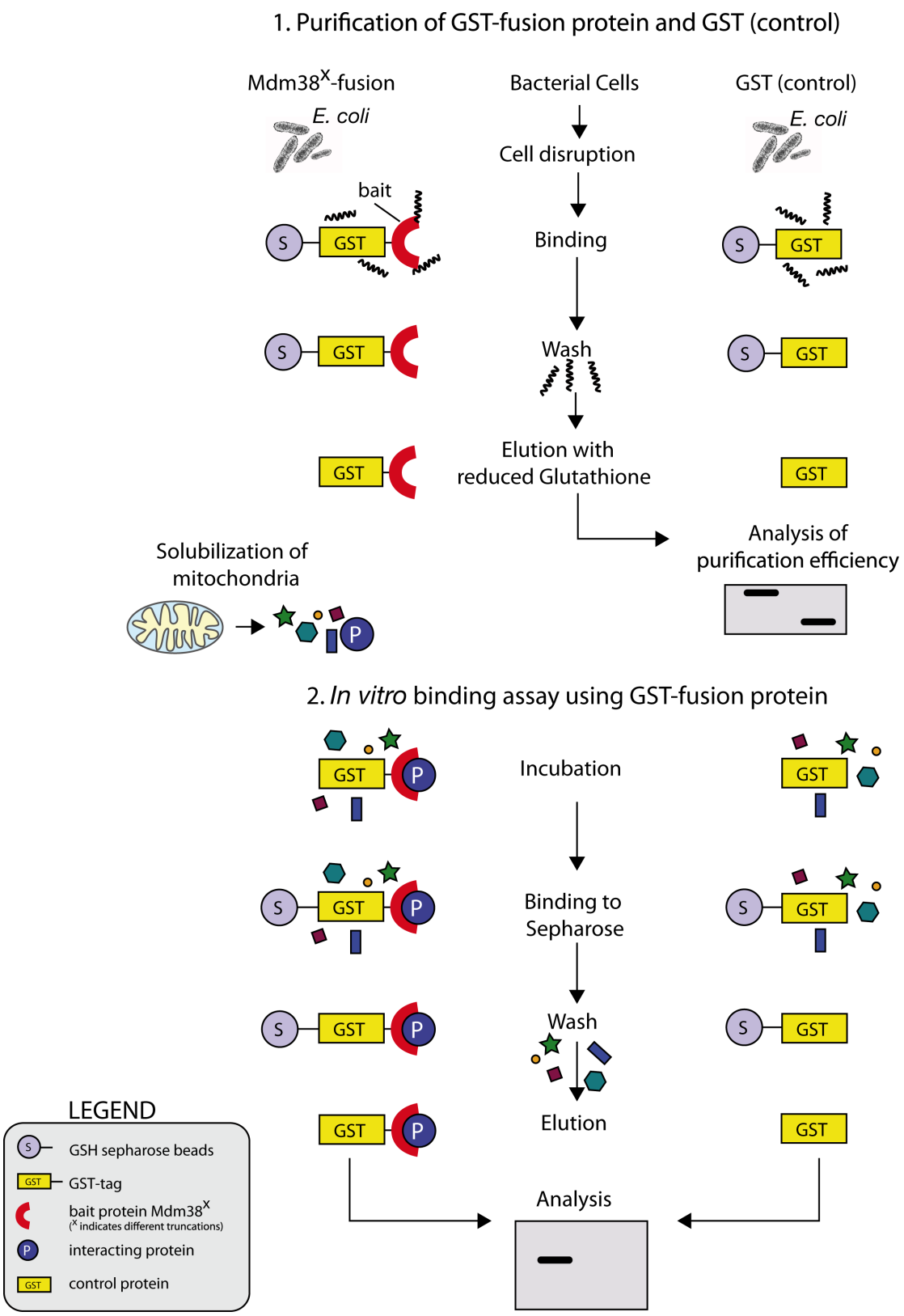

Figure 3.7: Schematic overview of the *in vitro* binding experiment procedure
Bait protein and GST (control) were purified with GSH-Sepharose. Mitochondria were solubilized and subsequently incubated with the bait or GST. Interacting proteins were bound to GSH-Sepharose and unspecific binding was removed by extensive washing. Elution was performed by the addition of SDS-Sample buffer. Interacting proteins were analyzed by SDS-PAGE and immunoblotting. For further explanation see 3.1.1.2.

3.1.2 Analysis of interaction partners of Mdm38

Previous analyses revealed that Mdm38 interacts with the mitochondrial ribosome and newly synthesized mt-encoded proteins, which is why it is suggested to be involved in the biosynthesis of mt-encoded proteins, particularly in their export from the matrix into the inner membrane (Frazier et al. 2006). Different studies concerning mitochondrial export machinery could demonstrate the physical interaction of Oxa1 (Jia et al. 2003; Szyrach et al. 2003) and Mba1 (Preuss et al. 2001; Ott et al. 2006) with the mt-ribosome, especially in terms of the assembly of newly synthesized Cox2 into the inner membrane (Hell et al. 1997; Hell et al. 2001). The exact insertion mechanism for all other mt-encoded proteins remained indeterminate, although Frazier et al. (2006) could provide support to the presumption, that Mdm38 plays a role in coupling ribosome function to protein transport across the inner membrane.

In order to elucidate the exact role of Mdm38 in the biogenesis of mt-encoded proteins, the established *in vitro* binding assay (see 3.1.1.2) was supposed to be used to identify proteins which interact with the C-terminal domain of Mdm38.

3.1.2.1 The C-terminus of Mdm38 interacts with proteins of the mitochondrial translation and export machinery *in vitro*

In vitro binding analysis was performed as described in 3.1.1.2 (Figure 3.7). Purified $Mdm38^{CTD}$ and GST (control) were incubated with solubilized mitochondrial extracts and interacting proteins were specifically co-purified. The samples were subjected to SDS-PAGE (see 2.4.2.1) and Western blotting (see 2.4.2.4). Interacting proteins were identified via immunodetection (see 2.4.4.5) (Figure 3.8).

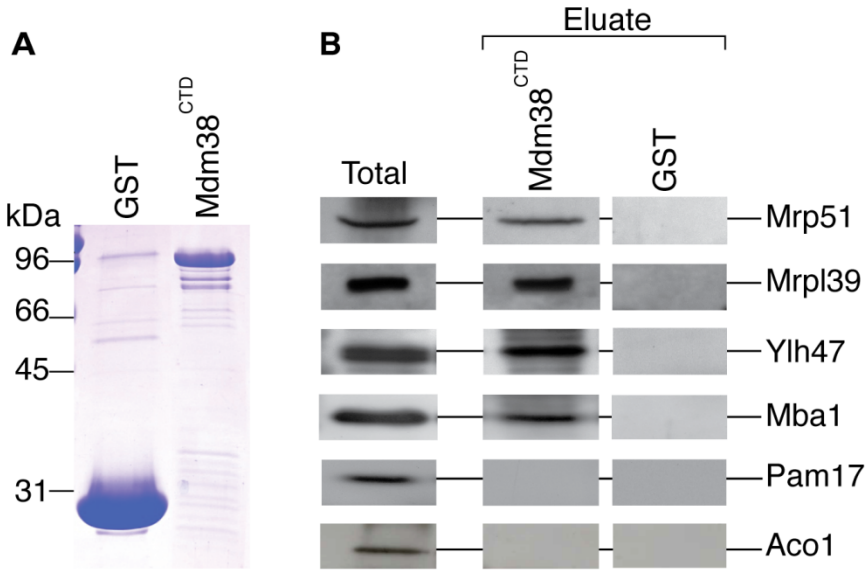

Figure 3.8: *In vitro* binding assay of Mdm38^{CTD}
Mdm38^{CTD} interacts specifically with the mitochondrial ribosome *in vitro*, as indicated by the presence of Mrp51 and Mrpl39 in the eluate. GST and GST-Mdm38^{CTD} were affinity-purified using GSH-Sepharose, and eluates were analyzed by SDS-PAGE and Coomassie staining (A). Wild type mitochondria were lysed (0.3 % Triton) and incubated with purified GST or GST-Mdm38^{CTD}. GST and GST-Mdm38^{CTD} were bound to GSH-Sepharose, unspecific binding was removed by extensive washing, and bound proteins were eluted and visualized by Western blotting using antibodies directed against the indicated proteins (B).

The presence of Mrpl39 and Mrp51 in the eluate indicated that Mdm38^{CTD} specifically interacts with mitochondrial ribosomes. Furthermore, the ribosome receptor protein Mba1 and the Mdm38 yeast homologue Ylh47 could be shown to interact specifically with Mdm38^{CTD}, as no interaction of these proteins with GST or with control proteins Pam17 and Aco1 could be observed. It can be suggested that the interaction of the mt-protein translation/export machinery components occurs at the C-terminus of Mdm38. Although interaction of Mdm38 with Ylh47 and ribosomal proteins had been shown before (Frazier et al. 2006), interaction partners of Mba1 have yet to be described. Previous studies have indicated that Mba1 binds to the large subunit of the mitochondrial ribosome and is involved in the co-translational insertion of nascent chains into the inner membrane (Preuss et al. 2001; Ott et al. 2006), however, the molecular function of Mba1 in the mitochondrial protein biosynthesis machinery and its role in mitochondrial translation was still unclear at the beginning of this study.

3.1.2.2 Interaction of Mdm38 with mitochondrial ribosomes is independent of Mba1

Here, it could be shown that Mdm38^{CTD} interacts with Mba1. Mba1 is a matrix protein, peripherally attached to the inner membrane, while Mdm38 possesses a predicted transmembrane span and exposes its large C-terminal domain into the mitochondrial matrix. Since Mba1 was shown to serve as a ribosome receptor, delivering proteins to Oxa1 (Preuss et al. 2001), it was speculated that the interaction between Mdm38 and the ribosome could be dependent on Mba1. To analyze this, the *in vitro* binding analysis (see 3.1.1.2) of ribosomal proteins with Mdm38^{CTD} was performed using solubilized *Δmba1* mitochondria (Figure 3.9).

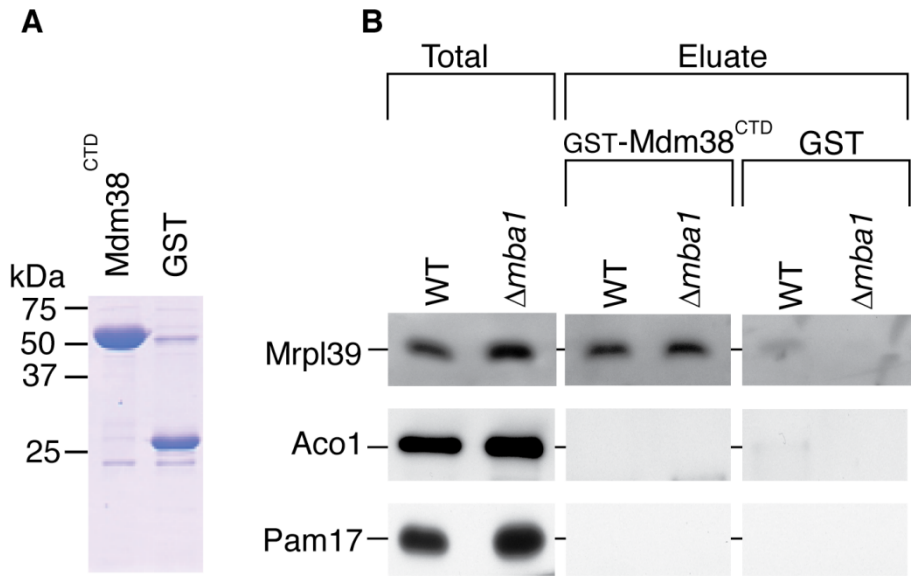

Figure 3.9: *In vitro* binding of Mdm38^{CTD} to mt-ribosome is independent of Mba1
Mdm38^{CTD} interacts specifically with the mitochondrial ribosome as indicated by the presence of Mrpl39 in the eluate, independent of the presence of Mba1. GST and GST-Mdm38^{CTD} were affinity purified on GSH-Sepharose. The amount of protein in the eluate was analyzed by SDS-PAGE and Coomassie staining (A). Wild type and *Δmba1* mitochondria were lysed (0.3 % Triton) and incubated with purified GST or GST-Mdm38^{CTD}. GST and GST-Mdm38^{CTD} were bound to GSH-Sepharose and unspecific binding was removed by extensive washing. Bound proteins were eluted and visualized by Western blotting using antibodies directed against the indicated proteins (B).

Since the level of mt-ribosome which co-isolated with Mdm38^{CTD} (indicated by the presence of Mrpl39 in the eluate) was identical from both, wild type and *Δmba1* mitochondria, it was shown that Mdm38 interacts with mitochondrial ribosome independent of Mba1. Little protein was bound to GST, indicating the specificity of the interaction between the mt-ribosome and Mdm38^{CTD}.

3.1.2.3 *In vivo* interaction of Mdm38 and Mba1 is independent of mitochondrial ribosomes

In vitro interaction analyses revealed that Mba1 interacts with Mdm38 (see 3.1.2.1), but does not mediate the association of Mdm38 to the mitochondrial ribosome. It could also be speculated that the interaction of Mdm38 and Mba1 occurs indirectly via the mitochondrial ribosome. To validate this speculation, the Mba1-Mdm38 interaction was analyzed *in vivo,* in ribosome-deficient yeast strains (*rho*^{0}-background). Complex isolations of Mdm38 were performed as described in Frazier et al. (2006), using WT and *rho*^{0} yeast strains expressing Protein A-tagged Mdm38. Mitochondrial extracts were incubated with IgG-Sepharose and extensively washed. Protein complexes were eluted via TEV cleavage and subsequently subjected to SDS-PAGE (see 2.4.2.1) and immunoblotting (see 2.4.2.4). Bound proteins were visualized using antibodies directed against the indicated proteins (Figure 3.10).

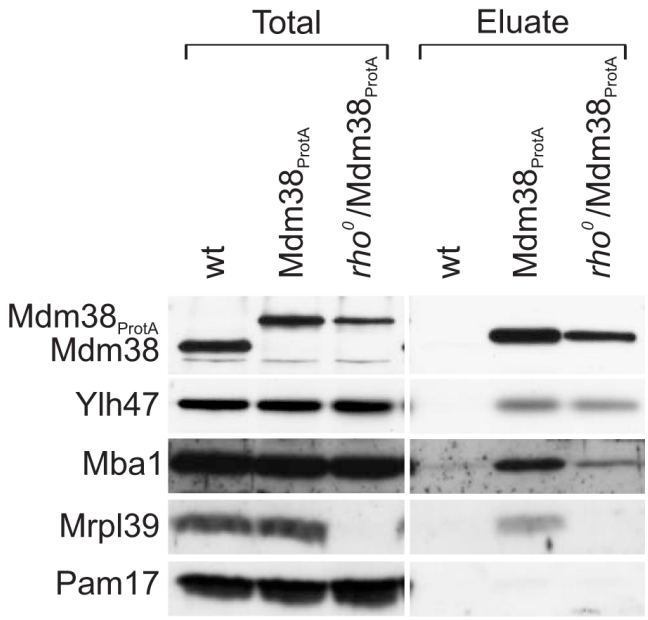

Figure 3.10: The interaction of Mdm38 and Mba1 is independent of the mt-ribosome
For protein isolation, mitochondria expressing Mdm38^{ProtA} either in a WT or a *rho*^{0}-background were lysed in solubilization buffer containing 1% digitonin. Mitochondrial extracts were incubated with IgG Sepharose. After 2 h of incubation, impurities were removed from the resin through extensive washing and native complexes were eluted by TEV cleavage. Proteins are visualized by immunodetection. Left 3 lanes (Total) show the mitochondrial extract; right 3 lanes (Eluate) show bound proteins. (Load: 4% of the total sample; 100% of the eluate).

Co-isolation experiments show that Mdm38 forms a complex with Mba1, Ylh47, and the mt-ribosome *in vivo*. Lack of mt-ribosomes did not influence the Mdm38 and Ylh47 interaction and Mba1 could be specifically co-purified with Mdm38^{ProtA} from *rho^0*-mitochondria. However, the amount of Mba1 specifically bound to Mdm38 was reduced in *rho^0*-mitochondria. Whether the mt-ribosome stabilizes or even stimulates the interaction between both proteins cannot be answered yet. This observation coincides with the publication by Preuss (2001), which postulates that Mba1 is part of an Oxa1-independent, novel protein insertion pathway. Mdm38 was also proposed to be involved in the export of newly synthesized mt-encoded proteins (Frazier et al. 2006). Whether both proteins interact by building a novel, Oxa1-independent insertion machinery can only be speculated at this point.

3.1.3 Growth phenotype and genetic interaction of Mdm38 and Mba1

Previous analyses of the growth behavior of *Δmdm38* cells (Frazier et al. 2006) and *Δmba1* cells (Ott et al. 2006) indicated a growth defect in both strains on non-fermentable carbon sources. In order to confirm the previously observed growth defects and to analyze the genetic interaction of both proteins, growth tests of WT, *Δmdm38*, *Δmba1* and *Δmdm38/Δmba1* yeast strains were performed (Figure 3.11, upper section). Growth test analyses confirmed the previously described phenotypes for the Δ*mdm38* and *Δmba1* strains on non-fermentable carbon sources. Interestingly, the double mutant displayed a severe respiration-deficient phenotype on non-fermentable carbon sources, suggesting that Mdm38 and Mba1 have overlapping functions for the assembly, maintenance, or the functionality of the respiratory chain.

Nowikovsky et al. (2007) characterized Mdm38 as an essential component of the mitochondrial K^+/H^+ exchange system. It was suggested that the observed *Δmdm38* phenotype on non-fermentable carbon sources is caused by an increased K^+ content and osmotic swelling, due to complete loss of mitochondrial K^+/H^+ exchange activity (Nowikovsky et al. 2004; Froschauer et al. 2005). Interestingly, it was shown that addition of Nigericin could rescue the *Δmdm38* growth-phenotype and improved the growth on non-fermentable carbon sources. To understand the interaction of Mdm38 and Mba1 in more detail, Nigericin sensitivity was examined in *Δmdm38/Δmba1* cells (Figure 3.11, lower section).

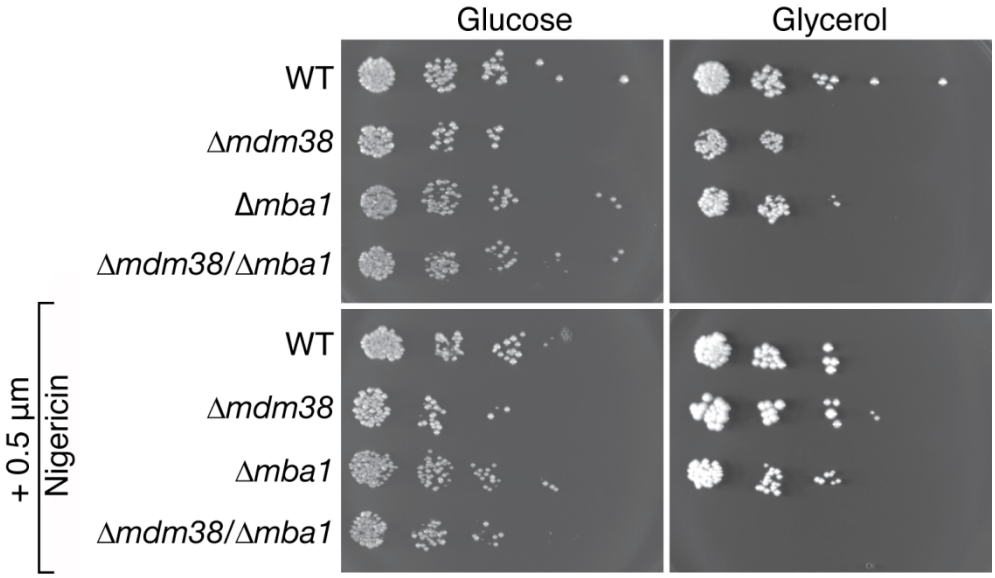

Figure 3.11: Treatment with Nigericin cannot rescue the *mdm38Δ/mba1Δ* phenotype
Indicated strains were grown on YPS medium and subjected to serial 10-fold dilutions. The dilutions were spotted on YP plates containing 2% glucose or 3% glycerol, and incubated at 30°C for 2 or 3 days, respectively. Plates containing Nigericin: 0.5 µM.

Although Nigericin restored the *Δmdm38* growth defect as previously reported by Nowikovsky et al. 2004, it did not compensate for the severe growth defect of the double mutant strain (*Δmdm38/Δmba1*). Furthermore, Nigericin did not improve the growth behavior of *Δmba1* cells, indicating that Mba1 is probably not involved in K^+/H^+ exchange. In conclusion, the observed data lead to the suggestions that the interaction of Mdm38 and Mba1 is probably independent of the putative ion homeostasis role of Mdm38. Whether the role of Mdm38 in K^+/H^+ exchange is direct or indirect cannot yet be dissected. However, an interaction of both ribosome receptor proteins, Mdm38 and Mba1, could be demonstrated. Obviously, both proteins play an important role in the functionality of mt-protein translation machinery, and therefore in the respiratory chain biogenesis.

3.1.4 Mdm38 interacts with *COX1*- and *COB*-specific translation activator proteins

Mdm38 interacts specifically with newly synthesized mt-encoded proteins (Frazier et al. 2006), additionally Mba1 was suggested to interact with translation products predominantly during their synthesis (Preuss et al. 2001; Frazier et al. 2006). Therefore, a possible interaction of Mdm38 with translation activator proteins was analyzed in

detail. Since Mdm38 was shown to be required for the biogenesis of cytochrome *b (COB)* and to be involved in transport of Cox1 across the inner membrane (Frazier et al. 2006), the interaction of Mdm38 and Pet309, a *COX1* translation activator protein (1.2.3.1.1 for further details), and Cbs1 (translation activator protein, controlling the *COB* translation; see 1.2.3.1.1 for further details) was analyzed using co-immunoprecipitation (see 2.4.3.1) (Figure 3.12).

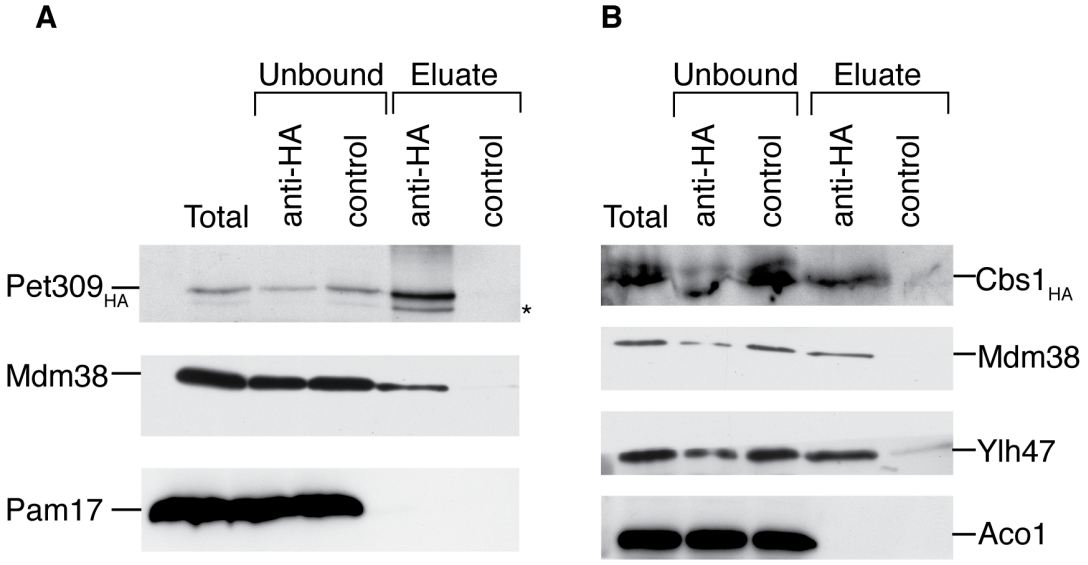

Figure 3.12: Mdm38 interacts with COX1 and *COB* specific translation activator proteins
Mitochondria expressing $Pet309_{HA}$ (A) or $Cbs1_{HA}$ (B) were solubilized in 1% digitonin buffer and subjected to co-immunoprecipitation with anti-HA or anti-FLAG antibodies (control). Bound protein was analyzed by immunodecoration using the indicated antibodies (Load: 5% of the total, 100% of the eluate). * Unspecific signal.

Pet309 (A) and Cbs1 (B) could efficiently be precipitated from mitochondrial extracts with HA antibodies. Mdm38 could be specifically co-immunoprecipitated with both proteins, whereas the control proteins Pam17 and Aco1 could not.

Interestingly, the yeast homologue of Mdm38, Ylh47, was co-immunoprecipitated with Cbs1, suggesting that both proteins are components of one complex (B). In conclusion, Mdm38 interacts in one complex with Pet309 (A), as well as with Cbs1 (B), however, whether the observed interactions are indirect or direct can only be speculated at this point. A role of Mdm38 for mt-protein biosynthesis was already shown, and since the protein also interacts with Mba1 (see 3.1.2.1 and 3.1.2.3) and very specifically with the mitochondrial ribosome (see 3.1.2.1 and 3.1.2.2), a putative mt-translation function of Mdm38 is conceivable.

3.2 Structural characterization of Mdm38

Mdm38 appears to be a mitochondrial protein of dual function, as on the one hand it is involved in ion transport (Froschauer et al. 2005), and on the other hand it interacts with both the mitochondrial ribosomes (Frazier et al. 2006) and the ribosome receptor protein Mba1 (see 3.1.2). Although there is data on the possible functions of Mdm38, there is still no structural information available. To understand the possible dual function of Mdm38, its structure was analyzed: The C-terminal domain of Mdm38 ($Mdm38^{CTD}$) was purified in preparative amounts and subjected to crystallization screens. The truncation construct, $Mdm38^{CTD,}$ was chosen for these screens as it includes the largest feasible soluble protein domain of Mdm38 and was previously shown to bind both mt-ribosomes and Mba1 (see 3.1.2).

All analyses concerning the crystallization and structural evaluation of Mdm38 were performed in collaboration with Dr. Domenico Lupo (AG Prof. Sinning/Heidelberg, Germany).

3.2.1 Purification of Mdm38

Prerequisites of protein crystallography are high amounts of highly pure and homogenous protein samples. Therefore, the expression and purification of GST-$Mdm38^{CTD}$-His_6 was optimized in large scale: *E. coli* BL21 (DE3) cells expressing the recombinant truncation construct were cultivated in LB-medium. The over-expression of the protein was induced by IPTG (see 2.2.1.2). Cells were harvested by centrifugation and disrupted by pressure (1000 psi) using an EmulsiFlex device (see 2.4.1.1). The GST-$Mdm38^{CTD}$-His_6 fusion protein was subsequently purified by applying two affinity chromatography steps: first on GSH-Sepharose 4B (elution by proteolytic cleavage with thrombin) and second on Ni^{2+}NTA Agarose (elution with 300 mM Imidazole). The batch method was used in both affinity chromatography steps. In order to concentrate the sample prior to size-exclusion chromatography, the elution fraction obtained from Ni^{2+}NTA chromatography was subsequently subjected to ultra filtration devices (see 2.4.1.4). Finally, the eluate was subjected to size-exclusion chromatography using a *16/60 Superdex200 prep grade* column on an Äkta-purifier. An overview of the purification procedure is also depicted in figure 3.13.

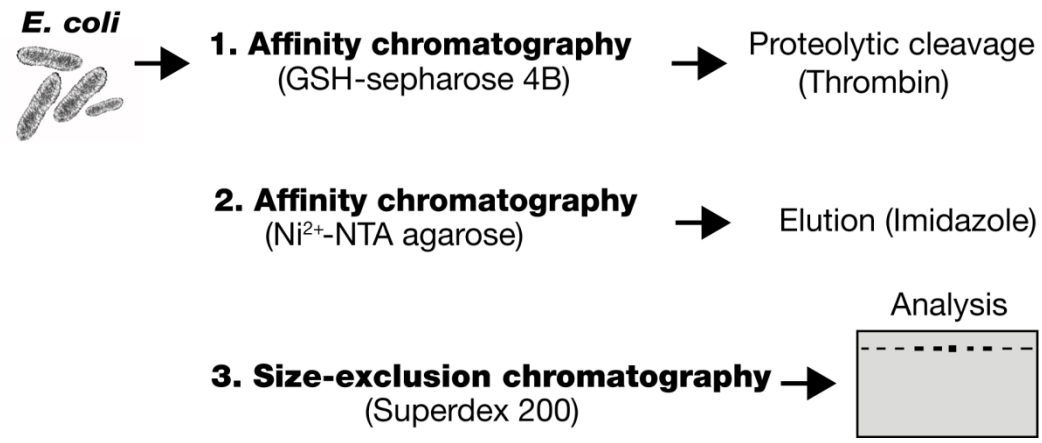

Figure 3.13: Overview of the GST-Mdm38^{CTD}-His$_6$ construct purification procedure
Purification of GST-Mdm38^{CTD}-His$_6$ was performed in 3 steps. After cell disruption the recombinant protein was purified on GSH-Sepharose. For further purification the eluate was subjected to Ni^{2+} NTA Agarose and finally to size-exclusion chromatography.

Purification fractions of different chromatographic steps were analyzed by SDS-PAGE and subsequent Coomassie staining.

Figure 3.14 shows the two-step affinity-purification procedure for the Mdm38^{CTD} construct. Figure 3.15 shows an elution spectrum of size-exclusion chromatography analysis of Mdm38^{CTD}.

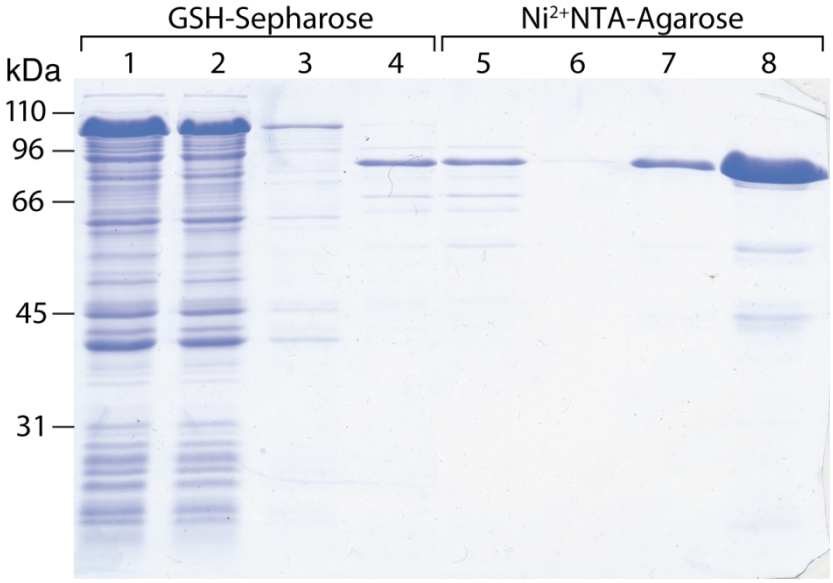

Figure 3.14: Purification of GST-Mdm38^{CTD}-His$_6$ on GSH-Sepharose and Ni^{2+}NTA Agarose
Overview of the GST-Mdm38^{CTD}-His$_6$ construct purification steps of from *E. coli* cell disruption to protein enrichment after the second affinity chromatography purification step. Load: 1 µl sample per lane. Fractions: 1: Lysate (cells disrupted via Emulsi Flex); 2: Unbound; 3: Wash; 4: Eluate; 5: Unbound; 6: Wash; 7: Eluate; 8: Centrifugal-filtration.

The overview (Figure 3.14) of the dual affinity chromatography purification steps indicates that the construct could be efficiently purified in sufficient amounts, as each lane on the SDS-PAGE gel contains 1% of the sample fraction. Figure 3.15 (A+B) shows analyses of size-exclusion chromatography on a *16/60 Superdex200 prep grade* column. Flow rate was 1 ml/min and the eluate was collected in 1.5 ml fractions.

A

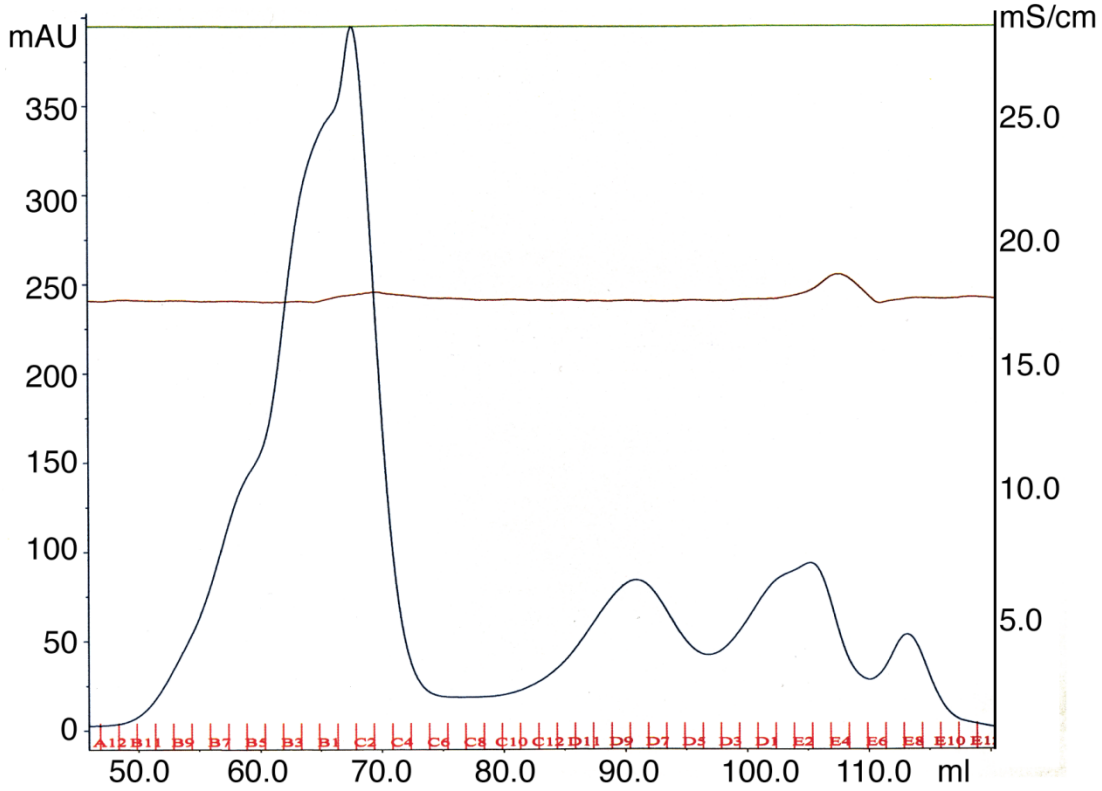

B

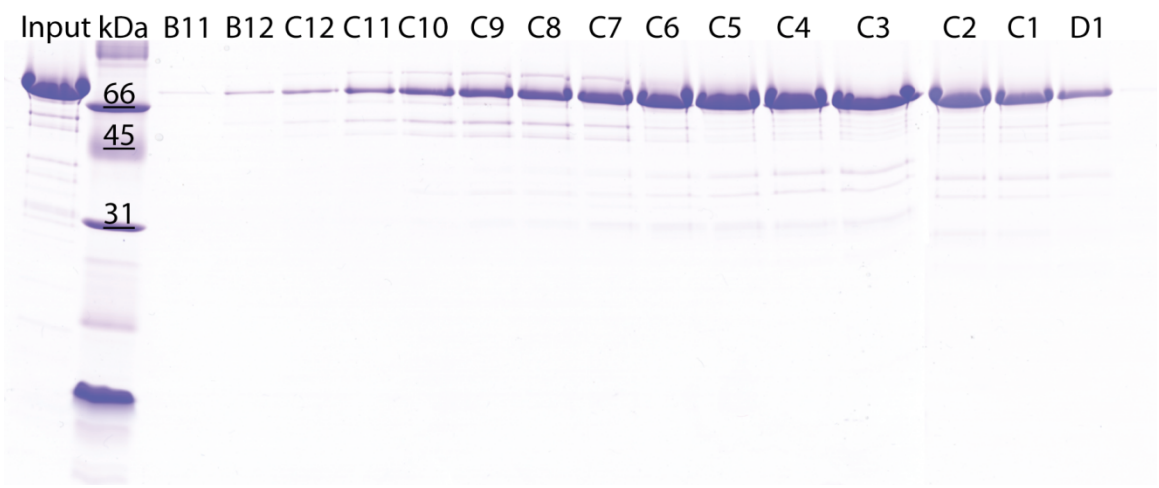

Figure 3.15: Size-exclusion chromatography of Mdm38^{CTD}-His$_6$ on S´dex 200 (Äkta Purifier)
Purified Mdm38^{CTD}-His$_6$ was subjected to size-exclusion chromatography for further purification. The sample was eluted in 1.5 ml fractions, which were analyzed by SDS-PAGE and subsequent Coomassie Brilliant Blue staining. A depicts the elution-profile of size-exclusion chromatography. In detail: blue line indicates absorption at a wavelength of 280 nm, brown line indicates the conductivity, red numbers indicate the collected fractions. B shows the Coomassie stained SDS-gel (load: 1% fraction per lane).

Gelfiltration of Mdm38^{CTD}-His$_6$ showed a prominent peak (Figure 3.15 A) in the absorption spectrum, which was identified as pure Mdm38^{CTD}-His$_6$ by subsequent SDS-analysis and mass spectrometry (data not shown). Comparison of the elution profile of Mdm38^{CTD}-His$_6$ with molecular weight marker proteins revealed a molecular mass of approximately 70 kDa, obviously not corresponding to the expected mass of 45 kDa. At that point in time, it could only be speculated if Mdm38 assembled into higher oligomeric forms. The purification of GST-Mdm38^{CTD}-His$_6$ protein was performed using 50 g of *E. coli* cells (wet weight) yielding 10 mg of purified protein, which is a sufficient quantity for crystallization trails.

3.2.2 Crystallization and X-ray diffraction of Mdm38

In order to obtain structural information on Mdm38^{CTD}, 10 mg of purified fusion protein were analyzed by our collaboration partner Dr. Domenico Lupo, University of Heidelberg, who performed the structural analyses. Mdm38^{CTD} was subjected to crystallization trails using the sitting drop method. First crystals appeared after 10 days in a condition containing 0.2 M potassium iodine (KI) and 20% PEG 3350. Crystals were flash frozen using 20% glycerol as cryoprotectant and analyzed at the European Synchrotron Radiation Facility (ESRF) in Grenoble (France). Data of a well diffracting crystal were collected and processed with the X-ray Detector Software (XDS) program package (Kabsch 1993). As no homologous protein structure was available in the database (based on primary sequence predictions), it was impossible to determine the structure of Mdm38 by molecular replacement. Therefore, a seleno-methionine labeled Mdm38^{CTD} construct had to be purified, in order to solve the structure by "Multiple Anomalous Dispersion" (MAD) phasing. BL21 (DE3) cells expressing the GST-Mdm38^{CTD}-His$_6$ construct were cultured in presence of L-seleno methionine (see 2.2.1.1 and 2.2.1.2). The L-seleno methionine GST-Mdm38^{CTD}-His$_6$ construct was also

purified by double affinity chromatography (Figure 3.16) and subsequent size-exclusion chromatography (Figure 3.17) (for an overview of the full purification procedure see figure 3.13). The purification on 30 g of *E. coli* cells (wet weight) provided 6 mg of SeMet-labeled Mdm38^{CTD}-His$_6$ fusion protein.

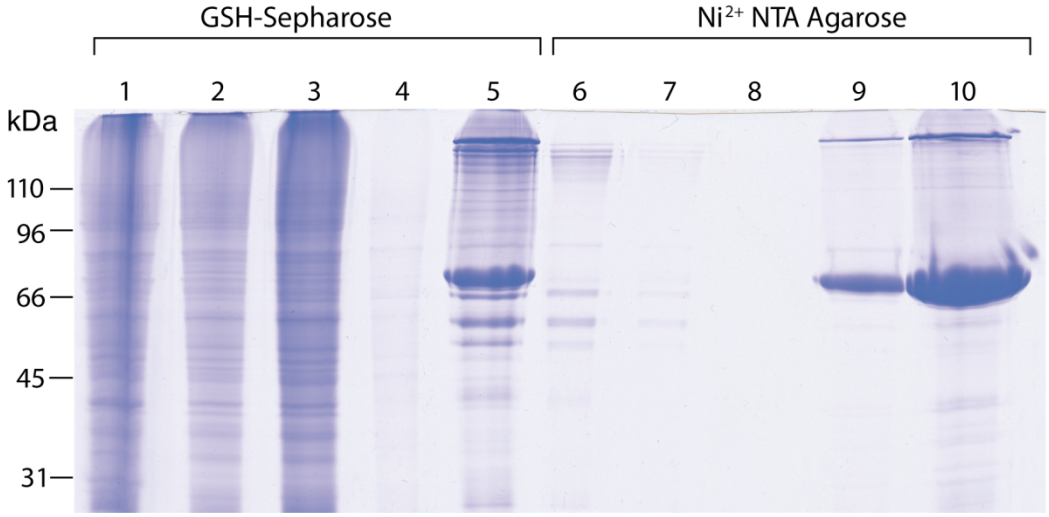

Figure 3.16: Purification of L-seleno methionine labeled GST-Mdm38^{CTD}-His$_6$ on GSH-Sepharose and Ni^{2+}NTA Agarose
Overview of purification steps of the L-seleno methionine labeled GST-Mdm38^{CTD}-His$_6$ construct from *E. coli*. Fractions: 1: Lysate (cells disrupted via French press); 2: Unbound; 3+4: Wash; 5: Eluate; 6: Unbound; 7+8: Wash; 9: Eluate; 10: Centrifugal filtration

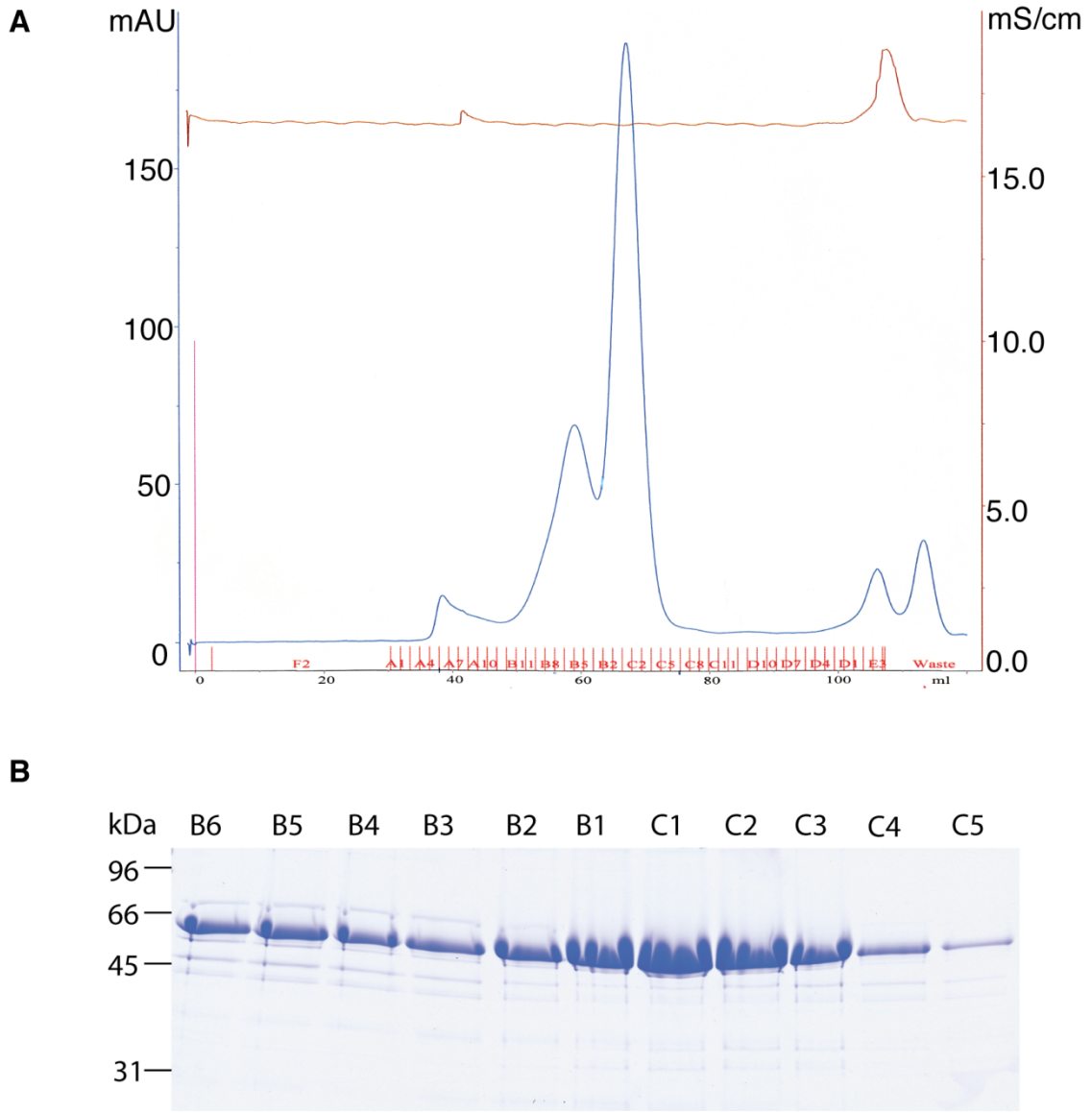

Figure 3.17: Size-exclusion chromatography of Seleno-Methionine-labeled Mdm38^{CTD}-His$_6$ on S´dex 200
SeMet-labeled Mdm38^{CTD}-His$_6$ construct obtained by double affinity chromatographic purification (Figure 3.16) was subjected to size-exclusion chromatography for further purification. The sample was eluted in 1.5 ml fractions, which were analyzed by SDS-PAGE and subsequent Coomassie staining. A: elution-profile of the size-exclusion chromatography. In detail: blue line indicates the absorption at 280 nm, brown line indicates the conductivity, red numbers indicate the collected fractions. B shows the Coomassie stained SDS-gel; only fractions B6 to C5 are shown (load: 1% of each obtained fraction was loaded with the concentrated sample corresponding to 10 fold more).

Purified SeMet-labeled Mdm38^{CTD}-His$_6$ was analyzed by Dr. Domenico Lupo, using the same crystallization conditions as previously used for the non-labeled construct. The screen was successful and the crystal could be measured at the ESRF (France). Data were processed with the program HKL2000 (Otwinowski et al. 1997) and phases were calculated using the program Solve (Terwilliger et al. 1999), allowing for the

construction of an initial model with the program Resolve (Terwilliger 2001; Terwilliger 2003). Manual correction of the model in Coot (Emsley et al. 2004) and subsequent running of Arp/wArp (Perrakis et al. 1999), using native data of 2.3 Å resolution, led to a final model. The model was used as a template for molecular replacement leading to data with a higher resolution of 2.1 Å. Moreover, it was subjected to iterative cycles of manual model building/validation in Coot and refinement with Refmac (CCP4, 1994).

The structure of Mdm38^{CTD} was solved and the model refined to 2.1 Å, with good crystallographic statistics (Table 3.1).

Data collection	**Mdm38 protein**
Space group	C2
Cell Parameters Axis a, b and c (in Å) Angles α, β and γ (in °)	124.527; 52.033; 47.232 90.00; 108.65; 90.00
Beamline	ESRF ID14-2
Wavelength (Å)	0.93340
Resolution (Å)*	30-2.1 (2.2-2.1)
Completeness (%)*	97.8 (97.6)
R_{sym} (%)*	5.1 (40.5)
I/σ*	15.8 (3.1)
Reflections (Total/Unique)	44 933/16 561

Refinement	**Statistics**
Resolution (Å)*	30-2.1 (2.2-2.1)
R_{cryst} (%)*	21.4 (26.0)
R_{free} (%)*	24.8 (34.0)
rmsd bond lengths (Å)	0.015
rmsd bond angles (°)	1.440
No. of atoms/B-factors	•
Protein	1 849/42.44
Others	9/73.34
Water	66/42.99

Table 3.1: Data collection and refinement statistics of the Mdm38^{CTD} crystal
$R_{sym} = \sum_{hkl} \sum_i |I(hkl; i) - \langle I(hkl)\rangle| / \sum_{hkl} \sum_i I(hkl;i)$
R_{cryst} ; $R_{free} = \sum_{hkl} | F_{obs}(hkl) - F_{calc}(hkl)| / \sum_{hkl} F_{obs}(hkl)$ whereby the summation runs over the working set and test set reflections, respectively.
*Values in parentheses are for the outmost resolution shell.

Mass spectrometric analysis of a single crystal was indicative of a possible proteolytic activity during crystallogenesis, which limited the structure of Mdm38^{CTD} to a 28.2 kDa fragment ranging from aa 159 to 408 (data not shown). The structure of the crystallized fragment depicts predominantly an α-helical fold (Figure 3.18), containing only the region between amino acid 182 to 408, as the first 23 N-terminal amino acids could not be resolved.

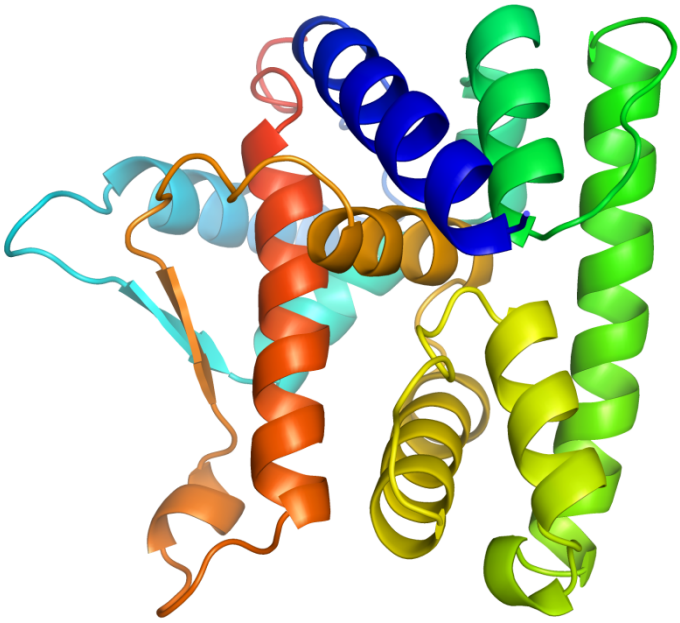

Figure 3.18: Structural model of Mdm38, amino acids 182-408
The crystal structure of Mdm38 (aa 182-408) was determined to a 2.1 Å resolution. Mdm38 forms a monomer in the crystal structure, which consists of 9 α-helices and 2 ß-sheets. Blue color indicates the N-terminus; red color indicates the C-terminus. Figure was generated with Pymol (DeLano, 2002)

3.2.3 Tertiary structure of Mdm38 displays high homology to 14-3-3 proteins

Primary amino acid sequence analysis found no homologous proteins of $Mdm38^{CTD}$, thus suggesting that it adopts a completely novel fold. The coordinates of the $Mdm38^{CTD}$ crystal structure were analyzed by the DALI-server (Holm et al. 2010) to search for structural homologues within the database of known protein structures (the search was performed by Dr. Lupo, University Heidelberg). According to the DALI score, $Mdm38^{CTD}$ showed the highest homology to different members of the 14-3-3-protein superfamily. Human 14-3-3-epsilon (ε) protein showed the highest homology to the $Mdm38^{CTD}$ fragment structure, which superposes with 96 C_{α}-atoms showing an average deviation of 4.2 Å (Figure 3.19). Therefore the structure of Mdm38 (aa 159-408) will be referred to as $Mdm38^{14\text{-}3\text{-}3}$.

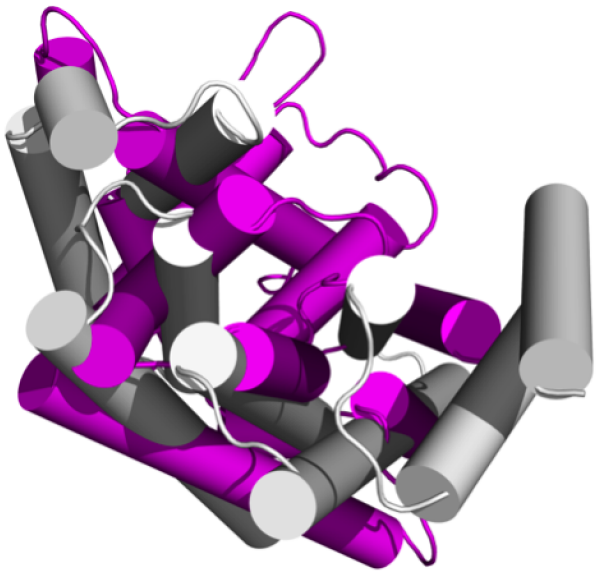

Figure 3.19: Superposition of yeast Mdm38^{CTD} with human protein 14-3-3 epsilon
According to the DALI server, the human 14-3-3 epsilon protein has the highest structural homology to the crystallized fragment of Mdm38^{CTD}. Pink depicts Mdm38^{CTD} fragment, and grey depicts human 14-3-3 epsilon. The average derivation of structure homology between both proteins is 4.2 Å.

3.2.3.1 Identification of a putative substrate-binding groove within the crystallized Mdm38^{CTD} construct

Within eukaryotic cells, 14-3-3 proteins are involved in several molecular and cellular functions by interacting with more than 200 binding partners, which have important roles in signal transduction, cell cycle regulation, apoptosis, stress responses, and malignant transformation (Darling et al. 2005). Apparently, the 14-3-3 proteins can regulate their target protein's function individually by several distinct mechanisms. In order to acquire information on specific domains which could be involved in the interaction between Mdm38 and the mitochondrial translation machinery, the structure of the Mdm38$^{14\text{-}3\text{-}3}$ protein was compared in more detail with those of 14-3-3 proteins. Special interest was devoted to a highly conserved region within the 14-3-3 protein family specialized in substrate accommodation, namely a central channel of dimensions 35 Å tall, 35 Å wide and 20 Å deep. Intriguingly, this region aligned in the superposition performed by the DALI server with a highly conserved cavity in Mdm38$^{14\text{-}3\text{-}3}$. This cavity might be a potential binding site for ribosomal proteins or ribosomal RNA (Figure 3.20).

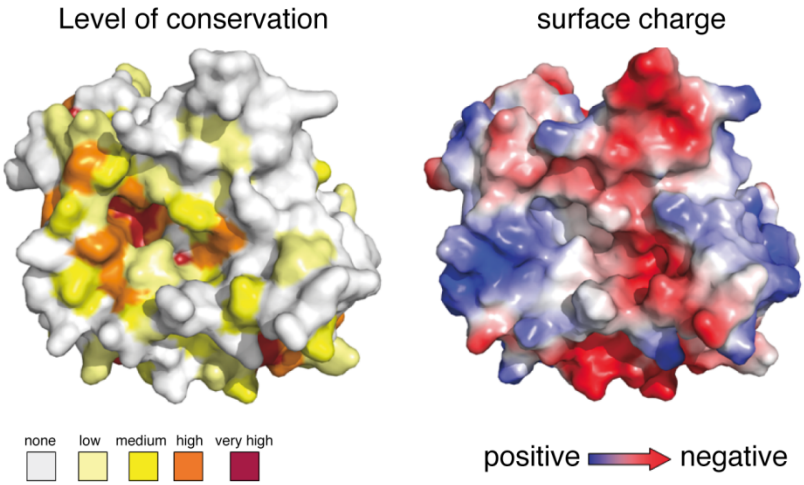

Figure 3.20: Hypothetical 14-3-3-like substrate binding groove within Mdm38
Superposition provided by the DALI Server revealed a putative 14-3-3 like substrate binding groove within Mdm38$^{14\text{-}3\text{-}3}$. Left side: Level of surface charge conservation*. Right side: Colors indicate surface charge of Mdm38$^{14\text{-}3\text{-}3}$. (* Indicated via ConSurf analyses of 100 members of the Mdm38/LETM1 family). Structural analyses have been performed by Dr. Lupo/Heidelberg.

3.2.3.2 Cloning and expression of the Mdm38 truncation construct containing only the predicted substrate-binding domain

The discovery of a 14-3-3-like substrate-binding domain in Mdm38$^{14\text{-}3\text{-}3}$ was an important reason to investigate the role of Mdm38 within the mt-translation machinery. Previous studies indicated that Mdm38^{CTD} interacts with the mt-ribosome as well as with two other export machinery components, Ylh47 and Mba1 (see 3.1.2.3). Since the size of the Mdm38$^{14\text{-}3\text{-}3}$ fragment (28.2 kDa) differed significantly from the size of the Mdm38^{CTD} construct (47.8 kDa), potentially missing interaction sites were examined. Interestingly the putative substrate-binding groove within Mdm38 contained a highly conserved positively charged patch, suggestive of an interaction site for negatively charged RNA or ribosomal proteins (Figure 3.20). Therefore, a recombinant Mdm38 truncation construct was generated, encompassing only aa 182-408, termed Mdm38$^{14\text{-}3\text{-}3}$. In analogy to the Mdm38^{CTD} construct, this construct was also generated with a N-terminal GST and a C-terminal His$_6$ tag. Figure 3.21 gives a schematic overview of the recombinant Mdm38$^{14\text{-}3\text{-}3}$ construct.

Figure 3.21: Overview on the double-tagged Mdm38$^{14\text{-}3\text{-}3}$ construct

3.2.3.3 *In vitro* binding analyses confirmed the interaction between Mdm38$^{14\text{-}3\text{-}3}$ and the mitochondrial ribosome

In order to assess if the 28.2 kDa Mdm38$^{14\text{-}3\text{-}3}$ construct was sufficient to interact with mitochondrial ribosomes, *in vitro* binding studies using purified GST-Mdm38$^{14\text{-}3\text{-}3}$-His$_6$ as bait were performed as described in 3.1.1.2 (Figure 3.7). Therefore GST-Mdm38$^{14\text{-}3\text{-}3}$-His$_6$ was purified, incubated with solubilized mitochondria and immobilized on GSH-Sepharose beads. In order to check for unspecific binding, GST-Mdm38^{CTD}-His$_6$ and GST were treated in the same fashion. Elution was performed with SDS-sample buffer; samples were analyzed by SDS-PAGE (see 2.4.2.1), and immunodecoration (see 2.4.2.5). It could be shown that mitochondrial ribosomes bound specifically to both Mdm38 constructs but not to the GST alone (Figure 3.22).

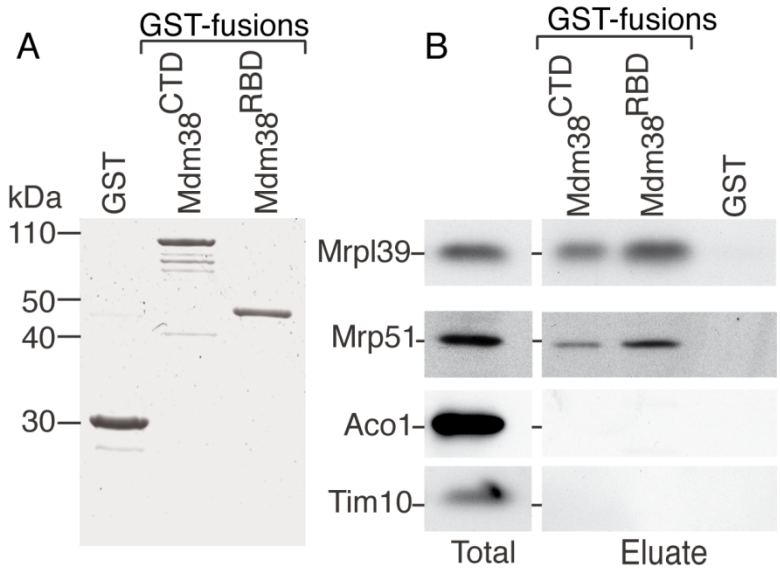

Figure 3.22: *In vitro* binding analysis using GST-Mdm38$^{14\text{-}3\text{-}3}$–His$_6$
In vitro binding analysis using GST, Mdm38^{CTD} and Mdm38^{RBD*}-GST fusion constructs revealed strong interaction of Mdm38^{RBD*} with mitochondrial ribosomes and strengthened the hypothesis of

a putative 14-3-3-like substrate-binding domain within Mdm38. A: Overview on the purification efficiency of GST and GST fusion constructs prior to incubation with solubilized mitochondria. B: Totals indicate the amount of mitochondrial proteins within the sample; Eluates indicate the amount of specifically pulled out mitochondrial proteins. Mrpl39 and Mrp51 signals demonstrate the interaction of the fusion constructs with the mt-ribosome, Aconitase 1 (Aco1) and Tim10 served as controls. (* $Mdm38^{RBD}$ also referred to as $Mdm38^{14\text{-}3\text{-}3}$).

Mitochondrial ribosome interaction with the Mdm38 constructs was monitored by Mrpl39 and Mrp51. The $Mdm38^{RBD}$ construct ($Mdm38^{RBD}$ = $Mdm38^{14\text{-}3\text{-}3}$) showed a stronger interaction with mitochondrial ribosomes than the $Mdm38^{CTD}$ construct. This *in vitro* observation demonstrates that the region of aa 182-408 within Mdm38 mediates its interaction with mitochondrial ribosomes. It is conceivable that the interaction occurs in the putative substrate-binding groove, but this hypothesis has still to be verified. According to its high ability to bind to mitochondrial ribosomes, $Mdm38^{14\text{-}3\text{-}3}$ will in the following be referred to as Mdm38 ribosome-binding domain ($Mdm38^{RBD}$).

3.2.3.4 Interaction of the Mdm38 ribosome-binding domain with *E. coli* ribosomes

In vitro binding experiments using $Mdm38^{RBD}$ illustrated its affinity to mitochondrial ribosomes (see 3.2.3.3). To verify the specific interaction of Mdm38 to mitochondrial ribosomes, the interaction of Mdm38 to *E. coli* ribosomes was analyzed. *E. coli* possess 70S ribosomes, which could be used as a model for the yeast mitochondrial 74S ribosomes. Interestingly, the specificity of $Mdm38^{RBD}$ is even higher than initially assumed, as the recombinant fusion protein was detected to bind to *E. coli* ribosomes within the bacterial cell. This interaction is very stable and survives the affinity purification procedure on GSH-Sepharose. In conclusion, $Mdm38^{RBD}$ could be purified with bound *E. coli* ribosomes (Figure 3.23).

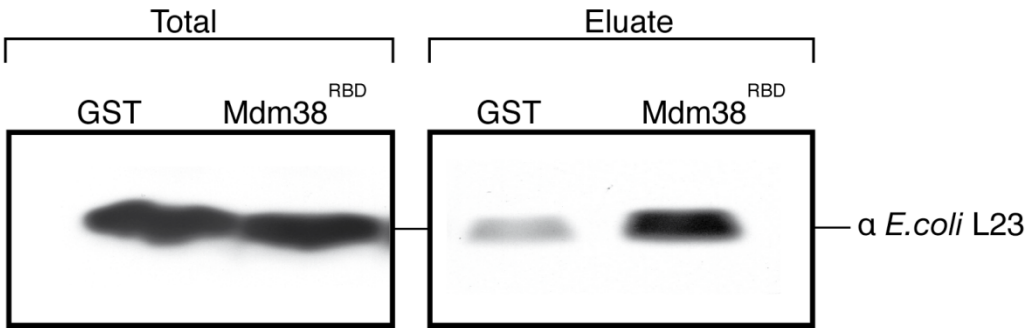

Figure 3.23: $Mdm38^{RBD}$ interacts with the *E. coli* ribosome
Specific interaction of $Mdm38^{RBD}$ with the *E. coli* ribosome is indicated by the presence of L23 ribosomal protein in the eluate. Total: fractions of GST and GST-$Mdm38^{RBD}$-$_{His6}$ after *E. coli* cell wall disruption and separation from insoluble components. Eluate: fractions of affinity purified GST and GST-$Mdm38^{RBD}$-His_6 with the specifically bound *E. coli* ribosome.

Mdm38^{RBD} specifically bound the *E. coli* ribosome as indicated by the presence of the protein L23 in the eluate, whereas only a minor amount of *E. coli* ribosome interacted with GST. In order to analyze whether the interaction between Mdm38 and *E. coli* ribosomes occurred during the purification procedure performed for the crystallized construct, binding of the *E. coli* ribosome was assessed in the presence and in the absence of Triton X-100. The presence of Triton X-100 during cell opening (1x PBS buffer with 0.3% Triton X-100) disrupted the interaction of Mdm38^{RBD} and *E. coli* ribosomes during *E. coli* cell wall rupture by French press. However, addition of isolated *E. coli* ribosomes (kindly provided by the group of Prof. Rodnina, MPIbpc Göttingen) to purified Mdm38^{RBD} (affinity purification on GSH-Sepharose and Ni^{2+} NTA Agarose) revealed efficient *in vitro* interaction as L23 was specifically bound and eluted in complex with Mdm38^{RBD}.

In *E. coli*, L23 is located at the peptide exit tunnel of the 50S ribosomal subunit (Gu et al. 2003). Its yeast homologue, Mrp20 (Fearon et al. 1992) is also located next to the peptide exit tunnel and interacts with Oxa1, the main component of the mitochondrial export translocase complex (Jia et al. 2003). Since it was predicted that Mdm38 is involved in mt-encoded protein export (Frazier et al. 2006) and the truncation construct Mdm38^{RBD} shows an affinity to yeast and *E. coli* ribosomal proteins, it can be concluded that the 14-3-3-like substrate binding groove within Mdm38^{RBD} probably plays an essential role in its interaction with 70S/74S ribosomal proteins.

3.3 *In vivo* characterization of Mdm38 domains

3.3.1 C-terminal truncation and Protein A-tagging of Mdm38

The results obtained by *in vitro* analyses indicated that Mdm38 can be dissected into three different domains: the N-terminal domain, including the transmembrane span, the central domain, including the ribosome-binding site, and the C-terminal domain, including the two coiled coil motifs. In order to analyze the function of the different domains of Mdm38 and to confirm the presence of the ribosome-binding site, two C-terminal Mdm38 truncation constructs were generated by chromosomal integration of a Protein A- His6 tag (see 2.3.5.1) according to Knop et al. (1999).

3.3.1.1 Generation of C-terminal truncation constructs

Figure 3.2 gives an overview of the Mdm38 amino acid sequence highlighting the predicted transmembrane span and coiled coils. The protein and its domains are shown schematically in figure 3.1. To demonstrate the importance of Mdm38 domain function, C-terminal truncations were constructed as shown in figure 3.24. The Protein A-tag (ProtA) was chosen for purification due to its high affinity to IgG-Sepharose. The presence of a His_6 tag allowed for a second affinity purification step while the specific TEV-cleavage site located between the protein and the double tag permitted an efficient tag removal.

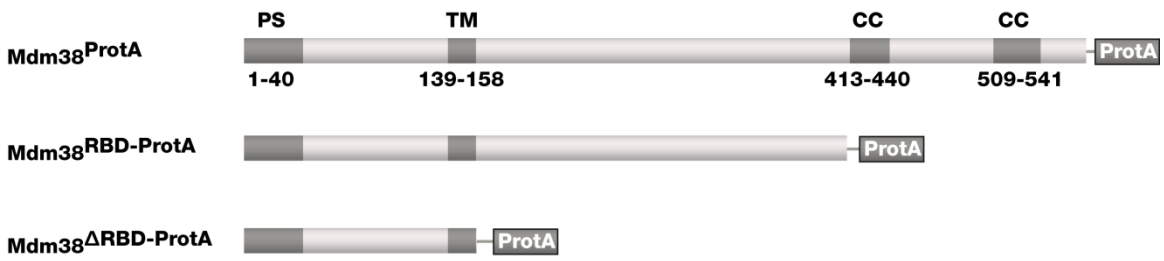

Figure 3.24: Scheme of Mdm38-Protein A-His_6 truncation constructs

3.3.1.2 Phenotype and expression-test of Mdm38-Protein A-truncations

To analyze the importance of both domains (the ribosome-binding domain and the C-terminal coiled coil domain) in regards to Mdm38 function, the growth phenotypes of yeast strains expressing the $Mdm38^{ProtA}$ truncations were analyzed on fermentable and non-fermentable carbon sources (Figure 3.25).

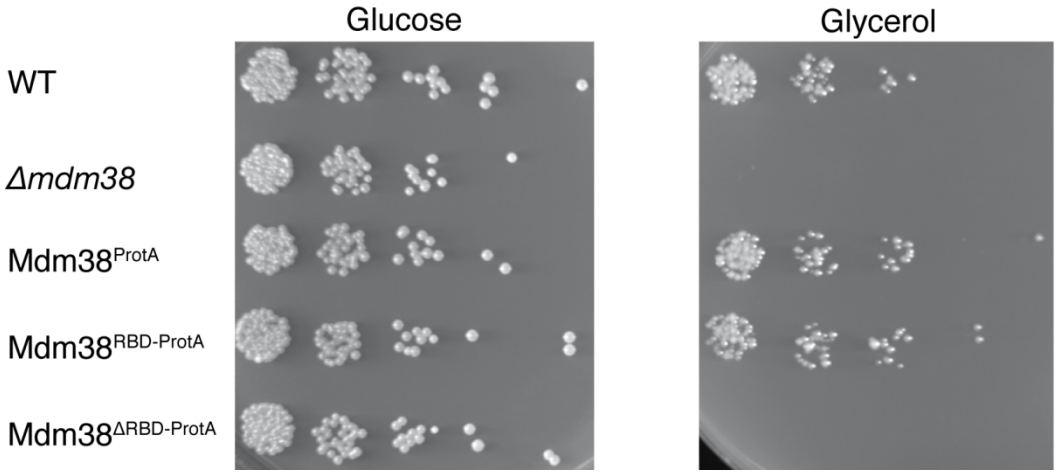

Figure 3.25: The RBD-domain of Mdm38 is essential for growth on non-fermentable carbon sources
Wild type cells (WT) and cells lacking Mdm38, or containing truncated forms of Mdm38 were cultivated in YPS medium and spotted in serial dilutions on YP-plates containing 2% glucose (YPD) or 3% glycerol (YPG). YPD plates were incubated at 30°C for 2 days, while YPG plates were incubated at 30°C for 3 days.

The growth phenotype analyses revealed a similar growth behavior of all tested strains on YPD, indicating that the Mdm38 protein is not essential for yeast cells viability on fermentable carbon sources (Figure 3.25). Additionally, on non-fermentable carbon sources, the growth phenotype of the WT, Mdm38^{ProtA} and Mdm38$^{RBD\text{-}ProtA}$ strain was not affected, indicating that mitochondrial function was not impaired in these strains. However, the growth behavior of the strain expressing Mdm38$^{\Delta RBD\text{-}ProtA}$ was severely affected, and the cells were unable to grow on non-fermentable carbon sources. These observations support the conclusion that the ribosome-binding domain of Mdm38 possibly plays an important role for mitochondrial respiratory function.

Nowikovsky et al. (2004) demonstrated that the addition of an artificial K^+/H^+ exchanger, Nigericin, to YPG plates fully compensated for the absence of Mdm38 in a *Δmdm38* strain. In order to assess which domain of Mdm38 could be involved in ion homeostasis, the growth phenotype of Mdm38-ProtA truncation constructs were analyzed on YPG/YPD plates supplemented with Nigericin (Figure 3.26).

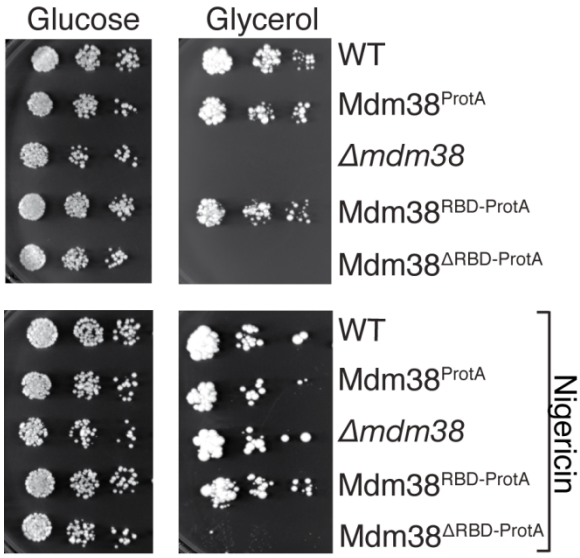

Figure 3.26: Growth defect of Mdm38^{RBD} cannot be complemented by Nigericin addition
Wild type (WT) and cells containing the Mdm38 truncated tagged protein were cultivated in YPS medium and spotted in serial dilutions on YP-plates containing 2% glucose (YPD) or 3% glycerol (YPG), as well as on YPD an YPG plates supplemented with 0.5 µM Nigericin. YPD plates (+/- Nigericin) were incubated at 30°C for 2 days. YPG plates (+/- Nigericin) were incubated at 30°C for 3 days.

Interestingly, the deletion of the ribosome-binding domain of Mdm38 led to a severe growth defect, which could not be complemented by the addition of Nigericin (Figure 3.26), in contrast to the *Δmdm38* strain. Based on this observation it can be concluded that the observed growth defect of Mdm38$^{\Delta RBD\text{-}ProtA}$ is probably unrelated to the role of Mdm38 in ion transport.

It was important to demonstrate that the observed growth phenotype was caused by the absence of the RBD and not by impaired expression levels or instability of the Mdm38^{ProtA} constructs within the cell. Therefore, mitochondrial proteins of both Mdm38 truncated constructs were separated by SDS-PAGE (see 2.4.2.1) and transferred to PVDF membranes by Western blotting (see 2.4.2.4). Immunodecoration with antibodies directed against either ProtA or the Mdm38 C-terminus (see 2.4.4.5) demonstrated that protein levels were not affected in the Mdm38 C-terminal truncated constructs (Figure 3.27). All indicated strains expressed similar amounts of Mdm38 or C-terminal truncated Mdm38.

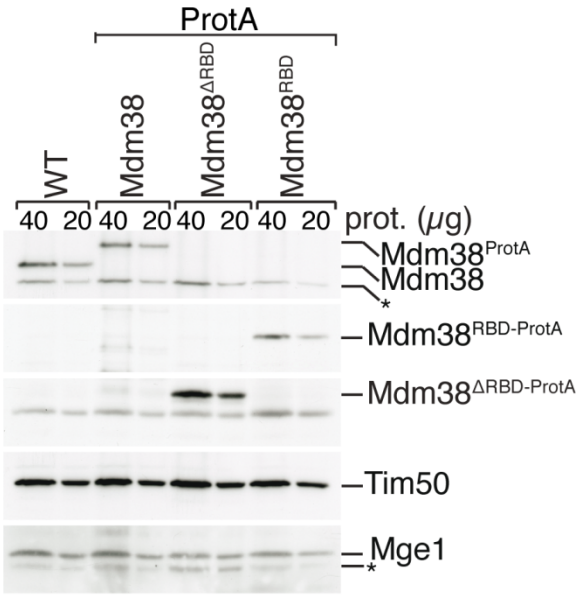

Figure 3.27: Expression and stability of Mdm38-ProtA constructs
20 and 40 µg of isolated mitochondria were separated by SDS-PAGE and subsequently subjected to immunodecoration. All indicated strains expressed similar amounts of Mdm38 or C-terminal truncated Mdm38. Mge1 and Tim50 were used as controls. * Unspecific signal.

3.3.2 Analyses of different Mdm38 domains

3.3.2.1 Mdm38 interaction with mitochondrial protein-translation machinery components is dependent on the ribosome-binding domain

Since *in vitro* analyses showed the existence of a ribosome-binding domain in Mdm38 (aa 182-408), it was important to test whether this interaction could also be verified *in vivo.* Furthermore, it was important to analyze, which other components of the mitochondrial translation machinery interact with Mdm38 lacking its C-terminal domain. Therefore, native complexes containing Mdm38 (full length or truncations) were isolated from yeast mitochondria: Mdm38^{ProtA} and Mdm38$^{RBD\text{-}ProtA}$ complexes were isolated from mitochondria solubilized under conditions shown to maintain the Mdm38-ribosome interaction (Frazier et al. 2006). The native Mdm38 complexes were released from the IgG-Sepharose by TEV protease cleavage (see 2.4.3.2). The samples were subjected to SDS-PAGE (see 2.4.2.1) and analyzed by immunoblotting (see 2.4.2.5), using antibodies directed against the indicated proteins (Figure 3.28).

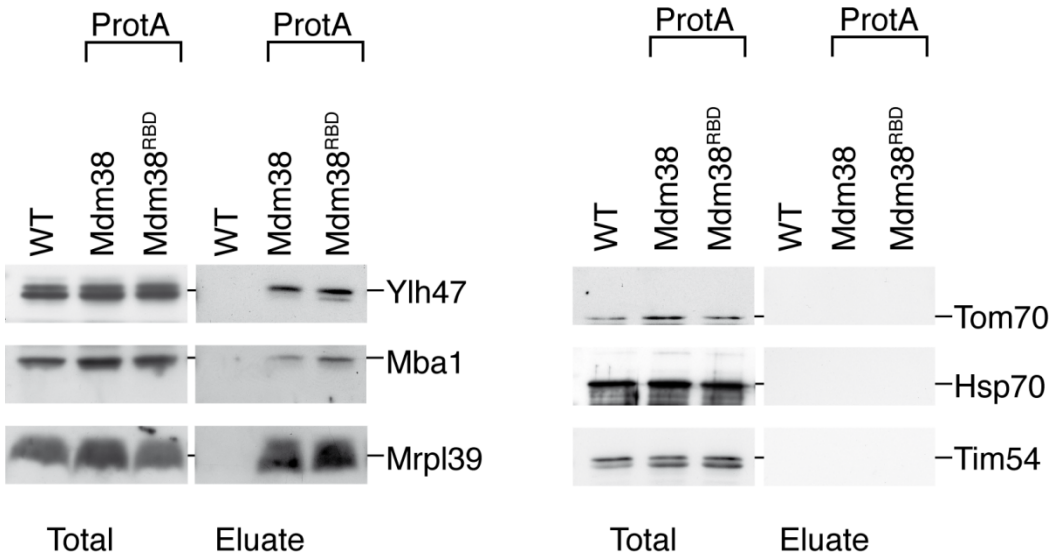

Figure 3.28: Native complex isolation of Mdm38^{ProtA} and Mdm38^{RBD}
Wild type (WT), Mdm38^{ProtA}, and Mdm38^{RBD} mitochondria were solubilized in 1% digitonin buffer and subjected to IgG chromatography. Bound proteins were eluted by TEV protease cleavage and analyzed by SDS-PAGE and Western blotting. Left panel shows total fractions, right panel shows eluate fractions. (Load: 5% of total, 100% of eluate).

The mitochondrial ribosome could be co-isolated with Mdm38 and Mdm38^{RBD} *in vivo*, as indicated by the presence of Mrpl39 in the eluate. Hence the interaction of Mdm38 to the ribosome is independent of the predicted C-terminal coiled coil domains. Furthermore, Ylh47, the yeast homologue of Mdm38, and the ribosome receptor Mba1 could be identified as interacting components.

3.3.2.2 The biogenesis of respiratory chain complexes III and IV depends on the Mdm38 ribosome-binding domain

In vitro and *in vivo* experiments demonstrated that the 14-3-3-like domain of Mdm38 interacts with proteins of the mt-protein translation machinery. Deletion of this region led to a severe growth defect, as seen in Mdm38$^{\Delta RBD}$ cells on a non-fermentable carbon source. Apparently, interaction between Mdm38, the mt-ribosomes and mt-protein members of the translation machinery is essential for yeast cell respiration. Therefore, it was important to analyze the levels of respiratory chain complexes in yeast strains containing or lacking the Mdm38 RBD.

In order to visualize respiratory chain complexes, mitochondria expressing Mdm38^{ProtA}, Mdm38$^{RBD\text{-}ProtA}$ or Mdm38$^{\Delta RBD\text{-}ProtA}$ were solubilized in digitonin buffer and subjected to Blue native PAGE (see 2.4.2.2) (Figure 3.29).

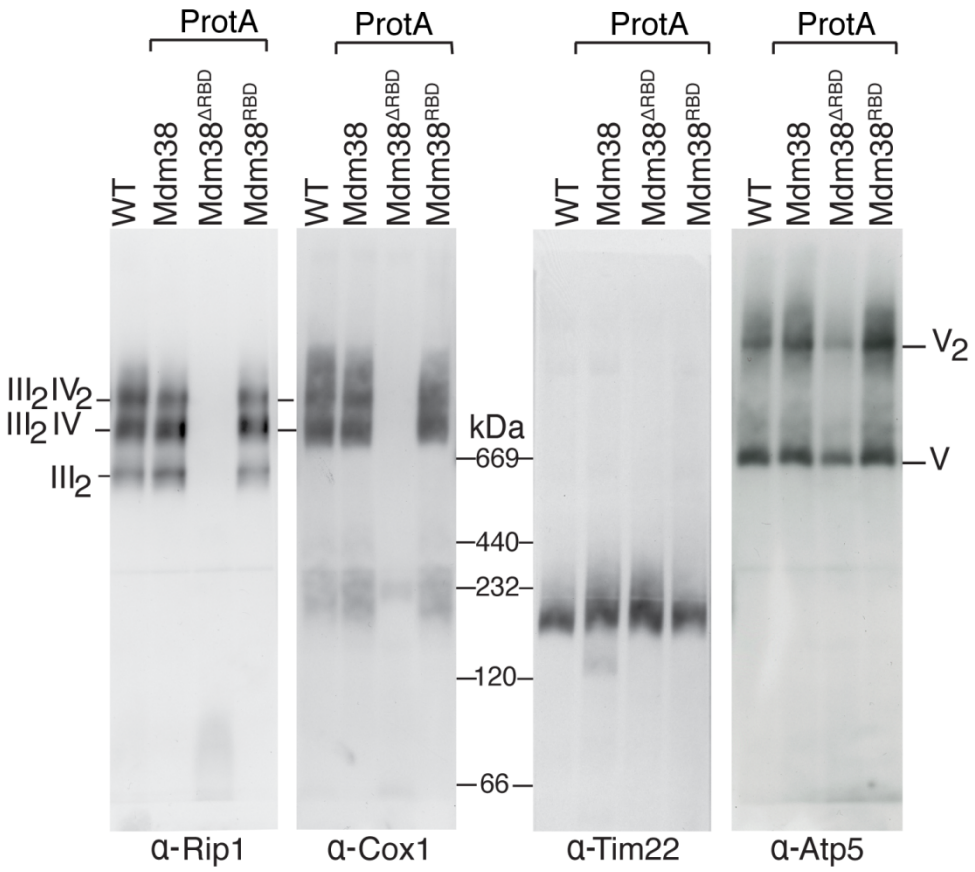

Figure 3.29: Blue native PAGE analysis of different Mdm38^{ProtA} truncations
Mitochondrial protein complexes were resolved by BN-PAGE, transferred to PVDF membranes and analyzed by immunodecoration with antibodies against Rip1 (complex III), Cox1 (complex IV), Tim54 (TIM22 complex), and Atp5 (F_oF_1-ATPase). Positions of molecular-weight markers in kDa are indicated.

The level of respiratory chain supercomplexes (III_2IV and III_2IV_2) were identical in mitochondria isolated from WT, Mdm38^{ProtA}, and Mdm38$^{RBD\text{-}ProtA}$ cells. In contrast, mitochondria isolated from Mdm38$^{\Delta RBD\text{-}ProtA}$ cells had undetectable respiratory chain complexes III and IV. As a control, the TIM22 complex (carrier translocases complex of the inner mitochondrial membrane, see also 1.1.3) was present in similar amounts in both Mdm38^{ProtA} truncations as well as in wild type and full length Mdm38^{ProtA} cells. To test if the observed defects were indeed generated by the lack of an Mdm38 ribosome-binding domain, and not due to loss of mitochondrial DNA, the levels of F_1F_0-ATPase were examined. The F_1F_0-ATPase contains 3 mt-encoded subunits (Atp6, Atp8, and Atp9). All isolated mitochondria contained fully assembled monomeric (V) and dimeric (V_2) complexes. In Mdm38$^{\Delta RBD\text{-}ProtA}$ mitochondria, only a slight reduction of the dimeric ATPase could be detected. Interestingly, the lack of Mdm38^{RBD} only affects the expression of the subunits of complexes III and IV, therefore it was necessary to

determine which step of respiratory chain biosynthesis is dependent on Mdm38. Moreover, the level of respiratory chain subunits were compared in all above–mentioned strains. To analyze the protein steady states, wild type mitochondria and mitochondria expressing the Mdm38^{ProtA} versions were separated by SDS-PAGE (5 µg and 10 µg, respectively) and analyzed by immunodecoration with antibodies directed against indicated proteins (Figure 3.30).

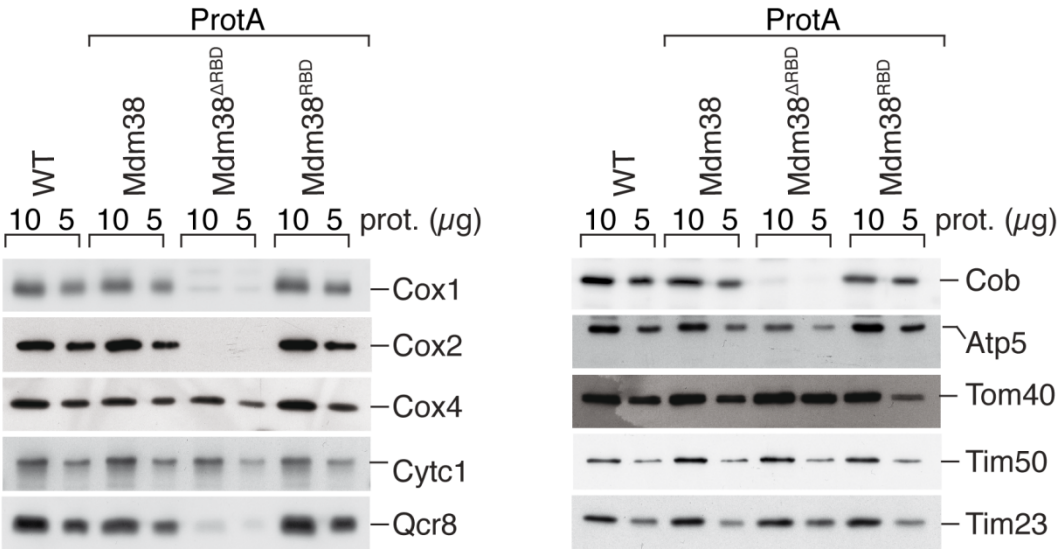

Figure 3.30: Steady state analysis of wild type mitochondria in comparison with mitochondria expressing Mdm38^{ProtA}, Mdm38$^{RBD\text{-}ProtA}$ or Mdm38 $^{\Delta RBD\text{-}ProtA}$
Mitochondria (5 or 10 µg) isolated from the indicated strains were analyzed by Western blotting using antibodies directed against the indicated proteins. Cox1 (Subunit I of cytochrome *c* oxidase); Cox2 (Subunit II of cytochrome *c* oxidase); Cox4 (Subunit IV of cytochrome *c* oxidase); Cyt*c*1, (cytochrome *c*1); Ocr8 (Subunit 8 of ubiquinol cytochrome-c reductase); Cob (cytochrome *b*, subunit of ubiquinol-cytochrome c reductase); Atp5 (Subunit 5 of the stator stalk of mitochondrial F_1F_0 ATP synthase); Tom40 (component of the translocase of the outer membrane, TOM); Tim50 (component of the translocases of the inner membrane, TIM23); Tim23 (component of the translocases of the inner membrane, TIM23).

Western blotting analysis revealed significantly reduced steady state levels of different mitochondria encoded proteins, demonstrating that loss of the RBD domain within Mdm38 led to specific effects in the biogenesis of respiratory chain complexes III and IV. The amount of Cox1 and Cob was significantly reduced in Mdm38$^{\Delta RBD\text{-}ProtA}$ mitochondria. Furthermore, Cox2 was completely absent at steady states. In addition, Qcr8 could not be detected, but it is known that defects in the biogenesis of complex III or IV usually lead to turnover of the nuclear-encoded subunits. However, Cox4 levels were identical in WT and Mdm38$^{\Delta RBD\text{-}ProtA}$ mitochondria, demonstrating that this nuclear-encoded protein remained stable, additionally seen in the absence of fully assembled complexes (Mick et

al. 2007). Steady state levels of additional outer and inner mitochondrial membrane proteins were tested, with all being present in similar amounts in all four strains, demonstrating the specificity of the observed defect in Mdm38$^{\Delta RBD\text{-}ProtA}$ mitochondria.

3.3.2.3 The ribosome-binding domain of Mdm38 is necessary for efficient translation of *COX1* and *COX2*

The absence of complexes III and IV in mitochondria lacking the ribosome-binding domain of Mdm38 were shown to be caused by significantly decreased levels of Cox1, Cox2, and cytochrome *b*. All three proteins are mitochondria encoded, which confirmed an important role in regards to Mdm38-ribosome-binding during synthesis of these proteins. In order to determine if the observed effects are caused by defective mitochondrial translation or degradation of the translated products, *in vivo* labeling of yeast cells expressing Mdm38^{PotA}, Mdm38$^{RBD\text{-}ProtA}$, or Mdm38$^{\Delta RBD\text{-}ProtA}$ was performed. In this assay, cytosolic translation was inhibited via cycloheximide treatment and mitochondrial translation products were labeled with [^{35}S] methionine. Subsequently, mitochondrial proteins were separated by SDS-PAGE and radioactive signals were quantified by digital autoradiography (see 2.4.4.1) (Figure 3.31).

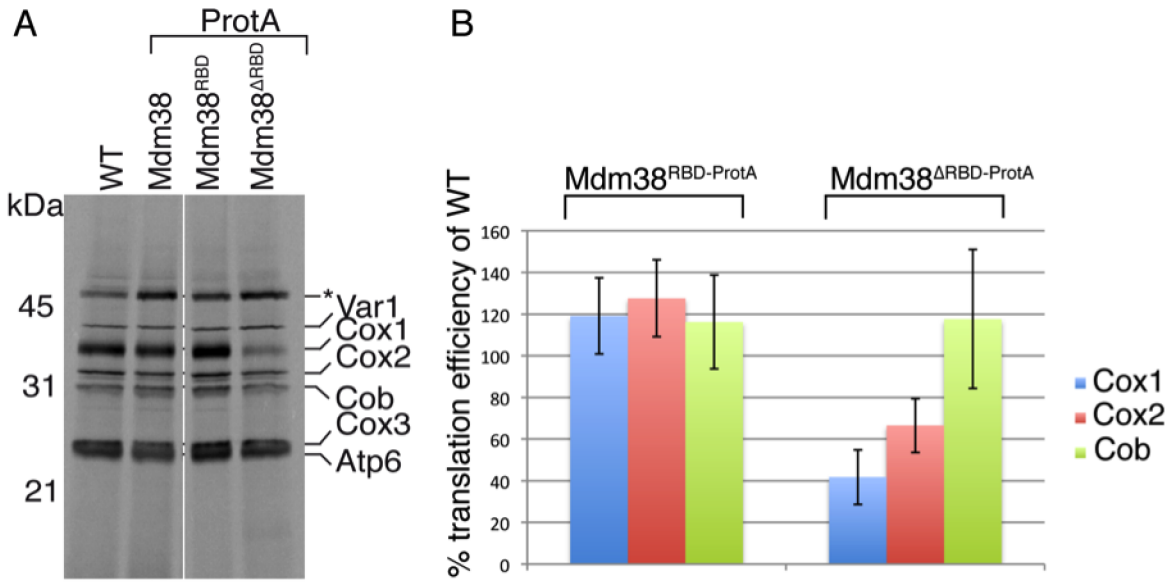

Figure 3.31: *In vivo* translation of yeast cells expressing different Mdm38^{ProtA} constructs
Yeast cells containing mitochondria harboring the different Mdm38^{ProtA} truncation constructs were incubated in translation buffer. Mitochondrial translation products were labeled with [^{35}S] methionine and subsequently separated by SDS-PAGE (A). The intensity of all radioactive signals was quantified by digital autoradiography. B: Quantitative analyses of mt-encoded proteins Cox1,

Cox2 and Cob. Four independent experiments were quantified using ImageQuant TL software (GE Healthcare), values represent the mean ratios of Cox1/Va1, Cox2/Var1, and Cob/Var1, relative to wild type (WT; 100%), respectively. Error bars indicate SEM (n=4). Abbreviations: Var1 (mt-ribosomal protein), cytochrome oxidase subunits 1, 2 and 3: Cox1, Cox2 and Cox3, respectively; Cob (cytochrome *b*); Atp6 (Fo-ATPase subunit 6); * unspecific signal (oligomer of ATPase subunits).

The analyses revealed significantly reduced levels of Cox1 and Cox2 within mitochondria harboring Mdm38$^{\Delta RBD\text{-}ProtA}$, demonstrating that the previously observed defects were indeed due to defective translation of *COX1* and *COX2*. These results were also verified by *in organello* labeling of mitochondrial translation products. In conclusion, mitochondria harboring Mdm38$^{\Delta RBD\text{-}ProtA}$ are defective in *COX1* and *COX2* translation.

Additionally, the stability of newly synthesized mt-translation products was examined by *in vivo* labeling followed by pulse–chase analysis: mitochondrial translation products were labeled with [^{35}S] methionine (pulse) in wild type, Mdm38^{ProtA}, Mdm38$^{RBD\text{-}ProtA}$ and Mdm38$^{\Delta RBD\text{-}ProtA}$ mutant cells and further incubated for 80 minutes (chase). Samples were taken after indicated time points (Figure 3.32).

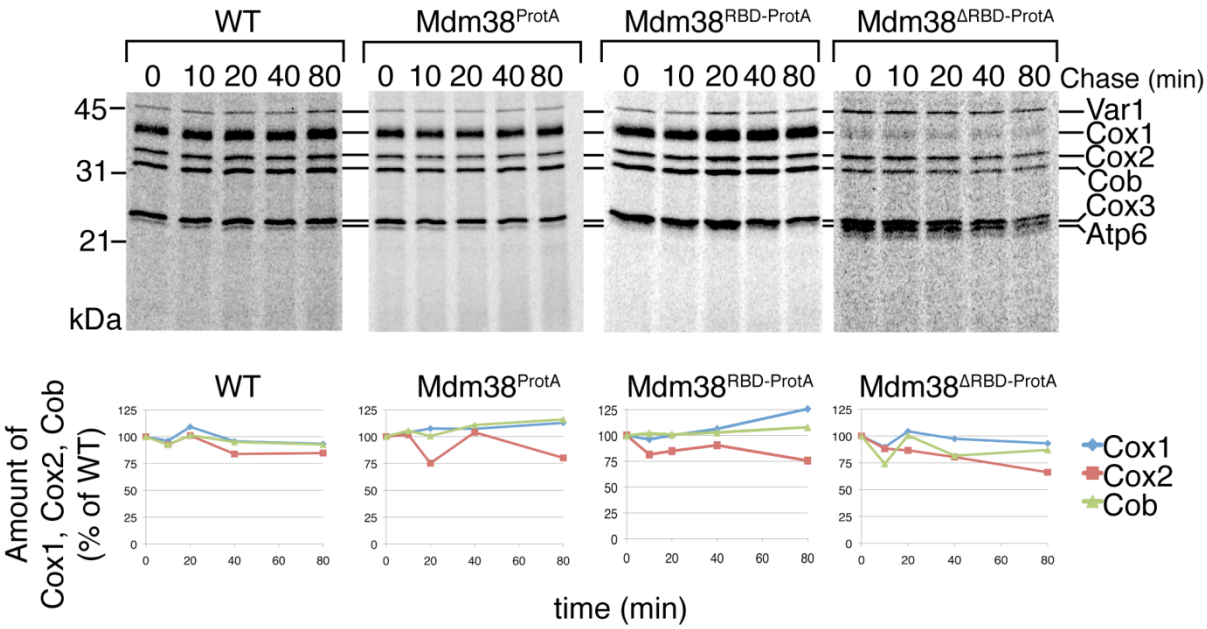

Figure 3.32: Synthesized mt-translation products are stable in Mdm38$^{\Delta RBD\text{-}ProtA}$ mutant cells
Mitochondrial translation products were labeled with [^{35}S] methionine (pulse). Translations were stopped by the addition of excess unlabeled methionine and chloramphenicol. Samples were taken after 10-, 20-, 40-, 80-min chase and analyzed by digital autoradiography. Abbreviations: Var1 (mt-ribosomal protein), cytochrome oxidase subunits 1, 2 and 3; Cox1, Cox2 and Cox3, respectively; Cob (cytochrome *b*); Atp6 (subunit 6 of the F_0ATPase). Values represent mean ratios of Cox1/Var1, Cox2/Var1 and Cob/Var1, relative to 0-min chase (100%).

Comparable amounts of Cox1 were synthesized in WT, Mdm38^{ProtA} and Mdm38$^{RBD\text{-}ProtA}$ mitochondria. In contrast, the level of Cox1 synthesized in Mdm38$^{\Delta RBD\text{-}ProtA}$ mutant cells was significantly reduced. However, during the chase period, the level of Cox1 remained constant, indicating that Cox1 was stable in the Mdm38$^{\Delta RBD\text{-}ProtA}$ mutant. In conclusion, the ribosome-binding domain of Mdm38 is required for efficient Cox1 synthesis, but not for stability. When the domain is absent, Cox1 is synthesized at a reduced rate. Hence the observed severe reduction of respiratory chain complexes III and IV (see 3.3.2.2) were due to reduced Cox1 and Cox2 synthesis. This data allows for the assumption that the Mdm38 ribosome-binding domain is required for translation of Cox1 and Cox2.

3.4 Identification of a putative ribosome-binding domain in LETM1

3.4.1. Expression of LETM1 in *E. coli*

The human protein LETM1 is an orthologue of the yeast protein Mdm38 (see 1.2.3). Mutations in *LETM1* have been shown to be involved in the manifestation of Wolf-Hirschhorn Syndrome (Endele et al. 1999). Several publications have shown that LETM1 has similar functions as Mdm38: Knockdown of *LETM1* in HeLa cells led to impaired formation of respiratory chain complexes I, II and IV (Tamai et al. 2008). Moreover, LETM1 was additionally shown to interact with mitochondrial ribosomes (Piao et al. 2009). Therefore, it was of particular interest to analyze LETM1 in more detail and to assess if LETM1 contains an Mdm38^{RBD}-like domain.

Both proteins are predicted to possess a single transmembrane domain and coiled coil motifs at their C-terminal ends. Amino acid sequence comparison of the Mdm38 ribosomal binding domain with LETM1 revealed the presence of a 92 amino acid long insertion in the LETM1 sequence, which cannot be found in Mdm38 (Figure 3.33).

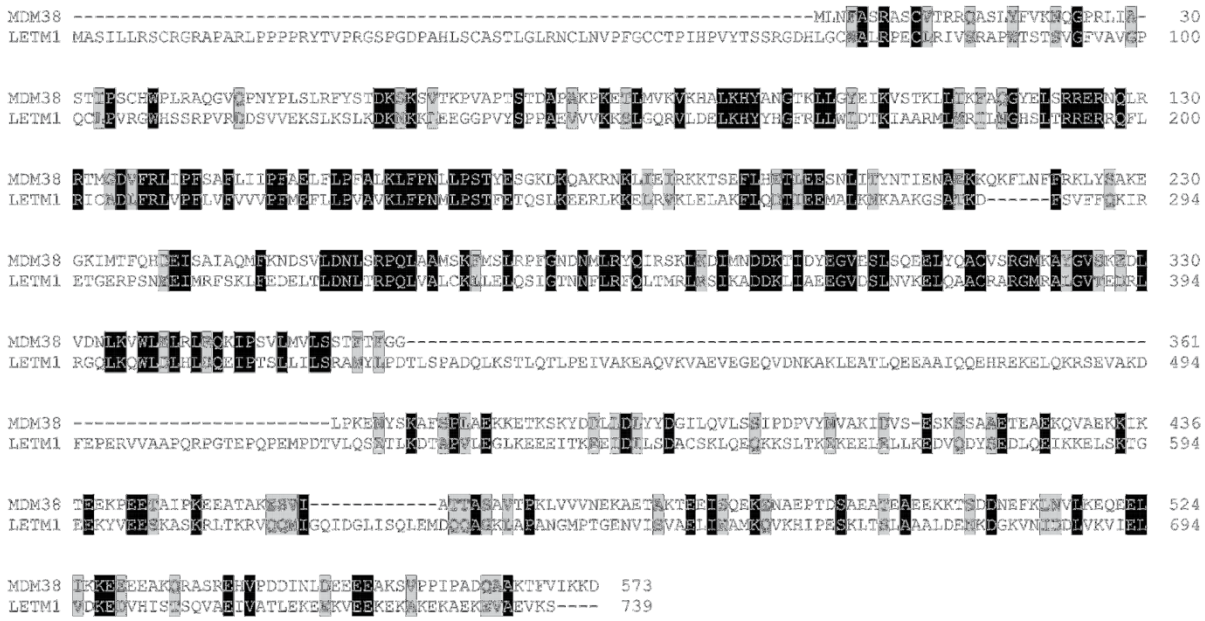

Figure 3.33: Amino acid sequence comparison of Mdm38^{RBD} and LETM1
Sequence alignment of Mdm38 and human LETM1. Black boxes indicate identical amino acids, and gray boxes indicate similar amino acids. Dotted line indicates a span of 92 amino acids present only in LETM1.

Two main questions were to be analyzed: First, whether the LETM1 domain, which is similar to Mdm38^{RBD}, was responsible for LETM1's interaction with mt-ribosomes and second, if the additional amino acids present in this area (although not conserved in Mdm38), will influence LETM1 binding to mt-ribosomes. In order to perform *in vitro* binding analyses and also to purify the LETM1 fragment for crystallization, a truncation construct of the protein was generated. Therefore, the sequence encoding aa 250-612 of LETM1 was cloned into pGEX-4T2, an *E. coli* expression vector. The LETM1 fragment (aa 250-612) and a C-terminal His$_6$ tag were amplified by PCR, digested by *BamH*I and *Not*I (see 2.3.4.1), and ligated into pGEX-4T2 (see 2.3.2.5). The LETM1 sequence was confirmed by DNA sequencing (see 2.3.3.3) and subsequently transformed into the C43 *E. coli* strain for protein expression (see 2.3.3.2). After harvesting cells by centrifugation, the solubility of the construct was examined. 0.5 g of *E. coli* cells were disrupted by French press, insoluble material was separated from soluble by centrifugation, and was analyzed by SDS-PAGE and Coomassie staining. The GST-LETM1$^{250-612}$–His$_6$ construct was highly soluble and therefore used for further analyses.

3.4.2 Purification of the LETM1 construct via chromatography

As the amount of GST-Mdm38^{CTD}-His$_6$ purified was sufficient for crystallization screens (see 3.2.3.1), the GST-LETM1$^{250-612}$–His$_6$ was subjected to the same purification procedures utilized for Mdm38^{CTD}. Therefore, *E. coli* C43 cells expressing GST-LETM1$^{250-612}$-His$_6$ were cultivated in LB-medium and the over-expression of the construct was induced by IPTG (see 2.2.1.2). The cells were harvested by centrifugation and disrupted by Emulsi Flex (1000 psi) (see 2.4.1.1). During subsequent centrifugation, the soluble fraction (containing the construct) was separated from insoluble material. Protein purification was achieved through two affinity chromatography steps followed by size-exclusion chromatography. GST-LETM1$^{250-612}$-His$_6$ was incubated with GSH-Sepharose; unspecific binding was removed by extensive washing and the purified construct was eluted by thrombin cleavage. Subsequently, the eluate was bound to Ni^{2+}NTA Agarose, washed and eluted with 300 mM Imidazole. Protein concentration of the eluate was further enriched by centrifugal filtration. In a last purification step the concentrated eluate was subjected to size-exclusion chromatography using a *16/60 Superdex200 prep grade* column coupled to an Äkta-purifier-FPLC-system (see 2.4.1.4). Analyses of different chromatography steps were performed by SDS-PAGE and subsequent Coomassie staining (Figure 3.34).

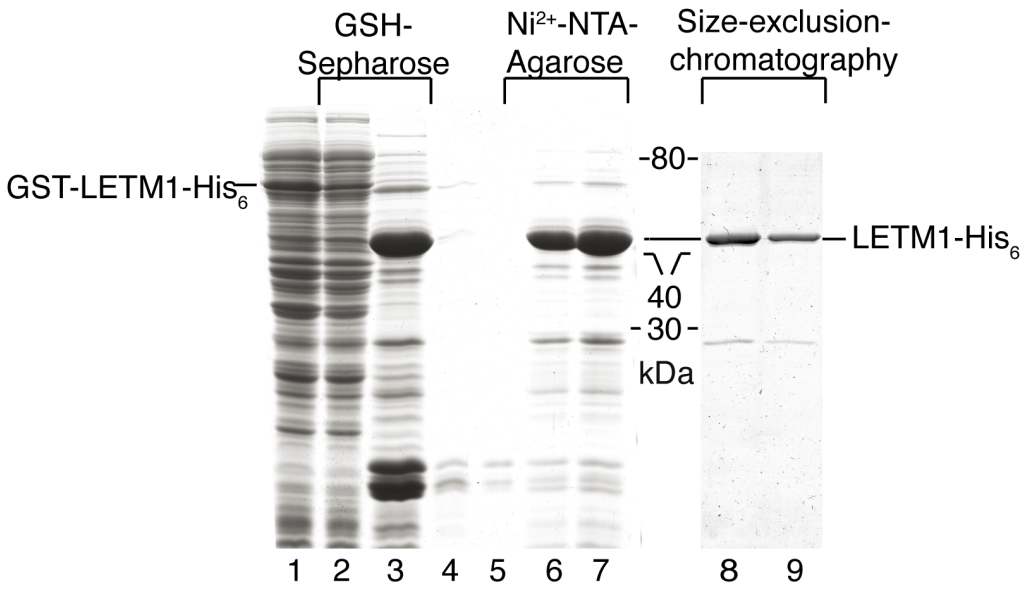

Figure 3.34: Purification of LETM1$^{250-612}$
Purification of GST-LETM1$^{250-612}$–His$_6$ by three different chromatography steps: GSH, Ni^{2+}-NTA affinity chromatography and size-exclusion chromatography. After each step, purified proteins

were separated on SDS-PAGE and visualized by Coomassie staining. Lanes: 1: total; 2: unbound; 3: eluate; 4:unbound; 5: wash; 6: eluate; 7: concentrated eluate; 8 and 9 show the main fractions of purified protein after gel-filtration.

Protein purification was performed on 40 g of *E. coli* cells (wet weight) and subsequently provided 6 mg of pure GST-LETM1$^{250-612}$–His$_6$ fusion protein, which was subjected to crystallization trails by Dr. Lupo (Heidelberg). However, while several buffers were tested, it was not successfully crystallized, and therefore the crystallization conditions still need to be optimized.

3.4.3 LETM1 interacts with the mitochondrial ribosome *in vitro*

In order to analyze if LETM1$^{250-612}$ is capable of binding to mitochondrial ribosomes, *in vitro* binding studies were performed using the GST-LETM1$^{250-612}$-His$_6$ construct as bait. The same protocol as previously used for the Mdm38 binding studies was employed (see 3.1.1.2). GST-LETM1$^{250-612}$-His$_6$ and GST were purified from *E. coli* and incubated with solubilized human mitochondrial extracts (mitochondria were isolated from HEK293T cells, provided by Robert Reinhold). Fusion proteins were rebound to GSH-Sepharose and extensively washed, proceeding elution via the addition of SDS sample buffer. Samples were subjected to SDS-PAGE (see 2.4.2.1) and Western blotting (see 2.4.2.4). Bound proteins were visualized using antibodies directed against the indicated proteins (Figure 3.35).

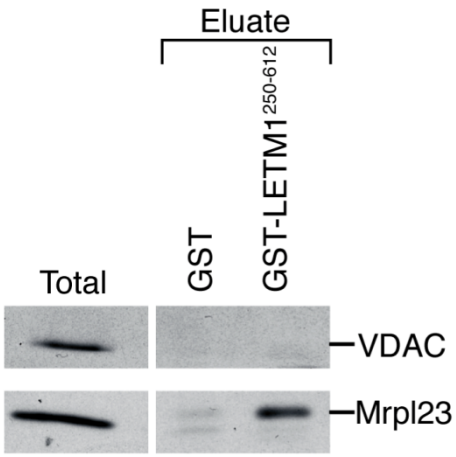

Figure 3.35: GST-LETM1$^{250-612}$–His$_6$ interacts with the mitochondrial ribosomal protein Mrpl23
The GST and GST-LETM1$^{250-612}$–His$_6$ fusion construct were used in an *in vitro* binding analysis, which revealed strong interaction of the LETM1$^{250-612}$ construct with mitochondrial ribosomes. Totals indicate the amount of mitochondrial proteins within the sample; Eluates indicate specifically co-purified mitochondrial ribosomes determined by the presence of Mrpl23, a subunit of the human ribosome (39S). VDAC served as control protein.

In vitro binding analyses revealed that the LETM1$^{250-612}$ construct is able to bind human mitochondrial ribosomes, indicated by the presence of Mrpl23 in the eluate. The presence of the additional 92 amino acids within its structure, which are not homologue to Mdm38, did not affect its interaction with the ribosome.

In conclusion, it could be shown that Mdm38 and LETM1 can interact with mitochondrial ribosomes and therefore are presumably functional homologues in mitochondria of yeast and humans.

4. DISCUSSION

Mdm38 was shown to interact independently from Oxa1 with newly synthesized mt-encoded proteins and was therefore proposed to play a role in mitochondrial protein biosynthesis and export (Frazier et al. 2006). This hypothesis is supported by the fact that the protein exposes a long C-terminal domain into the matrix, which is proposed to interact with the mitochondrial ribosome (Frazier et al. 2006). Further studies postulated Mdm38 to be involved in K^+/H^+ antiport (Nowikovsky et al. 2004). Thus, a major aim of the present work was to obtain greater insight into the function of Mdm38 in order to refine the current model of mitochondrial protein-biosynthesis as well as the export mechanism to the inner membrane. The search for interaction partners of Mdm38 was proposed to assist in the characterization of its function on a molecular level (4.1). Furthermore, structural analyses of Mdm38 were supposed to elucidate which of its putative domains are involved in its two proposed functions, ion homeostasis and mt-protein synthesis and subsequent export (4.2). To allow for further analysis of the homology between yeast Mdm38 and human LETM1, the latter was subjected to structural characterization in order to identify the region interacting with the mt-ribosome (4.3), allowing for the creation of a functional model of Mdm38 (4.4).

4.1. Function of Mdm38-Mba1 interaction within the mitochondrial translation machinery

Structural predictions of Mdm38 indicated a putative transmembrane span in its N-terminal domain and two coiled coil domains in its C-terminal domain (Frazier et al. 2006). Since coiled-coil motifs are known to mediate protein-protein interactions, a truncation construct of Mdm38, including the full C-terminal domain ($Mdm38^{CTD}$), was generated (see 3.1.1.1). Binding assays using $Mdm38^{CTD}$ showed an interaction with the yeast homologue Ylh47 and the mitochondrial ribosome (see 3.1.2.1), which was in agreement with a previous publication that also demonstrated this interaction (Frazier et al. 2006). Moreover, the *in vitro* binding studies revealed a novel interaction partner of Mdm38, namely Mba1 (see 3.1.2.1). Mba1 was previously shown to interact with Oxa1 (Ott et al. 2006), and, even more interestingly, it was postulated to act as a ribosome receptor, critical for protein synthesis coordination (Ott et al. 2006). A prior study already postulated Mba1 to be a component of an Oxa1-unrelated export machinery

(Preuss et al. 2001).

It was important to assess whether Mba1 is involved in the interaction of Mdm38 with the mt-ribosome and whether the lack of Mba1 would affect the ribosome binding capacity of Mdm38. *In vitro* binding assays incubating purified Mdm38^{CTD} with *Δmba1* mitochondrial extract revealed that mt-ribosomes could be specifically isolated, indicating that the binding of Mdm38 to the mt-ribosome is independent of Mba1 (see 3.1.2.2). In conclusion, these binding assays point to an interaction between Mdm38 and Mba1, both likely acting as ribosome receptors at the inner membrane. However, the interaction of Mdm38 with the mt-ribosome is independent of Mba1, and therefore it was important to assess whether the interaction between Mdm38 and Mba1 was relevant *in vivo*. Mdm38^{ProtA} was isolated from mitochondria revealing co-isolation of Mba1, however, the mt-ribosome was additionally specifically purified. It was thus imaginable that the interaction between Mdm38 and Mba1 was indirect and mediated by the mt-ribosome. To validate this suggestion, complex isolation was performed using mitochondria isolated from a ribosome-deficient (rho^0) strain containing Mdm38^{ProtA}. This experiment successfully demonstrated an interaction of Mdm38 with Mba1, as Mba1 co-purified with Mdm38^{ProtA} under the described conditions (see 3.1.2.3).

Since Mdm38 and Mba1 were already detected in a complex (see 3.1.2.3), it was important to assess whether they display a genetic interaction. Therefore, yeast strains harboring *Δmdm38*, *Δmba1,* or simultaneous deletion of both proteins (*Δmdm38*/*Δmba1*) were constructed (Bauerschmitt et al. 2010). Previous studies had already described that single deletion of either Mdm38 (Frazier et al. 2006) or Mba1 (Ott et al. 2006) leads to a growth defect, however, simultaneous deletion aggravated the single mutations and the *Δmdm38*/*Δmba1* cells exhibited severe respiratory defects on non-fermentable carbon sources (see 3.1.3). It can be speculated that both proteins have overlapping roles in either the assembly, the maintenance, or the function of the respiratory chain.

Interestingly, the Oxa1 C-terminal domain was shown to interact with mt-ribosomes (Jia et al. 2003; Szyrach et al. 2003). Therefore it was important to analyze if Oxa1 and Mdm38 have overlapping functions and whether strains lacking the C-terminal domain of Oxa1 and Mdm38 would show growth defects. Therefore, yeast strains of combined mutations of *Δmdm38* and *oxa1ΔC* were created and analyzed for their growth behavior on a non-fermentable carbon source (Bauerschmitt et al. 2010).

Interestingly, simultaneous deletion of *oxa1ΔC* and *Δmdm38* did not aggravate the growth defect observed for *Δmdm38* alone, leading to the suggestion that Mdm38 and Oxa1 do not possess an overlapping function.

Mdm38, Mba1, and Oxa1 are ribosome-associated membrane proteins, however, only Mdm38 and Mba1 display a genetic interaction. The fact that Mdm38 was proposed to play a role in ion homeostasis (Nowikovsky et al. 2004), and was shown to interact with Mba1 raised the question whether Mba1 was also involved in the K^+/H^+ antiport. Therefore, the *Δmdm38/Δmba1* mutant strain was analyzed for its growth on plates supplemented with Nigericin. Nigericin is an artificial K^+/H^+ ionophore and was previously shown to complement the observed *Δmdm38* growth defect (Nowikovsky et al. 2007). However, addition of Nigericin could not complement the severe growth defect of *Δmdm38/Δmba1* mutant cells (see 3.1.3.1), indicating that the interaction of both proteins is unrelated to K^+/H^+ exchange activity. Thus, a different purpose for the observed interaction of both proteins had to be taken into account. In order to identify the molecular basis of the observed growth defects in *Δmdm38/Δmba1* mutant cells, the activity of respiratory chain complexes III and IV was determined (Bauerschmitt et al. 2010). It attracted attention that both *Δmdm38* and *Δmba1* mutant mitochondria displayed reduced activities for both complexes, whereas the *Δmdm38/Δmba1* mutant mitochondria displayed an even stronger defect in complexes III and IV activity. These defects could further be confirmed by Blue native PAGE analysis, as mitochondria of both single-deletion strains contain only reduced amounts of complexes III and IV, whereas no complexes could be detected in the double mutant mitochondria (Bauerschmitt et al. 2010).

In order to determine the necessity of the presence of both proteins for the expression or stability of mitochondrial proteins, steady-states analyses of the different mutant mitochondria were performed. Surprisingly, *Δmdm38* mitochondria revealed a slightly increased amount of Mba1 and *vice versa*, suggesting an endogenous compensatory effect (Bauerschmitt et al. 2010). In conclusion, it could be assumed that the interaction between Mdm38 and Mba1 is essential for the biogenesis or the stability of respiratory chain complexes III and IV. The steady state levels of the two mitochondria encoded proteins Cyt *b* and Cox2 were reduced in *Δmdm38/Δmba1* mutant mitochondria, leading to the assumption that both proteins are somehow involved in either the synthesis, the assembly, or the transport of mitochondria encoded proteins.

The mitochondrial protein biosynthesis machinery is very complex and highly adapted to the requirements of the organelle, as exemplified by the unique translation system and ribosome tethering to the inner membrane. It is thus imaginable that the Mdm38-Mba1 interaction is also a specific adaption to these requirements. Both proteins had been formerly postulated to play a role as ribosome receptors (Frazier et al. 2006; Ott et al. 2006). In order to assess whether the localization of the mt-ribosome at the inner membrane depends on Mdm38 or Mba1, floatation centrifugation was performed. The level of mt-ribosomes remaining in the membrane fraction was analyzed in the background of different deletion strains (Bauerschmitt et al. 2010). Interestingly, the result demonstrated that the membrane association of mt-ribosomes is not compromised in the absence of Mba1 or Mdm38, leading to the presumption that both proteins could be involved in the translation of mt-encoded proteins. Therefore, mt-encoded translation products were analyzed *in organello* and *in vivo*. These experiments revealed severe translation defects of Cob and Cox1 in the *Δmdm38/Δmba1* double mutant (Bauerschmitt et al. 2010). Although Cob and Cox1 were not detectable, Atp6 and Atp9 translation products were synthesized at increased rates in the *Δmdm38/Δmba1* double mutant (Bauerschmitt et al. 2010). Since the translation of Cob and Cox1 was only mildly affected in the single mutant strains, Mdm38 and Mba1 are apparently able to partially substitute for one another in Cob and Cox1 expression, while loss of both proteins prevents translation of these mt-encoded proteins. Moreover, Atp6 and Atp9 translation was found to be misregulated in the *Δmdm38/Δmba1* strain. These results could explain the previously observed defects of complexes III and IV in the double mutant.

In order to assess whether the observed defects were merely caused by defects in translation or rather by transcriptional defects, the mRNA levels were analyzed by Northern blotting. The analysis indicated that both Cob and Cox1 mRNAs were almost absent in the *Δmdm38/Δmba1* double mutant (Bauerschmitt et al. 2010). However, this result did not necessarily indicate a defect in transcription, but points more towards a rapid degradation of mRNA due to its inability to be translated, since it was already previously observed that defects in translation lead to a rapid degradation of mRNAs (Manthey et al. 1995).

One of the most interesting adaptations of the mitochondrial translation machinery is the use of translational activator proteins (see 1.2.4). These proteins bind to the 5'

untranslated leader sequences (UTLs) of mRNAs and initiate the translation process. This regulatory system has adapted so well, that the translation of each mt-encoded mRNA is under the control of corresponding translation activator proteins (see 1.2.4). Since Cox1 translation was highly affected in the double mutant, the *COX1*-specific 5' and 3' UTLs were replaced with the flanking regions of COX2 (Perez-Martinez et al. 2003), which displayed no translation defect in the *Δmdm38/Δmba1* mutant. Previous studies had already shown that 5'UTLs in mt-mRNAs are interchangeable (Fox 1996), and indeed this exchange of UTLs in *Δmdm38/Δmba1* mutant cells leads to Cox1 translation in amounts comparable to WT cells (Bauerschmitt et al. 2010).

Obviously, Mdm38 and Mba1 are both involved in the translation regulation of Cox1 and Cob. Interestingly, coimmunoprecipitation experiments with the Cox1-specific translation activator $Pet309_{HA}$ and the Cob-specific translation activator $Cbs1_{HA}$ revealed Mdm38 to be in a complex with the translation activator proteins (see 3.1.4). Further, coimmunoprecipitation experiments showed that both Mdm38 and mt-ribosomes could be precipitated with $Pet309_{HA}$ (Bauerschmitt et al. 2010). Taken together, these observations indicate that Mdm38 and Pet309 both interact with the mt-ribosome. In conclusion, it is proposed that Mdm38 and Mba1 have an overlapping function in the mitochondrial translation of *COB* and *COX1*. It is imaginable that both proteins coordinate the translation process by interacting with the mt-ribosomes. In the absence of Mdm38 and Mba1, *COB* and *COX1* mRNAs cannot be translated and hence are rapidly degraded. As a result, neither Cob nor Cox1 can be synthesized, leading to the observed reductions of complexes III and IV levels, and consequently to growth defects of *Δmdm38/Δmba1* double mutant cells on non-fermentable carbon sources.

Interestingly, a 900 kDa multisubunit complex was identified, which contained several yet to be identified subunits, but also contained the *COB*- and *COX1*-specific mRNA translation activator proteins Cbp1 and Pet309 (Krause et al. 2004). Another study already proposed the existence of general translation regulator complexes at the inner mitochondrial membrane (Naithani et al. 2003), promoting adjacent translation of specific mRNAs, and thereby facilitating the assembly of respiratory chain complexes. It is tempting to speculate that Mdm38 and Mba1 interact with the mt-ribosome and distinct translation activators and finally contribute to the formation of such proposed translation regulation complexes.

4.2 Mdm38: The first putative mitochondrial 14-3-3-like protein in *S. cerevisiae*

Analyses of Mdm38-Mba1 interaction revealed a new function of Mdm38 in *COX1* and *COB* translation regulation. The protein was furthermore shown to interact with the mitochondrial ribosome (Frazier et al. 2006; Bauerschmitt et al. 2010), which is why it was of particular interest to determine which regions of Mdm38 are involved in ribosome binding, interaction with other components of the mt-protein translation machinery, and the postulated K^+/H^+ antiport (Nowikovsky et al. 2004). Structural analyses appeared to be beneficial for answering these questions.

The C-terminal domain of Mdm38 ($Mdm38^{CTD}$) was purified (see 3.2.1), crystallized, and the structure of $Mdm38^{CTD}$ was solved utilizing MAD with a seleno-methionine derivate of $Mdm38^{CTD}$ (see 3.2.2) (in cooperation with Dr. Lupo [University of Heidelberg]). Mass spectrometrical analysis of a single crystal revealed only a 28.2 kDa fragment (aa 159-408) of $Mdm38^{CTD}$ to have crystallized. The structure of this fragment was refined to a resolution of 2.1 Å and revealed a novel fold of mainly α-helical composition (see 3.2.2). Based on the crystal structure, a search against the database of known protein structures using the DALI-server was performed (in cooperation with Dr. Lupo). Highest homology, based upon Z-scores, was found for members of the 14-3-3 protein superfamily, with the human 14-3-3 protein epsilon having the highest Z-score and an average derivation of 4.2 Å to the crystallized Mdm38 fragment (see 3.2.3).

Generally, similarity in structure can indicate similarity in function. The superfamily of eukaryotic 14-3-3 proteins consists of a large number of highly conserved, acidic, 30 kDa proteins, which are expressed in a wide range of organisms and tissues. They are involved in numerous different regulatory processes such as cell signaling, cell cycle regulation, intracellular trafficking/targeting, cytoskeletal structure and transcription (Aitken 2006). The monomeric structure of 14-3-3 proteins consists of nine antiparallel α-helices, arranged in a U-like conformation, although 14-3-3 monomers mostly assemble into dimers. In many cases, the dimer docks on to phosphorylated substrates and subsequently modulates interactions between substrate proteins. It was shown that those dimers can act either as an adaptor linking two phosphorylated proteins (Ottmann et al. 2007), or, more commonly, bind to two tandemly phosphorylated 14-3-3-binding sites in the same protein (Johnson et al. 2010).

14-3-3 binding often results in conformational changes within the substrate which either activate or inhibit subsequent substrate processes (van Heusden 2009) and thereby allow for specific processes to occur. Three different 14-3-3 binding motifs were identified with the most prominent consisting of RXX (pS/pT) XP which has been termed the mode I motif (Johnson et al. 2010).

Since 14-3-3 proteins exist mainly in a dimeric state, it was of special interest to determine if Mdm38 is also present as a dimer. Indication for potential dimerization was reflected in the higher apparent molecular weight of the recombinant $Mdm38^{CTD}$ calculated from the size-exclusion chromatography profile (see 3.2.1) and the fact, that LETM1, the human homologue protein of Mdm38, was already supposed to assemble into tetramers (Jiang et al. 2009). However, structural analysis of the crystallized portion of Mdm38 ($Mdm38^{14\text{-}3\text{-}3}$) did not reveal any equivalence to the first two helices of 14-3-3 proteins (i.e. helices which are involved in 14-3-3-dimerization). Therefore, a 14-3-3-like dimerization of $Mdm38^{CTD}$ appeared to be unlikely. Nonetheless, a dimerization of Mdm38 was conceivable, since the protein was postulated to play a role in K^+/H^+ antiport (Nowikovsky et al. 2004; Nowikovsky et al. 2007; Nowikovsky et al. 2009). Hence, light scattering analysis was performed in collaboration with Dr. Lupo, in order to assess whether the coiled coil motifs at the C-terminal end of Mdm38 are involved in a putative dimerization. This analysis did not show an $Mdm38^{CTD}$ dimerization mediated by its coiled coil motifs, leading to the suggestion that a putative dimerization of Mdm38 could be mediated by the N-terminal portion of the protein. However, it seems to be improbable that ion homeostasis can be achieved in a monomeric protein state, which is why the data tempt to speculate that the postulated function of ion homeostasis is probably not mediated by the $Mdm38^{14\text{-}3\text{-}3}$ domain alone. This suggestion was further supported by the observation that mitochondria expressing Mdm38 without the 14-3-3-like domain are unable to grow on non-fermentable carbon source (see 3.3.1.2) and this phenotype cannot be complemented by addition of the artificial K^+/H^+ exchanger Nigericin (see 3.3.1.2). However, even the exact role of Mdm38 in K^+/H^+ antiport is still elusive, as a recent publication postulated Mdm38 rather to be one component of a K^+/H^+ exchange complex than to mediate this process alone (Zotova et al. 2010). Whether Mdm38 forms a heterodimer with its yeast homologue Ylh47 in order to fulfill 14-3-3-like regulatory or chaperone properties within mitochondria cannot be elucidated yet. Previous studies could not observe an

interaction of both proteins, which was essential for the yeast cell. Deletion of Ylh47 did not lead to growth defects of yeast cells and double deletion of Mdm38 and Ylh47 displayed a growth phenotype similar to the one of *Δmdm38* cells (Frazier et al. 2006). Mdm38 can hence be presumed to fulfill a yet to be determined 14-3-3-like function, independently of Ylh47. Even if a putative dimerization of Mdm38 may possibly be mediated by a region not further analyzed in the present work, the obtained data indicate a monomeric form of the protein. This would also correspond to various other 14-3-3 proteins, whose functions were shown to be independent of 14-3-3 dimerization (Campbell et al. 1997; Ichimura et al. 1997; Gu et al. 1998; Waterman et al. 1998; Zhou et al. 2003) Taken together, it is conceivable that a monomeric form of Mdm38 could be capable of mediating 14-3-3-like functions within mitochondria.

Until now, mitochondrial proteins with homology to 14-3-3 proteins have not been identified, allowing for the possibility for Mdm38 to be the first described mitochondrial 14-3-3-like protein. In order to gather more information on structure similarities between 14-3-3 proteins and Mdm38, the superposition of both structures was obtained from the DALI server. It revealed a 14-3-3-like putative substrate-binding groove within the Mdm38 structure, which can be presumed to be a region for potential interaction with ribosomal proteins or ribosomal RNA (see 3.2.3.1). Indeed, *in vitro* binding analyses using the Mdm38$^{14\text{-}3\text{-}3}$ domain revealed a specific interaction between Mdm38$^{14\text{-}3\text{-}3}$ and mitochondrial ribosomes (see 3.2.3.3).

Since 14-3-3-binding is known to mediate protein-protein interactions, it seems likely that Mdm38 mediates similar processes. Therefore the interaction of Mdm38 with the mitochondrial ribosome and distinct regulatory components, e.g. translation activator proteins, is conceivable to occur in order to coordinate mitochondrial protein biosynthesis. Whether substrate-phosphorylation is a prerequisite of substrate binding to Mdm38, as has been shown for most 14-3-3 proteins, cannot yet be answered. However, an atypical mode of binding has been previously documented in other 14-3-3-like *S. cerevisiae* proteins, such as Est1p. Here, the binding mechanism is likely to differ from typical 14-3-3 proteins as its structure lacks several crucial phosphoserine-binding residues (Fukuhara et al. 2005). This tempts to speculate that a classic substrate-phosphorylation, generally believed to be necessary for 14-3-3 protein binding, is possibly lacking in yeast and can therefore not be a prerequisite of interaction with Mdm38. However, the phosphoproteomics field is expanding and may

discover additional putative interaction partners of Mdm38 in the future.

A simple comparison of Mdm38 to the 14-3-3 superfamily is not suitable, as this family consists of a multitude of different 14-3-3 proteins with varying characteristics. In order to determine the exact function of Mdm38 focus has to be put on individual 14-3-3 proteins instead of the superfamily as a whole. Therefore it was of particular interest to compare Mdm38 to 14-3-3 proteins, which are known to be involved in guiding other proteins and mediating specific processes. Even though mitochondrial 14-3-3 proteins have yet to be identified, the model organism of this work, *S. cerevisiae*, has already been described to carry two 14-3-3 genes, namely *BMH1* and *BMH2*, which were examined for similarities to Mdm38 function.

While deletion of one *BMH* gene alone has little effect on cell viability, disruption of both is lethal to the yeast cell (van Heusden et al. 1995). Genetically modified *bmh* mutant strains indicated that Bmh1 and Bmh2 are both involved in controlling the *S. cerevisiae* proteome at post-transcriptional level. Furthermore, interaction between these proteins and different substrates was shown to be one step in the process of protein synthesis and degradation (Bruckmann et al. 2007). These observed functions were not in line with the predicted function of Mdm38, which was postulated to be involved in translation of mt-encoded proteins (Bauerschmitt et al. 2010). Since a homologous function between Bmh1, Bmh2 and Mdm38 appears to be unlikely, it was evident to concentrate on the protein, which was stated by the DALI server to share the highest structural homology with Mdm38 – the human 14-3-3 epsilon.

Human 14-3-3 epsilon was characterized to be involved in the regulation of general and specialized signaling pathways typical for 14-3-3 proteins (Kagan et al. 2002; Zuo et al. 2010; Sorokina et al. 2011). However, the functions of 14-3-3- epsilon do not correspond to those predicted for Mdm38, hence only structural homology is present.

A possible role of Mdm38 could be envisioned in either guiding the newly synthesized mt-encoded proteins to their destined positions at the inner membrane, or in rotating the mt-ribosome into an adequate position, allowing for the polypeptide to be inserted into the inner membrane immediately after emerging from the polypeptide exit tunnel. This hypothesis is further supported by the fact that guiding and mediating of transport pathways seems to be a highly conserved function of 14-3-3 proteins. The search for additional 14-3-3 proteins, which are involved in those functions, revealed an

interesting example of a 14-3-3 protein in plants. An analogous functionality of Mdm38 and a 14-3-3 plant protein seems possible, since mitochondria and chloroplasts are believed to be descendants from the same bacterial progenitor (Kutik et al. 2009). This theory is *inter alia* strongly supported by the existence of the mitochondrial protein Oxa1 and the chloroplast protein Alb3, which have been demonstrated to exhibit high functional conservation. The 14-3-3 protein (accession number AJ238681) is important for guiding hydrophobic chloroplast precursors into the organelle. It is to mention, that contrarily to mitochondrial presequences, chloroplast-destined precursors are enriched in serine and threonine residues which will be phosphorylated prior to their import across the outer membrane (Waegemann et al. 1996), and recognized by the mentioned 14-3-3 protein. They assemble into a cytosolic guidance-complex, which additionally consists of the 14-3-3 protein dimer and a Hsp70 chaperone (May et al. 2000). It is hypothesized that the interaction with the guidance-complex protects the precursor from misfolding within the cytosolic space. Although the 14-3-3-Hsp70-precursor protein complex is postulated to be a *bona fide* intermediate in the *in vivo* protein import pathway in plants (May et al. 2000), a similar guiding mechanism was already indicated for the transport of certain mitochondrial precursors through the cytosol to the TOM complex. Here the 14-3-3-like chaperone mitochondrial import stimulating factor (MSF) selectively binds to precursors with mitochondrial targeting sequences and subsequently guides them to the Tom37 and Tom 70 receptor proteins in a reaction requiring ATP hydrolysis by MSF (Hachiya et al. 1995). It is conceivable, that the 14-3-3-like structure of Mdm38 serves a similar purpose within the mitochondrion. Mitochondria encoded polypeptides synthesized in the mitochondrial matrix are highly hydrophobic and are therefore exceptionally prone to form aggregates. This conjuncture led to the evolution of a sophisticated protein-biosynthesis machinery within the mitochondrial matrix, capable of synthesizing polypeptides in direct proximity to the inner mitochondrial membrane.

Mdm38 was previously supposed to interact with newly synthesized mt-encoded proteins (Frazier et al. 2006) and it is imaginable that the 14-3-3-like binding motif within Mdm38 is involved in mediating efficient assembly of polypeptides at the inner membrane. This theory is further supported by Herrmann et al. (1994), who showed that newly synthesized mt-encoded proteins interact with mt-Hsp70, and speculated that this interaction evolved to prevent the newly synthesized, hydrophobic

polypeptides from misfolding or aggregating within the matrix. Although an interaction between Mdm38 and mt-Hsp70 (Ssc1 in yeast) within the context of mt-encoded protein transport or assembly has never been shown, an interaction between the *COX1*-specific mRNA translation activator Mss51 and Ssc1 was identified (Fontanesi et al. 2010). This observation is very interesting, given that also Mdm38 could clearly be shown to play a role in translation of *COX1* mRNA (Bauerschmitt et al. 2010). Mss51 and Ssc1 were supposed to be present in a dimeric state and to assemble into a higher oligomeric complex containing additional assembly factors of the cytochrome *c* oxidase. The interaction between Ssc1 and Mss51 has been postulated to mediate the translational and posttranslational functions of Mss51 (Fontanesi et al. 2010). However, the interaction of Mss51 and Ssc1 was also observed in a strain devoid of mitochondrial DNA (*rho*^{0}), indicating that the chaperone could be involved in two different functions, namely both impairing Mss51's function and protecting newly synthesized mt-encoded polypeptides from aggregation. The present work could not ascertain, whether Mdm38 and Ssc1 interact to build a guidance-complex analogous to the 14-3-3 protein in plant cells in order to protect mt-encoded polypeptides from misfolding within the mitochondrial matrix. However, a putative 14-3-3-like substrate-binding groove was suspected to be identified within Mdm38, which is conceivable to be a potential binding region for the mt-ribosomes or substrates involved in mt-translation. Accordingly, Mdm38 could play a role in guidance of hydrophobic polypeptides to their destined positions at the inner mitochondrial membrane. Furthermore, Mdm38 was shown to be essential for efficient Cox1 and Cob translation, (see 3.3.2.3) as it coimmunoprecipitated with the translation activator proteins Pet309, respectively Cbs1 (see 3.1.4). Whether Mdm38 also interacts with Mss51 could not unambiguously be shown, although initial experiments were indicative of a potential interaction. In conclusion, Mdm38 likely plays a regulatory role within the mitochondrial protein translation machinery, presumably as an adaptor protein. It can be envisioned to bind to the mitochondrial ribosome and specific translation activator proteins, regulating the translation of mt-encoded proteins. Furthermore, the location of Mdm38 within the inner membrane allows for the spatial restriction of the translation process, thereby defining the insertion position of the translation product to the inner mitochondrial membrane.

4.3 Implications between yeast and human proteins Mdm38 and LETM1

Mitochondria are also referred to as the "power plants" of the cell, as they provide the majority of the cellular energy in form of ATP. Furthermore, they are involved in many essential cellular and metabolic processes, as well as in signaling cascades (see 1.1.2 for a summary). These pathways are tightly intertwined and therefore mitochondrial dysfunction gives rise to mulitfactorial human diseases (Rinaldi et al. 2010), which in turn bring mitochondrial investigation into the focus of medical research. Unfortunately, treatments of mitochondrial diseases are extremely scarce, as exploration of the wide range of different disease pathologies are just entering the literature. *S. cerevisiae* as a model organism represents a powerful tool to study the genetic and molecular aspects of mitochondria within the cell, and therefore to understand the etiology of mitochondrial diseases. The general conservation of mitochondrial genes and pathways between yeast and human is very high and among the disease causing human gene mutations, about 40% have been shown to possess an orthologue in yeast (Bassett et al. 1996). Understanding the defect in yeast was helpful in many cases to elucidate human pathologies (Schwimmer et al. 2006; Spinazzola et al. 2009).

The *S. cerevisiae* protein of present interest, Mdm38, was as well shown to possess a human homologue, termed Leucine zipper/EF hand-containing transmembrane-1 (LETM1). Schlickum et al. (2004) previously reported LETM1 to be conserved between yeast and humans and to reside within mitochondria. Initial work described *LETM1* as a gene in the chromosomal region 4p16.3, which is hemizygously deleted in most patients suffering from Wolf-Hirschhorn Syndrome (WHS) (Endele et al. 1999). This disease occurs in approximately one out of 50.000 births and is accompanied by different typical symptoms such as cranio-facial defects, hypotonia, growth & mental retardation, epilepsy, seizures and microcephaly (Bergemann et al. 2005).

The study by Endele et al. (1999) suggested the protein encoded by *LETM1* to be a member of the superfamily of EF-hand Ca^{2+}-binding proteins. Furthermore, LETM1 was hypothesized to play a role in Ca^{2+} signaling and homeostasis. Deletion of *LETM1* would therefore impair Ca^{2+} homeostasis, which may contribute to the characteristic neuromuscular features and seizures seen in WHS patients. Indeed a function of LETM1 as Ca^{2+}/ H^{+} antiporter within the inner mitochondrial membrane was recently

demonstrated (Jiang et al. 2009).

One interesting similarity in regard to the homology between Mdm38 and LETM1 is their common role in ion homeostasis. Particularly, Mdm38 was postulated to play a role in K^+/H^+ rather than in Ca^{2+}/H^+ antiport, and despite the obvious difference in ion selectivity, LETM1 was shown to complement the *Δmdm38* growth phenotype on non-fermentable carbon sources (Nowikovsky et al. 2004). However, a recent publication on this topic suggested Mdm38 to be only one of several components of a putative mitochondrial K^+/H^+ exchanger (KHE) complex (Zotova et al. 2010).

The present work focused on an additional function of Mdm38, as here the protein was shown to be the first mitochondrial ribosome-interacting 14-3-3-like protein in mitochondria, which assists in the translation of mitochondria encoded *COX1* and *COB* mRNAs. Structural analyses performed in the present work identified a region possibly responsible for the characteristics of Mdm38 (see 3.2.3.3). In agreement with the role of Mdm38 in ribosome binding, LETM1 was also shown to interact with the mitochondrial ribosome protein L36 (Piao et al. 2009). The study suggested LETM1 to serve as an adaptor protein for complex formation with the mitochondrial ribosome, and thereby regulating mitochondrial biogenesis. Biochemical data obtained during the present work provided further support for an interaction between LETM1 and the mitochondrial ribosome (see 3.4.3). Based on sequence identity (Endele et al. 1999), Mdm38 and LETM1 proteins belong to the same family, and a ConSurf analysis revealed that the newly described 14-3-3-like substrate-binding groove in Mdm38 is conserved in all members of the Mdm38/LETM1 family (see 3.2.3.1). Sequence conservation is especially apparent in the positively charged patch on one side of the groove and it is tempting to speculate that the interaction between LETM1 and the ribosome occurs at this region.

A recent discovery indicated the yeast and human translation system to be more similar than previously expected, namely the detection of a *COX1* specific translation activator, TACO1, in the human system (Weraarpachai et al. 2009; Seeger et al. 2010). Although it is known that the translation system in yeast is mainly regulated on the translational level, mammalian mitochondrial mRNAs lack significant 5'UTLs, leading to the suggestion that their expression is regulated by a different mechanism. The identification of TACO1 casts the mammalian translation system in a different light and indicates that means for translation regulation of mitochondria encoded genes are

conserved in both yeast and mammal systems. Further indication of such conservation is provided by the presence of the LRPPRC protein in humans, a distant homologue of the yeast *COX1* mRNA translation activator protein Pet309 (Xu et al. 2004). LRPPRC was proposed to play a role in the translation or stabilization of the mRNA of mitochondria encoded COX subunits. Mutation of *LRPPRC* was shown to lead to Leigh syndrome French Canadian variant (LSFC) (Mootha et al. 2003), which differs in phenotype from other COX deficiencies as it predominantly affects the liver and brain instead of causing classical neurological symptoms (Xu et al. 2004). Perhaps the similarities between the human and the yeast translation system are stronger than currently predicted.

Mdm38 and LETM1 are both conserved in structure and function, as they both represent mitochondrial inner membrane proteins, which possess a large C-terminal domain exposed into the matrix. Coiled coil domains have been predicted in the C-termini of both proteins (Endele et al. 1999; Frazier et al. 2006); additionally the joint ability to interact with mitochondrial ribosomes, thereby maintaining respiratory chain functionality, could be demonstrated (Frazier et al. 2006; Tamai et al. 2008).

Lack of the Mdm38 ribosome-binding domain led to defects in *COX1* and *COB* translation (see 3.3.2.3) and therefore significantly reduced respiratory chain complexes III and IV (see 3.3.2.2). It is thus conceivable that in the affected mitochondria the membrane potential is reduced and, as a consequence, ion homeostasis is disturbed. This hypothesis can be considered supported by the afore-mentioned results, however, it is also imaginable, that the disturbance in ion homeostasis is caused by the loss of the ribosome-binding domain of Mdm38 and would therefore not be the result, but the reason for the observed defects in translation.

In regard to WHS it is conceivable that the observed symptoms may be induced by either a defect in ion homeostasis, or by respiratory chain dysfunction, caused by either misregulation of translation or lack of LETM1 mediated ribosome-inner membrane docking. However, it remains unclear, if both proteins fulfill a conserved ion homeostasis function. In contrast to Mdm38, LETM1 possesses an EF-hand motif, which is indicative of Ca^{2+}-binding, but it is still uncertain how the ribosome-binding ability of LETM1 and its role in Ca^{2+}/H^{+} antiport can be combined. As of today, Mdm38 was only shown to be a component of an K^{+}/H^{+} exchange complex (Zotova et al. 2010) and, furthermore, to be directly involved in the regulation of Cox1 and Cyt*b* translation (Bauerschmitt et al. 2010). The analysis of these seemingly diverse questions will

probably be the subject of future research. However, it is likely that analyses concerning the function of the yeast protein Mdm38 will lead to further illuminating insights into the function of LETM1 and its role in WHS.

4.4 Functional model of Mdm38

The present work characterized the function of the mitochondrial protein Mdm38. It revealed the protein to be involved in the translation-regulation of *COX1* and *COB*, probably in collaboration with Mba1 (see 4.1). Additionally, Mdm38 was shown to interact with *COX1*- and *COB*-specific translation activator proteins and the mitochondrial ribosome (see 4.1), so that Mdm38 can be envisioned to act as an adaptor protein supporting the translation process by interaction with the ribosome and the translation activators respectively. $Mdm38^{CTD}$ was subjected to X-ray structural determination, however only the region encompassing amino acids 182-408 could be solved, showing an alpha helical fold with high homology to 14-3-3 proteins (see 4.2). It can therefore be suggested, that Mdm38 represents the first identified 14-3-3-like protein in mitochondria. This suggestion would also be in line with the hypothesis of Mdm38 acting as an adaptor protein, as 14-3-3 proteins are known to mediate protein-protein interactions (Aitken 2006) (see 4.2). *In vitro* binding analyses using $Mdm38^{14\text{-}3\text{-}3}$ showed that the 14-3-3-like region is highly capable of interacting with the mt-ribosome (4.2). Analyses of the corresponding region in LETM1 revealed the human protein to also possess a high affinity for mitochondrial ribosome interaction (4.3). It can be assumed that the ability to interact with the mitochondrial ribosome is a conserved function within the Mdm38/LETM1 family.

This data allowed for a functional model of Mdm38 function to be drafted. Mdm38 and Mba1 interact in order to regulate *COX1* and *COB* translation. Both proteins are presumably located in, or respectively at, the inner membrane in close proximity to each other, so as to increase the efficiency of their collaboration. It is conceivable that the translation activator proteins bind to the specific mRNAs before interacting with Mdm38 (Fig. 4.1, step I). Subsequently, Mdm38 interacts with the translation activator proteins Pet309 or Cbs1, probably via its 14-3-3-like substrate-binding domain (Fig. 4.1, step II). Regarding the structural homology between this Mdm38 domain and 14-3-3 proteins, it is imaginable that Mdm38 binds to both, the translation activator protein

and the mitochondrial ribosome and thereby acts as an adaptor supporting or possibly even initiating the translation process (Fig.4.1, step III). It is conceivable that this function of Mdm38 is supported by Mba1, which tethers the ribosome to the inner membrane. If conformational changes within the ribosome or the translation activator proteins occur during this process cannot be elucidated yet. Whether Mdm38 interacts specifically with a single translation activator or whether it is in complex with Pet309, Cbs1, and the ribosome is yet to be clarified. In regard to the postulated role of Mdm38 in K^+/H^+ antiport (Nowikovsky et al. 2004), it is tempting to speculate that ion homeostasis could be involved in a signaling cascade which leads to Mdm38-translation activator interaction and translation initiation.

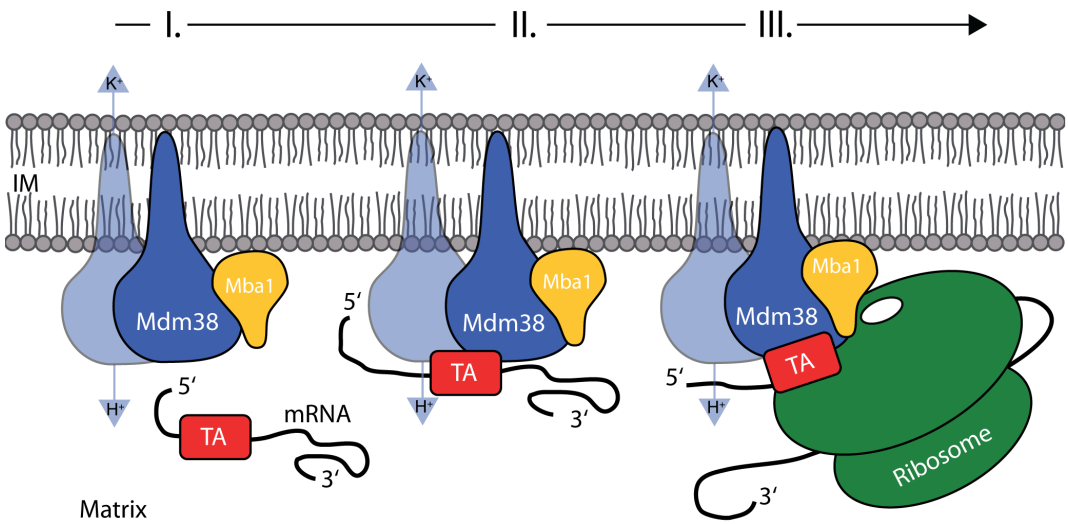

Fig 4.1: Functional model of Mdm38
Mdm38 and Mba1 are inserted or respectively peripherally attached to the inner mitochondrial membrane (I.). In order to enable new rounds of *COX1* and *COB* translation, Mdm38 interacts with translation activator proteins Pet309 or Cbs1 (referred to as translation activator; TA) (II.). Furthermore, the mt-ribosome binds to Mdm38 in a defined substrate-binding groove. Mdm38 serves as an adaptor and mediates the interactions between the mt-ribosome and the translation activator proteins. Mba1 fulfills a supporting function in stabilizing the ribosome at the inner membrane (III.). Ion homeostasis could be involved in a signaling cascade, which leads to Mdm38-translation activator interaction and translation initiation.

It is conceivable that Mdm38 permanently interacts with the mt-ribosome since the latter is tightly bound to the inner mitochondrial membrane, and Mdm38 is predicted to possess a transmembrane span anchoring the protein in the inner membrane (see 3.1.1.1). Moreover, it can be presumed that mitochondrial translation is organized into

defined compartments at the inner membrane in order to regulate respiratory chain biogenesis.

Analyses of translation activator protein Mss51 localization revealed it to be present in two different states: Either inactive, which prevents new rounds of *COX1* translation activation; or in a state allowing for new rounds of translation to be initiated (Mick et al. 2011)(see 1.2.4.1). This way of translation regulation is presumably not only Mss51-specific, but also applies on other translation activator proteins. It can therefore be presumed, that a general pool of translation activator proteins exists, which can be bound by specific adaptor proteins, such as Mdm38, shuttling the translation activator proteins to defined positions within the mitochondrial translation machinery complex. This organization can be imagined to guide the process of polypeptide synthesis to occur at distinct sites at the inner membrane, therefore allowing efficient insertion of the newly synthesized polypeptides. This hypothesis is supported by the fact that Mdm38 was previously postulated to be involved in the export of mt-encoded polypeptides into the inner membrane (Frazier et al. 2006), and Mba1 was shown to interact with the Oxa1 C-terminal domain (Ott et al. 2006).

Further indication for this hypothesis could be given by the structure of the bovine mitochondrial ribosome, which was shown to possess an additional opening in close proximity to the polypeptide exit tunnel, termed polypeptide accessible site (Sharma et al. 2003). This opening was postulated to be involved in the co-translational insertion of newly synthesized proteins, possibly in connection with Oxa1, and probably evolved as a specific adaption to the requirement of hydrophobic mt-encoded protein synthesis. However, it has to be taken into account that the mammalian mitochondrial ribosome differs from its yeast counterpart, exemplified by its different rRNA and protein content, which makes it difficult to draw conclusions suitable for both systems.

Although the regulation and mechanism of the mitochondrial translation machinery is not entirely clarified yet, it seems that certain mechanisms of mt-protein biosynthesis, as well as the assembly process of mature respiratory chain complexes can gradually be elucidated. It appears that these processes are more complex and more tightly regulated than expected, and therefore may also reveal unexpected characteristics.

5. SUMMARY

The present work focused on the role of the mitochondrial protein Mdm38 in regards to respiratory chain biogenesis. The obtained data revealed Mdm38 to be involved in the translation process of mitochondria encoded proteins and expanded the current knowledge on the interplay of the different components of the mitochondrial translation machinery.

For the first time, a genetic and physical interaction between Mdm38 and the ribosome receptor protein, Mba1, could be demonstrated. The interaction of both proteins is independent of the presence of the mitochondrial ribosome, but related to *COX1* and *COB* translation regulation. The presence of Mdm38 in complex with either Pet309 or Cbs1 additionally supports its role in translation. Structural characterization of the C-terminal domain of Mdm38 revealed a 28.2 kDa portion (aa 182-408) which interacts with the mitochondrial ribosome. The structure of this domain was solved at a resolution of 2.1 Å and displays high homology to 14-3-3 proteins. Hence, Mdm38 is assumed to be the first 14-3-3-like mitochondrial protein. The loss of Mdm38's ribosome-binding domain led to specific defects in *COX1* and *COB* translation and subsequently, defects in complexes III and IV assembly. Accordingly, the molecular function of Mdm38 is described as supporting or even regulating *COX1* and *COB* translation via its interaction with the mitochondrial ribosome. The ribosome-binding domain is structurally conserved among the LETM1/Mdm38 superfamily. LETM1 interacts with the mitochondrial ribosome via a region which is similar to the ribosome-interaction-region in its yeast counterpart, Mdm38. This is indicative for a conserved function from yeast to human.

REFERENCES

Acin-Perez, R., P. Fernandez-Silva, M. L. Peleato, A. Perez-Martos and J. A. Enriquez (2008). Respiratory active mitochondrial supercomplexes. *Mol Cell* 32(4): 529-539.

Aitken, A. (2006). 14-3-3 proteins: a historic overview. *Semin Cancer Biol* 16(3): 162-172.

Allen, S., V. Balabanidou, D. P. Sideris, T. Lisowsky and K. Tokatlidis (2005). Erv1 mediates the Mia40-dependent protein import pathway and provides a functional link to the respiratory chain by shuttling electrons to cytochrome c. *J Mol Biol* 353(5): 937-944.

Barrientos, A., A. Zambrano and A. Tzagoloff (2004). Mss51p and Cox14p jointly regulate mitochondrial Cox1p expression in Saccharomyces cerevisiae. *EMBO J* 23(17): 3472-3482.

Bassett, D. E., Jr., M. S. Boguski and P. Hieter (1996). Yeast genes and human disease. *Nature* 379(6566): 589-590.

Bauer, M., M. Behrens, K. Esser, G. Michaelis and E. Pratje (1994). PET1402, a nuclear gene required for proteolytic processing of cytochrome oxidase subunit 2 in yeast. *Mol Gen Genet* 245(3): 272-278.

Bauer, M. F., C. Sirrenberg, W. Neupert and M. Brunner (1996). Role of Tim23 as voltage sensor and presequence receptor in protein import into mitochondria. *Cell* 87(1): 33-41.

Bauerschmitt, H., D. U. Mick, M. Deckers, C. Vollmer, S. Funes, K. Kehrein, M. Ott, P. Rehling and J. M. Herrmann (2010). Ribosome-binding Proteins Mdm38 and Mba1 Display Overlapping Functions for Regulation of Mitochondrial Translation. *Mol. Biol. Cell* 21(12): 1937-1944.

Bergemann, A. D., F. Cole and K. Hirschhorn (2005). The etiology of Wolf-Hirschhorn syndrome. *Trends Genet* 21(3): 188-195.

Bohnert, M., P. Rehling, B. Guiard, J. M. Herrmann, N. Pfanner and M. van der Laan (2010). Cooperation of stop-transfer and conservative sorting mechanisms in mitochondrial protein transport. *Curr Biol* 20(13): 1227-1232.

Bolender, N., A. Sickmann, R. Wagner, C. Meisinger and N. Pfanner (2008). Multiple pathways for sorting mitochondrial precursor proteins. *EMBO Rep* 9(1): 42-49.

Bonnefoy, N., F. Chalvet, P. Hamel, P. P. Slonimski and G. Dujardin (1994). OXA1, a Saccharomyces cerevisiae nuclear gene whose sequence is conserved from prokaryotes to eukaryotes controls cytochrome oxidase biogenesis. *J Mol Biol* 239(2): 201-212.

Bonnefoy, N., H. L. Fiumera, G. Dujardin and T. D. Fox (2009). Roles of Oxa1-related inner-membrane translocases in assembly of respiratory chain complexes. *Biochim Biophys Acta* 1793(1): 60-70.

Boumans, H., L. A. Grivell and J. A. Berden (1998). The respiratory chain in yeast behaves as a single functional unit. *J Biol Chem* 273(9): 4872-4877.

Brown, N. G., M. C. Costanzo and T. D. Fox (1994). Interactions among three proteins that specifically activate translation of the mitochondrial COX3 mRNA in Saccharomyces cerevisiae. *Mol Cell Biol* 14(2): 1045-1053.

Bruckmann, A., P. J. Hensbergen, C. I. Balog, A. M. Deelder, H. Y. de Steensma and G. P. van Heusden (2007). Post-transcriptional control of the Saccharomyces cerevisiae proteome by 14-3-3 proteins. *J Proteome Res* 6(5): 1689-1699.

Burger, G., M. W. Gray and B. F. Lang (2003). Mitochondrial genomes: anything goes. *Trends Genet* 19(12): 709-716.

Campbell, J. K., R. Gurung, S. Romero, C. J. Speed, R. K. Andrews, M. C. Berndt and C. A. Mitchell (1997). Activation of the 43 kDa inositol polyphosphate 5-phosphatase by 14-3-3zeta. *Biochemistry* 36(49): 15363-15370.

Celis, J. E. (1994). Cell biology : a laboratory handbook. San Diego ; London, Academic Press.

Chacinska, A., B. Guiard, J. M. Muller, A. Schulze-Specking, K. Gabriel, S. Kutik and N. Pfanner (2008). Mitochondrial biogenesis, switching the sorting pathway of the intermembrane space receptor Mia40. *J Biol Chem* 283(44): 29723-29729.

Chacinska, A., C. M. Koehler, D. Milenkovic, T. Lithgow and N. Pfanner (2009). Importing mitochondrial proteins: machineries and mechanisms. *Cell* 138(4): 628-644.

Chacinska, A., M. Lind, A. E. Frazier, J. Dudek, C. Meisinger, A. Geissler, A. Sickmann, H. E. Meyer, K. N. Truscott, B. Guiard, N. Pfanner and P. Rehling (2005). Mitochondrial presequence translocase: switching between TOM tethering and motor recruitment involves Tim21 and Tim17. *Cell* 120(6): 817-829.

Chacinska, A., M. van der Laan, C. S. Mehnert, B. Guiard, D. U. Mick, D. P. Hutu, K. N. Truscott, N. Wiedemann, C. Meisinger, N. Pfanner and P. Rehling (2010). Distinct forms of mitochondrial TOM-TIM supercomplexes define signal-dependent states of preprotein sorting. *Mol Cell Biol* 30(1): 307-318.

Chan, N. C. and T. Lithgow (2008). The peripheral membrane subunits of the SAM complex function codependently in mitochondrial outer membrane biogenesis. *Mol Biol Cell* 19(1): 126-136.

Chen, X. J. and R. A. Butow (2005). The organization and inheritance of the mitochondrial genome. *Nat Rev Genet* 6(11): 815-825.

Christianson, T. and M. Rabinowitz (1983). Identification of multiple transcriptional initiation sites on the yeast mitochondrial genome by in vitro capping with guanylyltransferase. *J Biol Chem* 258(22): 14025-14033.

Costanzo, M. C. and T. D. Fox (1988). Specific translational activation by nuclear gene products occurs in the 5' untranslated leader of a yeast mitochondrial mRNA. *Proc Natl Acad Sci U S A* 85(8): 2677-2681.

Costanzo, M. C. and T. D. Fox (1990). Control of mitochondrial gene expression in Saccharomyces cerevisiae. *Annu Rev Genet* 24: 91-113.

Darling, D. L., J. Yingling and A. Wynshaw-Boris (2005). Role of 14-3-3 proteins in eukaryotic signaling and development. *Curr Top Dev Biol* 68: 281-315.

Daum, G., P. C. Bohni and G. Schatz (1982). Import of proteins into mitochondria. Cytochrome b2 and cytochrome c peroxidase are located in the intermembrane space of yeast mitochondria. *J Biol Chem* 257(21): 13028-13033.

Dieckmann, C. L., L. K. Pape and A. Tzagoloff (1982). Identification and cloning of a yeast nuclear gene (CBP1) involved in expression of mitochondrial cytochrome b. *Proc Natl Acad Sci U S A* 79(6): 1805-1809.

Dieckmann, C. L. and R. R. Staples (1994). Regulation of mitochondrial gene expression in Saccharomyces cerevisiae. *Int Rev Cytol* 152: 145-181.

Dieckmann, C. L. and A. Tzagoloff (1985). Assembly of the mitochondrial membrane system. CBP6, a yeast nuclear gene necessary for synthesis of cytochrome b. *J Biol Chem* 260(3): 1513-1520.

Dietze, I., B. Fritz, D. Huhle, W. Simoens, E. Piecha and H. Rehder (2004). Clinical, cytogenetic and molecular investigation in a fetus with Wolf-Hirschhorn syndrome with paternally derived 4p deletion. Case report and review of the literature. *Fetal Diagn Ther* 19(3): 251-260.

Dimmer, K. S., S. Fritz, F. Fuchs, M. Messerschmitt, N. Weinbach, W. Neupert and B. Westermann (2002). Genetic basis of mitochondrial function and morphology in Saccharomyces cerevisiae. *Mol Biol Cell* 13(3): 847-853.

Douglas, M. G. and R. A. Butow (1976). Variant forms of mitochondrial translation products in yeast: evidence for location of determinants on mitochondrial DNA. *Proc Natl Acad Sci U S A* 73(4): 1083-1086.

Dunstan, H. M., N. S. Green-Willms and T. D. Fox (1997). In vivo analysis of Saccharomyces cerevisiae COX2 mRNA 5'-untranslated leader functions in mitochondrial translation initiation and translational activation. *Genetics* 147(1): 87-100.

Dyall, S. D., M. T. Brown and P. J. Johnson (2004). Ancient invasions: from endosymbionts to organelles. *Science* 304(5668): 253-257.

Embley, T. M. and W. Martin (2006). Eukaryotic evolution, changes and challenges. *Nature* 440(7084): 623-630.

Emsley, P. and K. Cowtan (2004). Coot: model-building tools for molecular graphics. *Acta Crystallogr D Biol Crystallogr* 60(Pt 12 Pt 1): 2126-2132.

Endele, S., M. Fuhry, S. J. Pak, B. U. Zabel and A. Winterpacht (1999). LETM1, a novel gene encoding a putative EF-hand Ca(2+)-binding protein, flanks the Wolf-Hirschhorn syndrome (WHS) critical region and is deleted in most WHS patients. *Genomics* 60(2): 218-225.

Fearon, K. and T. L. Mason (1992). Structure and function of MRP20 and MRP49, the nuclear genes for two proteins of the 54 S subunit of the yeast mitochondrial ribosome. *J Biol Chem* 267(8): 5162-5170.

Finnegan, P. M., T. P. Ellis, P. Nagley and H. B. Lukins (1995). The mature AEP2 gene product of Saccharomyces cerevisiae, required for the expression of subunit 9 of ATP synthase, is a 58 kDa mitochondrial protein. *FEBS Lett* 368(3): 505-508.

Fiori, A., T. L. Mason and T. D. Fox (2003). Evidence that synthesis of the Saccharomyces cerevisiae mitochondrially encoded ribosomal protein Var1p may be membrane localized. *Eukaryot Cell* 2(3): 651-653.

Fiumera, H. L., S. A. Broadley and T. D. Fox (2007). Translocation of mitochondrially synthesized Cox2 domains from the matrix to the intermembrane space. *Mol Cell Biol* 27(13): 4664-4673.

Fontanesi, F., P. Clemente and A. Barrientos (2011). Cox25 teams up with Mss51, Ssc1, and Cox14 to regulate mitochondrial cytochrome c oxidase subunit 1 expression and assembly in Saccharomyces cerevisiae. *J Biol Chem* 286(1): 555-566.

Fontanesi, F., I. C. Soto, D. Horn and A. Barrientos (2010). Mss51 and Ssc1 facilitate translational regulation of cytochrome c oxidase biogenesis. *Mol Cell Biol* 30(1): 245-259.

Foster, L. J., C. L. de Hoog, Y. Zhang, X. Xie, V. K. Mootha and M. Mann (2006). A mammalian organelle map by protein correlation profiling. *Cell* 125(1): 187-199.

Foury, F., T. Roganti, N. Lecrenier and B. Purnelle (1998). The complete sequence of the mitochondrial genome of Saccharomyces cerevisiae. *FEBS Lett* 440(3): 325-331.

Fox, T. D. (1996). Genetics of mitochondrial translation. in *Translational Control*, Cold Spring Harbor Laboratory Press**:** 733-758.

Fox, T. D. (1996). Translational control of endogenous and recoded nuclear genes in yeast mitochondria: regulation and membrane targeting. *Experientia* 52(12): 1130-1135.

Frazier, A. E., R. D. Taylor, D. U. Mick, B. Warscheid, N. Stoepel, H. E. Meyer, M. T. Ryan, B. Guiard and P. Rehling (2006). Mdm38 interacts with ribosomes and is a component of the mitochondrial protein export machinery. *J Cell Biol* 172(4): 553-564.

Froschauer, E., K. Nowikovsky and R. J. Schweyen (2005). Electroneutral K+/H+ exchange in mitochondrial membrane vesicles involves Yol027/Letm1 proteins. *Biochim Biophys Acta* 1711(1): 41-48.

Fukuhara, N., J. Ebert, L. Unterholzner, D. Lindner, E. Izaurralde and E. Conti (2005). SMG7 is a 14-3-3-like adaptor in the nonsense-mediated mRNA decay pathway. *Mol Cell* 17(4): 537-547.

Funes, S., L. Gerdes, M. Inaba, J. Soll and J. M. Herrmann (2004). The Arabidopsis thaliana chloroplast inner envelope protein ARTEMIS is a functional member of the Alb3/Oxa1/YidC family of proteins. *FEBS Lett* 569(1-3): 89-93.

Funes, S., A. Hasona, H. Bauerschmitt, C. Grubbauer, F. Kauff, R. Collins, P. J. Crowley, S. R. Palmer, L. J. Brady and J. M. Herrmann (2009). Independent gene duplications of the YidC/Oxa/Alb3 family enabled a specialized cotranslational function. *Proc Natl Acad Sci U S A* 106(16): 6656-6661.

Funes, S., F. Kauff, E. O. van der Sluis, M. Ott and J. M. Herrmann (2011). Evolution of YidC/Oxa1/Alb3 insertases: three independent gene duplications followed by functional specialization in bacteria, mitochondria and chloroplasts. *Biol Chem*.

Gebert, N., M. T. Ryan, N. Pfanner, N. Wiedemann and D. Stojanovski (2010). Mitochondrial protein import machineries and lipids: A functional connection. *Biochim Biophys Acta*.

Geissler, A., T. Krimmer, U. Bomer, B. Guiard, J. Rassow and N. Pfanner (2000). Membrane potential-driven protein import into mitochondria. The sorting sequence of cytochrome b(2) modulates the deltapsi-dependence of translocation of the matrix-targeting sequence. *Mol Biol Cell* 11(11): 3977-3991.

Gietz, R. D. and R. H. Schiestl (2007). High-efficiency yeast transformation using the LiAc/SS carrier DNA/PEG method. *Nat Protoc* 2(1): 31-34.

Giraud, M. F., P. Paumard, V. Soubannier, J. Vaillier, G. Arselin, B. Salin, J. Schaeffer, D. Brethes, J. P. di Rago and J. Velours (2002). Is there a relationship between the supramolecular organization of the mitochondrial ATP synthase and the formation of cristae? *Biochim Biophys Acta* 1555(1-3): 174-180.

Graack, H. R. and B. Wittmann-Liebold (1998). Mitochondrial ribosomal proteins (MRPs) of yeast. *Biochem J* 329 (Pt 3): 433-448.

Graier, W. F., M. Frieden and R. Malli (2007). Mitochondria and Ca(2+) signaling: old guests, new functions. *Pflugers Arch* 455(3): 375-396.

Gray, M. W., G. Burger and B. F. Lang (1999). Mitochondrial evolution. *Science* 283(5407): 1476-1481.

Gray, M. W., G. Burger and B. F. Lang (2001). The origin and early evolution of mitochondria. *Genome Biol* 2(6): REVIEWS1018.

Green-Willms, N. S., T. D. Fox and M. C. Costanzo (1998). Functional interactions between yeast mitochondrial ribosomes and mRNA 5' untranslated leaders. *Mol Cell Biol* 18(4): 1826-1834.

Grivell, L. A. (1989). Nucleo-mitochondrial interactions in yeast mitochondrial biogenesis. *Eur J Biochem* 182(3): 477-493.

Grivell, L. A. (1995). Nucleo-mitochondrial interactions in mitochondrial gene expression. *Crit Rev Biochem Mol Biol* 30(2): 121-164.

Grivell, L. A. and R. J. Schweyen (1989). RNA splicing in yeast mitochondria: taking out the twists. *Trends Genet* 5(2): 39-41.

Gruschke, S., K. Grone, M. Heublein, S. Holz, L. Israel, A. Imhof, J. M. Herrmann and M. Ott (2010). Proteins at the polypeptide tunnel exit of the yeast mitochondrial ribosome. *J Biol Chem* 285(25): 19022-19028.

Gruschke, S. and M. Ott (2010). The polypeptide tunnel exit of the mitochondrial ribosome is tailored to meet the specific requirements of the organelle. *Bioessays* 32(12): 1050-1057.

Gu, M. and X. Du (1998). A novel ligand-binding site in the zeta-form 14-3-3 protein recognizing the platelet glycoprotein Ibalpha and distinct from the c-Raf-binding site. *J Biol Chem* 273(50): 33465-33471.

Gu, S. Q., F. Peske, H. J. Wieden, M. V. Rodnina and W. Wintermeyer (2003). The signal recognition particle binds to protein L23 at the peptide exit of the Escherichia coli ribosome. *RNA* 9(5): 566-573.

Hachiya, N., K. Mihara, K. Suda, M. Horst, G. Schatz and T. Lithgow (1995). Reconstitution of the initial steps of mitochondrial protein import. *Nature* 376(6542): 705-709.

Hartl, F. U., B. Schmidt, E. Wachter, H. Weiss and W. Neupert (1986). Transport into mitochondria and intramitochondrial sorting of the Fe/S protein of ubiquinol-cytochrome c reductase. *Cell* 47(6): 939-951.

He, S. and T. D. Fox (1997). Membrane translocation of mitochondrially coded Cox2p: distinct requirements for export of N and C termini and dependence on the conserved protein Oxa1p. *Mol Biol Cell* 8(8): 1449-1460.

Hell, K. (2008). The Erv1-Mia40 disulfide relay system in the intermembrane space of mitochondria. *Biochim Biophys Acta* 1783(4): 601-609.

Hell, K., J. Herrmann, E. Pratje, W. Neupert and R. A. Stuart (1997). Oxa1p mediates the export of the N- and C-termini of pCoxII from the mitochondrial matrix to the intermembrane space. *FEBS Lett* 418(3): 367-370.

Hell, K., W. Neupert and R. A. Stuart (2001). Oxa1p acts as a general membrane insertion machinery for proteins encoded by mitochondrial DNA. *EMBO J* 20(6): 1281-1288.

Herrmann, J. M., W. Neupert and R. A. Stuart (1997). Insertion into the mitochondrial inner membrane of a polytopic protein, the nuclear-encoded Oxa1p. *EMBO J* 16(9): 2217-2226.

Herrmann, J. M., R. A. Stuart, E. A. Craig and W. Neupert (1994). Mitochondrial heat shock protein 70, a molecular chaperone for proteins encoded by mitochondrial DNA. *J Cell Biol* 127(4): 893-902.

Hofmann, S., U. Rothbauer, N. Muhlenbein, K. Baiker, K. Hell and M. F. Bauer (2005). Functional and mutational characterization of human MIA40 acting during import into the mitochondrial intermembrane space. *J Mol Biol* 353(3): 517-528.

Holm, L. and P. Rosenstrom (2010). Dali server: conservation mapping in 3D. *Nucleic Acids Res* 38(Web Server issue): W545-549.

Hudspeth, M. E., W. M. Ainley, D. S. Shumard, R. A. Butow and L. I. Grossman (1982). Location and structure of the var1 gene on yeast mitochondrial DNA: nucleotide sequence of the 40.0 allele. *Cell* 30(2): 617-626.

Hutu, D. P., B. Guiard, A. Chacinska, D. Becker, N. Pfanner, P. Rehling and M. van der Laan (2008). Mitochondrial protein import motor: differential role of Tim44 in the recruitment of Pam17 and J-complex to the presequence translocase. *Mol Biol Cell* 19(6): 2642-2649.

Hwang, S. K., L. Piao, H. T. Lim, A. Minai-Tehrani, K. N. Yu, Y. C. Ha, C. H. Chae, K. H. Lee, G. R. Beck, J. Park and M. H. Cho (2010). Suppression of lung tumorigenesis by leucine zipper/EF hand-containing transmembrane-1. *PLoS One* 5(9).

Ichimura, T., M. Ito, C. Itagaki, M. Takahashi, T. Horigome, S. Omata, S. Ohno and T. Isobe (1997). The 14-3-3 protein binds its target proteins with a common site located towards the C-terminus. *FEBS Lett* 413(2): 273-276.

Jia, L., M. Dienhart, M. Schramp, M. McCauley, K. Hell and R. A. Stuart (2003). Yeast Oxa1 interacts with mitochondrial ribosomes: the importance of the C-terminal region of Oxa1. *EMBO J* 22(24): 6438-6447.

Jia, L., J. Kaur and R. A. Stuart (2009). Mapping of the Saccharomyces cerevisiae Oxa1-mitochondrial ribosome interface and identification of MrpL40, a ribosomal protein in close proximity to Oxa1 and critical for oxidative phosphorylation complex assembly. *Eukaryot Cell* 8(11): 1792-1802.

Jiang, D., L. Zhao and D. E. Clapham (2009). Genome-wide RNAi screen identifies Letm1 as a mitochondrial Ca2+/H+ antiporter. *Science* 326(5949): 144-147.

Johnson, C., S. Crowther, M. J. Stafford, D. G. Campbell, R. Toth and C. MacKintosh (2010). Bioinformatic and experimental survey of 14-3-3-binding sites. *Biochem J* 427(1): 69-78.

Kabsch, W. (1993). Automatic processing of rotation diffraction data from crystals of initially unknown symmetry and cell constants. *Journal of Applied Crystallography* 26(6): 795-800.

Kagan, A., Y. F. Melman, A. Krumerman and T. V. McDonald (2002). 14-3-3 amplifies and prolongs adrenergic stimulation of HERG K+ channel activity. *EMBO J* 21(8): 1889-1898.

Keating, K. S., N. Toor, P. S. Perlman and A. M. Pyle (2010). A structural analysis of the group II intron active site and implications for the spliceosome. *RNA* 16(1): 1-9.

Khalimonchuk, O., A. Bird and D. R. Winge (2007). Evidence for a pro-oxidant intermediate in the assembly of cytochrome oxidase. *J Biol Chem* 282(24): 17442-17449.

Kitakawa, M., H. R. Graack, L. Grohmann, S. Goldschmidt-Reisin, E. Herfurth, B. Wittmann-Liebold, T. Nishimura and K. Isono (1997). Identification and characterization of the genes for mitochondrial ribosomal proteins of Saccharomyces cerevisiae. *Eur J Biochem* 245(2): 449-456.

Kitakawa, M. and K. Isono (1991). The mitochondrial ribosomes. *Biochimie* 73(6): 813-825.

Knop, M., K. Siegers, G. Pereira, W. Zachariae, B. Winsor, K. Nasmyth and E. Schiebel (1999). Epitope tagging of yeast genes using a PCR-based strategy: more tags and improved practical routines. *Yeast* 15(10B): 963-972.

Kohler, R., D. Boehringer, B. Greber, R. Bingel-Erlenmeyer, I. Collinson, C. Schaffitzel and N. Ban (2009). YidC and Oxa1 form dimeric insertion pores on the translating ribosome. *Mol Cell* 34(3): 344-353.

Kozjak, V., N. Wiedemann, D. Milenkovic, C. Lohaus, H. E. Meyer, B. Guiard, C. Meisinger and N. Pfanner (2003). An essential role of Sam50 in the protein sorting and assembly machinery of the mitochondrial outer membrane. *J Biol Chem* 278(49): 48520-48523.

Krause, K., R. Lopes de Souza, D. G. Roberts and C. L. Dieckmann (2004). The mitochondrial message-specific mRNA protectors Cbp1 and Pet309 are associated in a high-molecular weight complex. *Mol Biol Cell* 15(6): 2674-2683.

Kutik, S., D. Stojanovski, L. Becker, T. Becker, M. Meinecke, V. Kruger, C. Prinz, C. Meisinger, B. Guiard, R. Wagner, N. Pfanner and N. Wiedemann (2008). Dissecting membrane insertion of mitochondrial beta-barrel proteins. *Cell* 132(6): 1011-1024.

Kutik, S., D. A. Stroud, N. Wiedemann and N. Pfanner (2009). Evolution of mitochondrial protein biogenesis. *Biochim Biophys Acta* 1790(6): 409-415.

Labouesse, M., P. Netter and R. Schroeder (1984). Molecular basis of the 'box effect', A maturase deficiency leading to the absence of splicing of two introns located in two split genes of yeast mitochondrial DNA. *Eur J Biochem* 144(1): 85-93.

Laemmli, U. K. (1970). Cleavage of structural proteins during the assembly of the head of bacteriophage T4. *Nature* 227(5259): 680-685.

Lazowska, J., C. Jacq and P. P. Slonimski (1980). Sequence of introns and flanking exons in wild-type and box3 mutants of cytochrome b reveals an interlaced splicing protein coded by an intron. *Cell* 22(2 Pt 2): 333-348.

Lee, C., A. S. Tibbetts, G. Kramer and D. R. Appling (2009). Yeast AEP3p is an accessory factor in initiation of mitochondrial translation. *J Biol Chem* 284(49): 34116-34125.

Lee, S. W., S. J. Berger, S. Martinovic, L. Pasa-Tolic, G. A. Anderson, Y. Shen, R. Zhao and R. D. Smith (2002). Direct mass spectrometric analysis of intact proteins of the yeast large ribosomal subunit using capillary LC/FTICR. *Proc Natl Acad Sci U S A* 99(9): 5942-5947.

Lenaz, G. and M. L. Genova (2009). Structural and functional organization of the mitochondrial respiratory chain: a dynamic super-assembly. *Int J Biochem Cell Biol* 41(10): 1750-1772.

Li, Y., J. Dudek, B. Guiard, N. Pfanner, P. Rehling and W. Voos (2004). The presequence translocase-associated protein import motor of mitochondria. Pam16 functions in an antagonistic manner to Pam18. *J Biol Chem* 279(36): 38047-38054.

Maleszka, R., P. J. Skelly and G. D. Clark-Walker (1991). Rolling circle replication of DNA in yeast mitochondria. *EMBO J* 10(12): 3923-3929.

Manthey, G. M. and J. E. McEwen (1995). The product of the nuclear gene PET309 is required for translation of mature mRNA and stability or production of intron-containing RNAs derived from the mitochondrial COX1 locus of Saccharomyces cerevisiae. *EMBO J* 14(16): 4031-4043.

Marzuki, S. and A. R. Hibbs (1986). Are all mitochondrial translation products synthesized on membrane-bound ribosomes? *Biochim Biophys Acta* 866(2-3): 120-124.

May, T. and J. Soll (2000). 14-3-3 proteins form a guidance complex with chloroplast precursor proteins in plants. *Plant Cell* 12(1): 53-64.

McMullin, T. W., P. Haffter and T. D. Fox (1990). A novel small-subunit ribosomal protein of yeast mitochondria that interacts functionally with an mRNA-specific translational activator. *Mol Cell Biol* 10(9): 4590-4595.

McQuibban, A. G., N. Joza, A. Megighian, M. Scorzeto, D. Zanini, S. Reipert, C. Richter, R. J. Schweyen and K. Nowikovsky (2010). A Drosophila mutant of LETM1, a candidate gene for seizures in Wolf-Hirschhorn syndrome. *Hum Mol Genet* 19(6): 987-1000.

Meinecke, M., R. Wagner, P. Kovermann, B. Guiard, D. U. Mick, D. P. Hutu, W. Voos, K. N. Truscott, A. Chacinska, N. Pfanner and P. Rehling (2006). Tim50 maintains the permeability barrier of the mitochondrial inner membrane. *Science* 312(5779): 1523-1526.

Meisinger, C., N. Pfanner and K. N. Truscott (2006). Isolation of yeast mitochondria. *Methods Mol Biol* 313: 33-39.

Meisinger, C., M. T. Ryan, K. Hill, K. Model, J. H. Lim, A. Sickmann, H. Muller, H. E. Meyer, R. Wagner and N. Pfanner (2001). Protein import channel of the outer mitochondrial membrane: a highly stable Tom40-Tom22 core structure differentially interacts with preproteins, small tom proteins, and import receptors. *Mol Cell Biol* 21(7): 2337-2348.

Miao, B., J. E. Davis and E. A. Craig (1997). Mge1 functions as a nucleotide release factor for Ssc1, a mitochondrial Hsp70 of Saccharomyces cerevisiae. *J Mol Biol* 265(5): 541-552.

Michaelis, U., A. Korte and G. Rodel (1991). Association of cytochrome b translational activator proteins with the mitochondrial membrane: implications for cytochrome b expression in yeast. *Mol Gen Genet* 230(1-2): 177-185.

Mick, D. U., T. D. Fox and P. Rehling (2011). Inventory control: cytochrome c oxidase assembly regulates mitochondrial translation. *Nat Rev Mol Cell Biol* 12(1): 14-20.

Mick, D. U., M. Vukotic, H. Piechura, H. E. Meyer, B. Warscheid, M. Deckers and P. Rehling (2010). Coa3 and Cox14 are essential for negative feedback regulation of COX1 translation in mitochondria. *J Cell Biol* 191(1): 141-154.

Mick, D. U., K. Wagner, M. van der Laan, A. E. Frazier, I. Perschil, M. Pawlas, H. E. Meyer, B. Warscheid and P. Rehling (2007). Shy1 couples Cox1 translational regulation to cytochrome c oxidase assembly. *EMBO J* 26(20): 4347-4358.

Milenkovic, D., V. Kozjak, N. Wiedemann, C. Lohaus, H. E. Meyer, B. Guiard, N. Pfanner and C. Meisinger (2004). Sam35 of the mitochondrial protein sorting and assembly machinery is a peripheral outer membrane protein essential for cell viability. *J Biol Chem* 279(21): 22781-22785.

Miroux, B. and J. E. Walker (1996). Over-production of proteins in Escherichia coli: mutant hosts that allow synthesis of some membrane proteins and globular proteins at high levels. *J Mol Biol* 260(3): 289-298.

Mitchell, P. and J. Moyle (1965). Evidence discriminating between the chemical and the chemiosmotic mechanisms of electron transport phosphorylation. *Nature* 208(5016): 1205-1206.

Mitchell, P. and J. Moyle (1968). Proton translocation coupled to ATP hydrolysis in rat liver mitochondria. *Eur J Biochem* 4(4): 530-539.

Model, K., C. Meisinger and W. Kuhlbrandt (2008). Cryo-electron microscopy structure of a yeast mitochondrial preprotein translocase. *J Mol Biol* 383(5): 1049-1057.

Model, K., C. Meisinger, T. Prinz, N. Wiedemann, K. N. Truscott, N. Pfanner and M. T. Ryan (2001). Multistep assembly of the protein import channel of the mitochondrial outer membrane. *Nat Struct Biol* 8(4): 361-370.

Mokranjac, D. and W. Neupert (2009). Thirty years of protein translocation into mitochondria: unexpectedly complex and still puzzling. *Biochim Biophys Acta* 1793(1): 33-41.

Mokranjac, D., M. Sichting, D. Popov-Celeketic, K. Mapa, L. Gevorkyan-Airapetov, K. Zohary, K. Hell, A. Azem and W. Neupert (2009). Role of Tim50 in the transfer of precursor proteins from the outer to the inner membrane of mitochondria. *Mol Biol Cell* 20(5): 1400-1407.

Moorman, A. F., G. J. Van Ommen and L. A. Grivell (1978). Transcription in yeast mitochondria: isolation and physical mapping of messenger RNAs for subunits of cytochrome c oxidase and ATPase. *Mol Gen Genet* 160(1): 13-24.

Mootha, V. K., P. Lepage, K. Miller, J. Bunkenborg, M. Reich, M. Hjerrild, T. Delmonte, A. Villeneuve, R. Sladek, F. Xu, G. A. Mitchell, C. Morin, M. Mann, T. J. Hudson, B. Robinson, J. D. Rioux and E. S. Lander (2003). Identification of a gene causing human cytochrome c oxidase deficiency by integrative genomics. *Proc Natl Acad Sci U S A* 100(2): 605-610.

Mullis, K. B. (1990). Target amplification for DNA analysis by the polymerase chain reaction. *Ann Biol Clin (Paris)* 48(8): 579-582.

Nagata, S., Y. Tsunetsugu-Yokota, A. Naito and Y. Kaziro (1983). Molecular cloning and sequence determination of the nuclear gene coding for mitochondrial elongation factor Tu of Saccharomyces cerevisiae. *Proc Natl Acad Sci U S A* 80(20): 6192-6196.

Naithani, S., S. A. Saracco, C. A. Butler and T. D. Fox (2003). Interactions among COX1, COX2, and COX3 mRNA-specific translational activator proteins on the inner surface of the mitochondrial inner membrane of Saccharomyces cerevisiae. *Mol Biol Cell* 14(1): 324-333.

Nargang, F. E., M. Preuss, W. Neupert and J. M. Herrmann (2002). The Oxa1 protein forms a homooligomeric complex and is an essential part of the mitochondrial export translocase in Neurospora crassa. *J Biol Chem* 277(15): 12846-12853.

Nowikovsky, K., R. J. Devenish, E. Froschauer and R. J. Schweyen (2009). Determination of yeast mitochondrial KHE activity, osmotic swelling and mitophagy. *Methods Enzymol* 457: 305-317.

Nowikovsky, K., E. M. Froschauer, G. Zsurka, J. Samaj, S. Reipert, M. Kolisek, G. Wiesenberger and R. J. Schweyen (2004). The LETM1/YOL027 gene family encodes a factor of the mitochondrial K+ homeostasis with a potential role in the Wolf-Hirschhorn syndrome. *J Biol Chem* 279(29): 30307-30315.

Nowikovsky, K., S. Reipert, R. J. Devenish and R. J. Schweyen (2007). Mdm38 protein depletion causes loss of mitochondrial K+/H+ exchange activity, osmotic swelling and mitophagy. *Cell Death Differ* 14(9): 1647-1656.

O'Brien, T. W. (2003). Properties of human mitochondrial ribosomes. *IUBMB Life* 55(9): 505-513.

Ott, M. and J. M. Herrmann (2010). Co-translational membrane insertion of mitochondrially encoded proteins. *Biochim Biophys Acta* 1803(6): 767-775.

Ott, M., M. Prestele, H. Bauerschmitt, S. Funes, N. Bonnefoy and J. M. Herrmann (2006). Mba1, a membrane-associated ribosome receptor in mitochondria. *EMBO J* 25(8): 1603-1610.

Ottmann, C., S. Marco, N. Jaspert, C. Marcon, N. Schauer, M. Weyand, C. Vandermeeren, G. Duby, M. Boutry, A. Wittinghofer, J. L. Rigaud and C. Oecking (2007). Structure of a 14-3-3 coordinated hexamer of the plant plasma membrane H+ -ATPase by combining X-ray crystallography and electron cryomicroscopy. *Mol Cell* 25(3): 427-440.

Otwinowski, Z. and W. Minor (1997). [20] Processing of X-ray diffraction data collected in oscillation mode. in *Methods in Enzymology*. Charles W. Carter, Jr., Academic Press. **Volume 276:** 307-326.

Payne, M. J., P. M. Finnegan, P. M. Smooker and H. B. Lukins (1993). Characterization of a second nuclear gene, AEP1, required for expression of the mitochondrial OLI1 gene in Saccharomyces cerevisiae. *Curr Genet* 24(1-2): 126-135.

Pel, H. J., C. Maat, M. Rep and L. A. Grivell (1992). The yeast nuclear gene MRF1 encodes a mitochondrial peptide chain release factor and cures several mitochondrial RNA splicing defects. *Nucleic Acids Res* 20(23): 6339-6346.

Perez-Martinez, X., S. A. Broadley and T. D. Fox (2003). Mss51p promotes mitochondrial Cox1p synthesis and interacts with newly synthesized Cox1p. *EMBO J* 22(21): 5951-5961.

Perez-Martinez, X., C. A. Butler, M. Shingu-Vazquez and T. D. Fox (2009). Dual functions of Mss51 couple synthesis of Cox1 to assembly of cytochrome c oxidase in Saccharomyces cerevisiae mitochondria. *Mol Biol Cell* 20(20): 4371-4380.

Perkins, G., C. Renken, M. E. Martone, S. J. Young, M. Ellisman and T. Frey (1997). Electron tomography of neuronal mitochondria: three-dimensional structure and organization of cristae and membrane contacts. *J Struct Biol* 119(3): 260-272.

Perrakis, A., R. Morris and V. S. Lamzin (1999). Automated protein model building combined with iterative structure refinement. *Nat Struct Biol* 6(5): 458-463.

Piao, L., Y. Li, S. J. Kim, H. S. Byun, S. M. Huang, S. K. Hwang, K. J. Yang, K. A. Park, M. Won, J. Hong, G. M. Hur, J. H. Seok, M. Shong, M. H. Cho, D. P. Brazil, B. A. Hemmings and J. Park (2009). Association of LETM1 and MRPL36 contributes to the regulation of mitochondrial ATP production and necrotic cell death. *Cancer Res* 69(8): 3397-3404.

Pierrel, F., M. L. Bestwick, P. A. Cobine, O. Khalimonchuk, J. A. Cricco and D. R. Winge (2007). Coa1 links the Mss51 post-translational function to Cox1 cofactor insertion in cytochrome c oxidase assembly. *EMBO J* 26(20): 4335-4346.

Poutre, C. G. and T. D. Fox (1987). PET111, a Saccharomyces cerevisiae nuclear gene required for translation of the mitochondrial mRNA encoding cytochrome c oxidase subunit II. *Genetics* 115(4): 637-647.

Preuss, M., K. Leonhard, K. Hell, R. A. Stuart, W. Neupert and J. M. Herrmann (2001). Mba1, a novel component of the mitochondrial protein export machinery of the yeast Saccharomyces cerevisiae. *J Cell Biol* 153(5): 1085-1096.

Preuss, M., M. Ott, S. Funes, J. Luirink and J. M. Herrmann (2005). Evolution of mitochondrial oxa proteins from bacterial YidC. Inherited and acquired functions of a conserved protein insertion machinery. *J Biol Chem* 280(13): 13004-13011.

Prokisch, H., C. Scharfe, D. G. Camp, 2nd, W. Xiao, L. David, C. Andreoli, M. E. Monroe, R. J. Moore, M. A. Gritsenko, C. Kozany, K. K. Hixson, H. M. Mottaz, H. Zischka, M. Ueffing, Z. S. Herman, R. W. Davis, T. Meitinger, P. J. Oefner, R. D. Smith and L. M. Steinmetz (2004). Integrative analysis of the mitochondrial proteome in yeast. *PLoS Biol* 2(6): e160.

Rabl, R., V. Soubannier, R. Scholz, F. Vogel, N. Mendl, A. Vasiljev-Neumeyer, C. Korner, R. Jagasia, T. Keil, W. Baumeister, M. Cyrklaff, W. Neupert and A. S. Reichert (2009). Formation of cristae and crista junctions in mitochondria depends on antagonism between Fcj1 and Su e/g. *J Cell Biol* 185(6): 1047-1063.

Rapaport, D. (2003). Finding the right organelle. Targeting signals in mitochondrial outer-membrane proteins. *EMBO Rep* 4(10): 948-952.

Rauch, A., S. Schellmoser, C. Kraus, H. G. Dorr, U. Trautmann, M. R. Altherr, R. A. Pfeiffer and A. Reis (2001). First known microdeletion within the Wolf-Hirschhorn syndrome critical region refines genotype-phenotype correlation. *Am J Med Genet* 99(4): 338-342.

Rehling, P., K. Brandner and N. Pfanner (2004). Mitochondrial import and the twin-pore translocase. *Nat Rev Mol Cell Biol* 5(7): 519-530.

Rehling, P., K. Model, K. Brandner, P. Kovermann, A. Sickmann, H. E. Meyer, W. Kuhlbrandt, R. Wagner, K. N. Truscott and N. Pfanner (2003). Protein insertion into the mitochondrial inner membrane by a twin-pore translocase. *Science* 299(5613): 1747-1751.

Reinders, J., R. P. Zahedi, N. Pfanner, C. Meisinger and A. Sickmann (2006). Toward the complete yeast mitochondrial proteome: multidimensional separation techniques for mitochondrial proteomics. *J Proteome Res* 5(7): 1543-1554.

Rimessi, A., C. Giorgi, P. Pinton and R. Rizzuto (2008). The versatility of mitochondrial calcium signals: from stimulation of cell metabolism to induction of cell death. *Biochim Biophys Acta* 1777(7-8): 808-816.

Rinaldi, T., C. Dallabona, I. Ferrero, L. Frontali and M. Bolotin-Fukuhara (2010). Mitochondrial diseases and the role of the yeast models. *FEMS Yeast Res* 10(8): 1006-1022.

Rodel, G. (1986). Two yeast nuclear genes, CBS1 and CBS2, are required for translation of mitochondrial transcripts bearing the 5'-untranslated COB leader. *Curr Genet* 11(1): 41-45.

Rosello, M., S. Monfort, C. Orellana, I. Ferrer-Bolufer, R. Quiroga, S. Oltra and F. Martinez (2009). Submicroscopic duplication of the Wolf-Hirschhorn critical region with a 4p terminal deletion. *Cytogenet Genome Res* 125(2): 103-108.

Saint-Georges, Y., P. Hamel, C. Lemaire and G. Dujardin (2001). Role of positively charged transmembrane segments in the insertion and assembly of mitochondrial inner-membrane proteins. *Proc Natl Acad Sci U S A* 98(24): 13814-13819.

Sambrook, J., E. F. Fritsch and T. Maniatis (1989). Molecular cloning : a laboratory manual. Cold Spring Harbor, Cold Spring Harbor Laboratory Press.

Sanger, F., S. Nicklen and A. R. Coulson (1977). DNA sequencing with chain-terminating inhibitors. *Proc Natl Acad Sci U S A* 74(12): 5463-5467.

Saracco, S. A. and T. D. Fox (2002). Cox18p is required for export of the mitochondrially encoded Saccharomyces cerevisiae Cox2p C-tail and interacts with Pnt1p and Mss2p in the inner membrane. *Mol Biol Cell* 13(4): 1122-1131.

Schagger, H. and K. Pfeiffer (2000). Supercomplexes in the respiratory chains of yeast and mammalian mitochondria. *EMBO J* 19(8): 1777-1783.

Schagger, H. and G. von Jagow (1991). Blue native electrophoresis for isolation of membrane protein complexes in enzymatically active form. *Anal Biochem* 199(2): 223-231.

Scheffler, I. E. (1999). Mitochondria. New York, Wiley-Liss.

Scheffler, I. E. (2001). A century of mitochondrial research: achievements and perspectives. *Mitochondrion* 1(1): 3-31.

Schlickum, S., A. Moghekar, J. C. Simpson, C. Steglich, R. J. O'Brien, A. Winterpacht and S. U. Endele (2004). LETM1, a gene deleted in Wolf-Hirschhorn syndrome, encodes an evolutionarily conserved mitochondrial protein. *Genomics* 83(2): 254-261.

Schwimmer, C., M. Rak, L. Lefebvre-Legendre, S. Duvezin-Caubet, G. Plane and J. P. di Rago (2006). Yeast models of human mitochondrial diseases: from molecular mechanisms to drug screening. *Biotechnol J* 1(3): 270-281.

Seeger, J., B. Schrank, A. Pyle, R. Stucka, U. Lorcher, S. Muller-Ziermann, A. Abicht, B. Czermin, E. Holinski-Feder, H. Lochmuller and R. Horvath (2010). Clinical and neuropathological findings in patients with TACO1 mutations. *Neuromuscul Disord* 20(11): 720-724.

Sharma, M. R., E. C. Koc, P. P. Datta, T. M. Booth, L. L. Spremulli and R. K. Agrawal (2003). Structure of the mammalian mitochondrial ribosome reveals an expanded functional role for its component proteins. *Cell* 115(1): 97-108.

Sickmann, A., J. Reinders, Y. Wagner, C. Joppich, R. Zahedi, H. E. Meyer, B. Schonfisch, I. Perschil, A. Chacinska, B. Guiard, P. Rehling, N. Pfanner and C. Meisinger (2003). The proteome of Saccharomyces cerevisiae mitochondria. *Proc Natl Acad Sci U S A* 100(23): 13207-13212.

Siep, M., K. van Oosterum, H. Neufeglise, H. van der Spek and L. A. Grivell (2000). Mss51p, a putative translational activator of cytochrome c oxidase subunit-1 (COX1) mRNA, is required for synthesis of Cox1p in Saccharomyces cerevisiae. *Curr Genet* 37(4): 213-220.

Sikorski, R. S. and P. Hieter (1989). A system of shuttle vectors and yeast host strains designed for efficient manipulation of DNA in Saccharomyces cerevisiae. *Genetics* 122(1): 19-27.

Simbeni, R., L. Pon, E. Zinser, F. Paltauf and G. Daum (1991). Mitochondrial membrane contact sites of yeast. Characterization of lipid components and possible involvement in intramitochondrial translocation of phospholipids. *J Biol Chem* 266(16): 10047-10049.

Smits, P., J. A. Smeitink, L. P. van den Heuvel, M. A. Huynen and T. J. Ettema (2007). Reconstructing the evolution of the mitochondrial ribosomal proteome. *Nucleic Acids Res* 35(14): 4686-4703.

Sorokina, E. M., S. I. Feinstein, S. Zhou and A. B. Fisher (2011). Intracellular targeting of peroxiredoxin 6 to lysosomal organelles requires MAPK activity and binding to 14-3-3 epsilon. *Am J Physiol Cell Physiol*.

Souza, R. L., N. S. Green-Willms, T. D. Fox, A. Tzagoloff and F. G. Nobrega (2000). Cloning and characterization of COX18, a Saccharomyces cerevisiae PET gene required for the assembly of cytochrome oxidase. *J Biol Chem* 275(20): 14898-14902.

Spinazzola, A. and M. Zeviani (2009). Disorders from perturbations of nuclear-mitochondrial intergenomic cross-talk. *J Intern Med* 265(2): 174-192.

Steele, D. F., C. A. Butler and T. D. Fox (1996). Expression of a recoded nuclear gene inserted into yeast mitochondrial DNA is limited by mRNA-specific translational activation. *Proc Natl Acad Sci U S A* 93(11): 5253-5257.

Szyrach, G., M. Ott, N. Bonnefoy, W. Neupert and J. M. Herrmann (2003). Ribosome binding to the Oxa1 complex facilitates co-translational protein insertion in mitochondria. *EMBO J* 22(24): 6448-6457.

Tamai, S., H. Iida, S. Yokota, T. Sayano, S. Kiguchiya, N. Ishihara, J. Hayashi, K. Mihara and T. Oka (2008). Characterization of the mitochondrial protein LETM1, which maintains the mitochondrial tubular shapes and interacts with the AAA-ATPase BCS1L. *J Cell Sci* 121(Pt 15): 2588-2600.

Tavares-Carreon, F., Y. Camacho-Villasana, A. Zamudio-Ochoa, M. Shingu-Vazquez, A. Torres-Larios and X. Perez-Martinez (2008). The pentatricopeptide repeats present in Pet309 are necessary for translation but not for stability of the mitochondrial COX1 mRNA in yeast. *J Biol Chem* 283(3): 1472-1479.

Taylor, A. B., B. S. Smith, S. Kitada, K. Kojima, H. Miyaura, Z. Otwinowski, A. Ito and J. Deisenhofer (2001). Crystal structures of mitochondrial processing peptidase reveal the mode for specific cleavage of import signal sequences. *Structure* 9(7): 615-625.

Terpstra, P. and R. A. Butow (1979). The role of var1 in the assembly of yeast mitochondrial ribosomes. *J Biol Chem* 254(24): 12662-12669.

Terpstra, P., E. Zanders and R. A. Butow (1979). The association of var1 with the 38 S mitochondrial ribosomal subunit in yeast. *J Biol Chem* 254(24): 12653-12661.

Terwilliger, T. C. (2001). Maximum-likelihood density modification using pattern recognition of structural motifs. *Acta Crystallogr D Biol Crystallogr* 57(Pt 12): 1755-1762.

Terwilliger, T. C. (2003). Automated main-chain model building by template matching and iterative fragment extension. *Acta Crystallogr D Biol Crystallogr* 59(Pt 1): 38-44.

Terwilliger, T. C. and J. Berendzen (1999). Automated MAD and MIR structure solution. *Acta Crystallogr D Biol Crystallogr* 55(Pt 4): 849-861.

Terziyska, N., B. Grumbt, C. Kozany and K. Hell (2009). Structural and functional roles of the conserved cysteine residues of the redox-regulated import receptor Mia40 in the intermembrane space of mitochondria. *J Biol Chem* 284(3): 1353-1363.

Teyssier, E., G. Hirokawa, A. Tretiakova, B. Jameson, A. Kaji and H. Kaji (2003). Temperature-sensitive mutation in yeast mitochondrial ribosome recycling factor (RRF). *Nucleic Acids Res* 31(14): 4218-4226.

Thomas, B. J. and R. Rothstein (1989). Elevated recombination rates in transcriptionally active DNA. *Cell* 56(4): 619-630.

Tong, W. H. and T. A. Rouault (2007). Metabolic regulation of citrate and iron by aconitases: role of iron-sulfur cluster biogenesis. *Biometals* 20(3-4): 549-564.

Towpik, J., A. Chacinska, M. Ciesla, K. Ginalski and M. Boguta (2004). Mutations in the yeast mrf1 gene encoding mitochondrial release factor inhibit translation on mitochondrial ribosomes. *J Biol Chem* 279(14): 14096-14103.

Truscott, K. N., W. Voos, A. E. Frazier, M. Lind, Y. Li, A. Geissler, J. Dudek, H. Muller, A. Sickmann, H. E. Meyer, C. Meisinger, B. Guiard, P. Rehling and N. Pfanner (2003). A J-protein is an essential subunit of the presequence translocase-associated protein import motor of mitochondria. *J Cell Biol* 163(4): 707-713.

Vambutas, A., S. H. Ackerman and A. Tzagoloff (1991). Mitochondrial translational-initiation and elongation factors in Saccharomyces cerevisiae. *Eur J Biochem* 201(3): 643-652.

van Bloois, E., S. Nagamori, G. Koningstein, R. S. Ullers, M. Preuss, B. Oudega, N. Harms, H. R. Kaback, J. M. Herrmann and J. Luirink (2005). The Sec-independent function of Escherichia coli YidC is evolutionary-conserved and essential. *J Biol Chem* 280(13): 12996-13003.

van der Laan, M., A. Chacinska, M. Lind, I. Perschil, A. Sickmann, H. E. Meyer, B. Guiard, C. Meisinger, N. Pfanner and P. Rehling (2005). Pam17 is required for architecture and translocation activity of the mitochondrial protein import motor. *Mol Cell Biol* 25(17): 7449-7458.

van der Laan, M., M. Rissler and P. Rehling (2006). Mitochondrial preprotein translocases as dynamic molecular machines. *FEMS Yeast Res* 6(6): 849-861.

van der Laan, M., N. Wiedemann, D. U. Mick, B. Guiard, P. Rehling and N. Pfanner (2006). A role for Tim21 in membrane-potential-dependent preprotein sorting in mitochondria. *Curr Biol* 16(22): 2271-2276.

van Heusden, G. P. (2009). 14-3-3 Proteins: insights from genome-wide studies in yeast. *Genomics* 94(5): 287-293.

van Heusden, G. P., D. J. Griffiths, J. C. Ford, A. W. T. F. Chin, P. A. Schrader, A. M. Carr and H. Y. Steensma (1995). The 14-3-3 proteins encoded by the BMH1 and BMH2 genes are essential in the yeast Saccharomyces cerevisiae and can be replaced by a plant homologue. *Eur J Biochem* 229(1): 45-53.

Velours, J., A. Dautant, B. Salin, I. Sagot and D. Brethes (2009). Mitochondrial F1F0-ATP synthase and organellar internal architecture. *Int J Biochem Cell Biol* 41(10): 1783-1789.

Vogel, F., C. Bornhovd, W. Neupert and A. S. Reichert (2006). Dynamic subcompartmentalization of the mitochondrial inner membrane. *J Cell Biol* 175(2): 237-247.

Voisine, C., E. A. Craig, N. Zufall, O. von Ahsen, N. Pfanner and W. Voos (1999). The protein import motor of mitochondria: unfolding and trapping of preproteins are distinct and separable functions of matrix Hsp70. *Cell* 97(5): 565-574.

Waegemann, K. and J. Soll (1996). Phosphorylation of the transit sequence of chloroplast precursor proteins. *J Biol Chem* 271(11): 6545-6554.

Wagner, K., N. Gebert, B. Guiard, K. Brandner, K. N. Truscott, N. Wiedemann, N. Pfanner and P. Rehling (2008). The assembly pathway of the mitochondrial carrier translocase involves four preprotein translocases. *Mol Cell Biol* 28(13): 4251-4260.

Waterman, M. J., E. S. Stavridi, J. L. Waterman and T. D. Halazonetis (1998). ATM-dependent activation of p53 involves dephosphorylation and association with 14-3-3 proteins. *Nat Genet* 19(2): 175-178.

Weraarpachai, W., H. Antonicka, F. Sasarman, J. Seeger, B. Schrank, J. E. Kolesar, H. Lochmuller, M. Chevrette, B. A. Kaufman, R. Horvath and E. A. Shoubridge (2009). Mutation in TACO1, encoding a translational activator of COX I, results in cytochrome c oxidase deficiency and late-onset Leigh syndrome. *Nat Genet* 41(7): 833-837.

Wiedemann, N., V. Kozjak, A. Chacinska, B. Schonfisch, S. Rospert, M. T. Ryan, N. Pfanner and C. Meisinger (2003). Machinery for protein sorting and assembly in the mitochondrial outer membrane. *Nature* 424(6948): 565-571.

Wiedemann, N., M. van der Laan, D. P. Hutu, P. Rehling and N. Pfanner (2007). Sorting switch of mitochondrial presequence translocase involves coupling of motor module to respiratory chain. *J Cell Biol* 179(6): 1115-1122.

Williams, E. H., C. A. Butler, N. Bonnefoy and T. D. Fox (2007). Translation initiation in Saccharomyces cerevisiae mitochondria: functional interactions among mitochondrial ribosomal protein Rsm28p, initiation factor 2, methionyl-tRNA-formyltransferase and novel protein Rmd9p. *Genetics* 175(3): 1117-1126.

Wurm, C. A. and S. Jakobs (2006). Differential protein distributions define two sub-compartments of the mitochondrial inner membrane in yeast. *FEBS Lett* 580(24): 5628-5634.

Xu, F., C. Morin, G. Mitchell, C. Ackerley and B. H. Robinson (2004). The role of the LRPPRC (leucine-rich pentatricopeptide repeat cassette) gene in cytochrome oxidase assembly: mutation causes lowered levels of COX (cytochrome c oxidase) I and COX III mRNA. *Biochem J* 382(Pt 1): 331-336.

Yoshida, M., E. Muneyuki and T. Hisabori (2001). ATP synthase--a marvellous rotary engine of the cell. *Nat Rev Mol Cell Biol* 2(9): 669-677.

Youle, R. J. and D. P. Narendra (2011). Mechanisms of mitophagy. *Nat Rev Mol Cell Biol* 12(1): 9-14.

Zambrano, A., F. Fontanesi, A. Solans, R. L. de Oliveira, T. D. Fox, A. Tzagoloff and A. Barrientos (2007). Aberrant translation of cytochrome c oxidase subunit 1 mRNA species in the absence of Mss51p in the yeast Saccharomyces cerevisiae. *Mol Biol Cell* 18(2): 523-535.

Zeth, K. (2010). Structure and evolution of mitochondrial outer membrane proteins of beta-barrel topology. *Biochim Biophys Acta* 1797(6-7): 1292-1299.

Zhou, Y., S. Reddy, H. Murrey, H. Fei and I. B. Levitan (2003). Monomeric 14-3-3 protein is sufficient to modulate the activity of the Drosophila slowpoke calcium-dependent potassium channel. *J Biol Chem* 278(12): 10073-10080.

Zick, M., R. Rabl and A. S. Reichert (2009). Cristae formation-linking ultrastructure and function of mitochondria. *Biochim Biophys Acta* 1793(1): 5-19.

Zollino, M., C. Di Stefano, G. Zampino, P. Mastroiacovo, T. J. Wright, G. Sorge, A. Selicorni, R. Tenconi, A. Zappala, A. Battaglia, M. Di Rocco, G. Palka, R. Pallotta, M. R. Altherr and G. Neri (2000). Genotype-phenotype correlations and clinical diagnostic criteria in Wolf-Hirschhorn syndrome. *Am J Med Genet* 94(3): 254-261.

Zollino, M., R. Lecce, R. Fischetto, M. Murdolo, F. Faravelli, A. Selicorni, C. Butte, L. Memo, G. Capovilla and G. Neri (2003). Mapping the Wolf-Hirschhorn syndrome phenotype outside the currently accepted WHS critical region and defining a new critical region, WHSCR-2. *Am J Hum Genet* 72(3): 590-597.

Zotova, L., M. Aleschko, G. Sponder, R. Baumgartner, S. Reipert, M. Prinz, R. J. Schweyen and K. Nowikovsky (2010). Novel components of an active mitochondrial K(+)/H(+) exchange. *J Biol Chem* 285(19): 14399-14414.

Zuo, S., Y. Xue, S. Tang, J. Yao, R. Du, P. Yang and X. Chen (2010). 14-3-3 epsilon dynamically interacts with key components of mitogen-activated protein kinase signal module for selective modulation of the TNF-alpha-induced time course-dependent NF-kappaB activity. *J Proteome Res* 9(7): 3465-3478.

ABBREVATIONS

General Abbreviations

aa	amino acids
AMPK	AMP-activated protein kinase
ATP	Adenosine triphosphate
BN-PAGE	Blue native-polyacrilamide gel electrophoresis
Bp	basepair
BSA	bovine serum albumine
C-terminus	carboxy terminus
CC	Coiled coils
CM	Cristae membrane
Coa 1	Cytochrome c oxidase assembly 1
Coa 3	Cytochrome c oxidase assembly 3
COX	Cytochrome *c* oxidase
Cryo EM	Cryo-electron-microscopy
CTD	C-terminal domain
Cyt *c*	Cytochrome *c*
Da	dalton
DNA	deoxyribonucleic acid
dNTP	2'deoxynucleoside-5'-triphosphate
DTT	dithiothreitol
E.coli	*Escherichia coli*
ECL	Enhanced chemical luminescence
EDTA	ethylenediaminetetraacetic acid
ER	Endoplasmic reticulum
EtOH	ethanol
FAD	flavin adenine dinucleotide
HCL	hydrochloric acid
IBM	Inner boundary membrane
IgG	Immunoglobulin G
IM	Inner membrane
IMS	Intermembrane space
IP	immunoprecipitation
IPTG	isopropyl-β-D-thiogalactopyranoside
kDa	Kilodalton
KHE	K^+/H^+ exchanger
LETM1	Leucine zipper/EF hand-containing transmembrane-1
MAD	Multiple Anomalous Dispersion
Mba1	Multicopy bypass of AFG 3 mutant 1
MDM	Mitochondrial distribution and morphology
Mge1	Mitochondrial GrpE homologue
MIA	Mitochondrial intermembrane space import and assembly
MPP	Mitochondrial processing peptidase
mRNA	Messenger RNA
MRP	Mitochondrial ribosomal protein
mt	mitochondrial
mt-DNA	Mitochondrial DNA
mt-ribosome	Mitochondrial ribosome
mtHsp70(Ssc1)	Mitochondrial heat shock protein Hsp70
N-terminus	Amino terminus
NAD^+	Nicotinamide adenine dinucleotide

No	number
O_2	Oxygen
OM	Outer membrane
ORF	Open reading frame
Oxa1	Oxidase assembly mutant 1
OXPHOS	Oxidative phosphorylation
PAGE	polyacrylamide gel electrophoresis
PAM	Presequence translocase associated motor
PBS	phosphate buffered saline
PCR	Polymerase chain reaction
Pefa bloc	4-2-aminoethyl-benzenesulfonyl fluoride hydrochloride
PFGE	Pulse field gel electrophoresis
pH	negative common logarithm of the proton
P_i	Inorganic phosphate
PMSF	phenylmethylsulphonyl fluoride
PS	Presequence
PVDF	polyvinylidene fluoride
RBD	Ribosome-binding domain
RET	Ribosomal polypeptide exit tunnel
RNA	ribonucleic acid
rpm	rotations per minute
S	Sedimentation coefficient
S. cerevisiae	*Saccharomyces cerevisiae*
SAM	Sorting and assembly machinery of outer membrane
SDS	Sodium dedecyl sulfate
SDS-PAGE	Sodium dodecyl sulfate-polyacrylamide gel electrophoresis
SeMet	Seleno-Methionine
TAE	Tris / Acetate / EDTA
TIM22	Carrier translocase of the inner membrane
TIM23	Presequence translocase of the inner membrane
TM	Transmembrane span
TOM	Translocase of outer membrane
Triton X-100	4-octylphenol polyethoxylate
tRNA	Transfer RNA
Tween20	polyoxyethylene (20) sorbitan monolaurate
UBQ	Ubiquinone
UV	ultraviolet
v/v	Volume per volume
w/v	Weight per volume
WB	Western blot
WHS	Wolf Hirschhorn Syndrome
wt	Wild type
YLH47	Yeast LETM1homologue of 47 kDa
$\Delta\Psi$	Membrane potential

Physical units

°C	Degree celsius
Å	Ångström
g	gram
h	hours
l	liter
M	Molar (mol/l)
m	meter
mAmp	milliampere
min	Minute(s)
OD	Optical density
pH	Potential hydrogen
rpm	Rotations per minute
s	Second(s)
U	Unit
V	volt
x g	Acceleration of gravity on earth

Prefixes

k	kilo-	10^{3}
c	centi-	10^{-2}
m	mili-	10^{-3}
µ	micro-	10^{-6}
n	nano-	10^{-9}
p	pico-	10^{-12}

Codes for amino acids

A	Ala	alanine
C	Cys	cysteine
D	Asp	asparatate
E	Glu	glutamate
F	Phe	phenylalanine
G	Gly	glycine
H	His	histidine
I	Iso	isoleucine
K	Lys	lysine
L	Leu	leucine
M	Met	methionine
N	Asn	asparagine
P	Pro	proline
Q	Gln	glutamine
R	Arg	arginine
S	Ser	Serine
T	Thr	threonine
V	Val	valine
W	Trp	tryptophane
Y	Tyr	tyrosine
x-	any	
z-	apolar residue	

CURRICULUM VITAE

Personal Data

Name	Christine Vollmer
Born	12.09.1980 in Göttingen

Education

10.2007-present	**PhD thesis** **Analysis of the role of Mdm38 in respiratory chain biogenesis** Department of Biochemistry II Center for Biochemistry and Molecular Cell Biology Georg-August University, Goettingen Supervisor: Prof. Dr. Peter Rehling
04.2006-03.2007	**Diploma thesis** **Isolierung und Anreicherung der Stickstoff-monoxid-Synthase (NOS) aus *Arabidopsis thaliana*** Albrecht-von-Haller-Institut für Pflanzenwissenschaften Georg-August University, Goettingen Supervisior: Prof.Dr. Rudolf Tischner
10.2000-03.2007	Graduate and undergraduate studies: Biology Georg-August University, Goettingen
06.2000	University entrance qualification: Abitur Gymnasium Witzenhausen